

Patrícia Sónia Ferraz Ferreira Alves

**Shrinkage and Warpage Behaviour on Injection
Moulding Parts**

Tese submetida à Universidade do
Minho para obtenção do grau de
Mestre em Projecto e Fabrico de
Moldes

**Universidade do Minho
2008**

Aos meus pais

Resumo

O processo de moldação por injeção é caracterizado pela elevada taxa de produção e qualidade nos seus produtos. Sendo perfeitamente viável a produção de peças com geometrias complexas a baixo custo, tendo em conta as excelentes propriedades que advêm do material polimérico. Contudo o material é sujeito a sucessivas transformações que dependem de diversas variáveis relacionadas com as propriedades do material, projecto do molde, performance do equipamento e dos parâmetros de processamento. Como resultado, as dimensões finais dos produtos resultantes do processo de moldação por injeção, infelizmente diferem das dimensões da cavidade do molde (fenómeno da contracção).

A indústria de plásticos pertence a uma nova era de processamento automatizado, estando neste momento preparada para ser competitiva devido a uma enorme diversidade de opções. O uso de instrumentação é uma prova viva da importância da automatização, uma vez que sem instrumentação não é possível o controlo do processo.

Hoje em dia, a elevada exigência e parâmetros apertados de qualidade nos produtos torna com que o interesse neste assunto seja cada vez mais relevante e presente. Por esta razão é fundamental um conhecimento exaustivo, do que na realidade acontece dentro da cavidade durante os ciclos de moldação.

O objectivo deste trabalho é fornecer informação sobre o efeito da segunda pressão e temperatura do molde na contracção e empeno, em diferentes materiais, com peças moldadas por injeção.

Um molde foi manufacturado sendo posteriormente instrumentado e a leitura dos respectivos sinais foi monitorizada continuamente através de um sistema de aquisição de dados. Simulações em Moldflow foram efectuadas para validar os resultados experimentais. Os resultados da contracção/empeno foram comparados com medições de orientação de fibras. Quatro materiais como o PC, PP, PP com 20% e 30% de fibras de vidro, foram usados nas moldações.

Abstract

Injection moulding is characterised by its high production rates and accurately sized products. It is possible to produce inexpensive complex geometry composite products with stiffness properties. However the material is subjected to successive transformations that depends on several variables related to material properties, the mould design, equipment performance and moreover process variables. As a result, the final dimensions of injection moulded products unfortunately differ from those of the mould cavity (shrinkage occurs).

The plastics industry has entered in the world of automated processing and it is now sorting out available options in order to be competitive. The use of instrumentation is very important in the automation, because without instrumentation, there is no process control.

Nowadays the products require higher demands on dimensional accuracy and stability, so the interest in this subject is more and more present. For this reasons an approach is need to a complete understanding of what happens inside the cavity during and after the moulding cycle.

The propose, of this work is to provide information about the effect of holding pressure and mould temperature on shrinkage and warpage on different materials in injection moulding parts.

An instrumented mould was manufactured and sensors signals were continuously monitored by a Data Acquisition System. In order to validate the experimental results, simulations in Moldflow were done. The results of shrinkage/warpage were compared with the fibre orientation measurements. Four materials were used for the mouldings: PC, PP, PP with 20% and with 30% of Glass Fibres.

TABLE OF CONTENTS

<u>1. Introduction</u>	<u>1</u>
<u>2. State of the Art</u>	<u>5</u>
<u>2.1. The thermo-mechanical environment</u>	<u>5</u>
<u>2.2. Shrinkage and warpage behaviour</u>	<u>7</u>
<u>2.3. Factors that influence shrinkage/warpage</u>	<u>10</u>
<u>2.3.1. Molecular structure</u>	<u>11</u>
<u>2.3.2. Moulded part geometry</u>	<u>16</u>
<u>2.4. Modelling of shrinkage/warpage</u>	<u>20</u>
<u>3. Experimental work</u>	<u>22</u>
<u>3.1. Part geometry</u>	<u>22</u>
<u>3.2. Material</u>	<u>22</u>
<u>3.3. Mould</u>	<u>25</u>
<u>3.3.1. Cooling channels layout optimization</u>	<u>26</u>
<u>3.4. Acquisition system and sensors</u>	<u>27</u>
<u>3.5. Injection moulding machine</u>	<u>29</u>
<u>3.6. Processing conditions</u>	<u>29</u>
<u>3.7. Shrinkage and warpage measurements procedure</u>	<u>30</u>
<u>3.7.1. Thickness and width shrinkage</u>	<u>30</u>
<u>3.7.2. Angle deformation</u>	<u>30</u>
<u>3.7.2.1. Experimental methodology</u>	<u>30</u>
<u>3.7.2.1. Simulation methodology</u>	<u>33</u>
<u>3.7.4. Fibre orientation</u>	<u>35</u>
<u>4. Experimental results and discussion</u>	<u>39</u>
<u>4.1. Cavity pressure evolution</u>	<u>39</u>
<u>4.1.1. Pressure evolution for PC</u>	<u>39</u>
<u>4.1.2. Pressure evolution for PP</u>	<u>40</u>
<u>4.1.3. Pressure evolution for reinforced PP</u>	<u>41</u>
<u>4.2. Moulding temperature evolution</u>	<u>43</u>
<u>4.2.1. Temperature evolution for PC</u>	<u>43</u>
<u>4.2.2. Temperature evolution for PP</u>	<u>44</u>
<u>4.2.3. Temperature evolution for PP20%</u>	<u>46</u>
<u>4.2.4. Temperature evolution for PP30%</u>	<u>49</u>
<u>4.3. As-moulding shrinkage</u>	<u>52</u>
<u>4.3.1. Unreinforced materials</u>	<u>52</u>

<u>4.3.1.1. Effect of holding pressure</u>	<u>52</u>
<u>4.3.1.2. Effect of mould temperature</u>	<u>54</u>
<u>4.3.2. Reinforced materials</u>	<u>56</u>
<u>4.3.2.1. Effect of holding pressure</u>	<u>56</u>
<u>4.3.2.2. Effect of mould temperature</u>	<u>58</u>
<u>4.4- Experimental warpage</u>	<u>60</u>
<u>4.4.1. Effect of processing conditions</u>	<u>61</u>
<u>4.4.2. Effect of fibre contents</u>	<u>62</u>
<u>4.5- Predicted warpage</u>	<u>64</u>
<u>4.5.1. Effect of processing conditions</u>	<u>64</u>
<u>4.5.2. Effect of fibre contents</u>	<u>65</u>
<u>4.6- Fibre orientation</u>	<u>66</u>
<u>4.6.1. Effect of processing conditions</u>	<u>67</u>
<u>5. Conclusions</u>	<u>69</u>
<u>6. Further Work</u>	<u>72</u>
<u>7. References</u>	<u>73</u>
<u>8. Appendix (Extra experimental data)</u>	<u>81</u>
<u>APPENDIX A1-Moulding pressure evolution</u>	<u>82</u>
<u>A1.1-Pressure evolution for reinforced PP</u>	<u>83</u>
<u>APPENDIX A2-Moulding temperature evolution</u>	<u>84</u>
<u>A2.1-Temperature evolution for PC</u>	<u>85</u>
<u>A2.2-Temperature evolution for PP</u>	<u>86</u>
<u>A2.3-Temperature evolution for reinforced PP20%</u>	<u>88</u>
<u>A2.4-Temperature evolution for reinforced PP30%</u>	<u>90</u>
<u>APPENDIX A3-3D Moldflow simulation results</u>	<u>92</u>
<u>A3.1-Simulation results for PC</u>	<u>93</u>
<u>A.3.1.1-Condition of $H_p=7\text{MPa}$ and $T_m=80^\circ\text{C}$</u>	<u>93</u>
<u>A.3.1.2-Condition of $H_p=51\text{MPa}$ and $T_m=80^\circ\text{C}$</u>	<u>95</u>
<u>A3.2-Simulation results for PP</u>	<u>97</u>
<u>A.3.2.1-Condition of $H_p=7\text{MPa}$ and $T_m=25^\circ\text{C}$</u>	<u>97</u>
<u>A.3.2.2-Condition of $H_p=7\text{MPa}$ and $T_m=40^\circ\text{C}$</u>	<u>99</u>
<u>A.3.2.3-Condition of $H_p=51\text{MPa}$ and $T_m=25^\circ\text{C}$</u>	<u>101</u>
<u>A.3.2.4-Condition of $H_p=51\text{MPa}$ and $T_m=40^\circ\text{C}$</u>	<u>103</u>
<u>A3.3-Simulation results for reinforced PP with 20% of GF</u>	<u>105</u>
<u>A.3.3.1-Condition of $H_p=7\text{MPa}$ and $T_m=25^\circ\text{C}$</u>	<u>105</u>
<u>A.3.3.2-Condition of $H_p=7\text{MPa}$ and $T_m=40^\circ\text{C}$</u>	<u>107</u>
<u>A.3.3.3-Condition of $H_p=36\text{MPa}$ and $T_m=25^\circ\text{C}$</u>	<u>109</u>

<u>A.3.3.4-Condition of $H_p=36\text{MPa}$ and $T_m=40^\circ\text{C}$</u>	<u>111</u>
<u>A3.4-Simulation results for reinforced PP with 30% of GF</u>	<u>113</u>
<u>A.3.4.1-Condition of $H_p=7\text{MPa}$ and $T_m=25^\circ\text{C}$</u>	<u>113</u>
<u>A.3.4.2-Condition of $H_p=7\text{MPa}$ and $T_m=40^\circ\text{C}$</u>	<u>115</u>
<u>A.3.4.3-Condition of $H_p=94\text{MPa}$ and $T_m=25^\circ\text{C}$</u>	<u>117</u>
<u>A.3.4.4-Condition of $H_p=94\text{MPa}$ and $T_m=40^\circ\text{C}$</u>	<u>119</u>

LIST OF FIGURES

Figure 1- Injection machine scheme (adapted from [3])	1
Figure 2- The three stages of injection moulding: injection, plastication (feeding), ejection [5]	3
Figure 3- Velocity, shear rate and temperature profiles through thickness [6]	5
Figure 4- Typical pressure evolution inside the mould impression [6]	6
Figure 5- The influence of some injection moulding variables in the pressure evolution profile inside the impression (adapted from [14])	7
Figure 6- Example of a thermal residual stress distribution after free quenching [8]	9
Figure 7- Molded plate: a) plate before solidification; b) plate solidified under a pressure profile in absence of mechanical equilibrium between layers; c) final stress distribution due to mechanical equilibrium between layers [18]	10
Figure 8- Polymer molecular structure: Amorphous and semi crystalline materials [23]	12
Figure 9- Influence of processing parameters on shrinkage behaviour (adapted from [20])	14
Figure 10- Part geometries: (a) Stepped transition (b) Tapered transition (c) Gradual transition [23]	17
Figure 11- Warpage of a ribbed component [20]	18
Figure 12- Corner warpage due to differential cooling [23]	19
Figure 13- Corner warpage due to uneven thermal behaviour [20]	19
Figure 14- Moulding geometry and nominal dimensions	22
Figure 15- Moulding blocks	26
Figure 16- Mould structure	26
Figure 17- Optimization results	27
Figure 18- Acquisition System	28

Figure 19- Injection moulding machine	29
Figure 20- Experimental angle deformation	31
Figure 21- Measure points	31
Figure 22- Lines for the angle measurements	32
Figure 23- Angles (1 to 4) to measure	32
Figure 24- Mesh model	33
Figure 25- Coordinates: a) On Moldflow model (before and after deformation) b) Equation	34
Figure 26- Planes on Moldflow model (before and after deformation)	34
Figure 27- Angles between planes on Moldflow model (before and after deformation)	35
Figure 28- Positions of the Specimens used to study the fibre orientation	36
Figure 29- Specimens for polishing	36
Figure 30- Equipments	37
Figure 31- Possible forms of fibre sections in a polishing surface: ϕ is the out of orientation angle [70].	37
Figure 32- Influence of the Holding Pressure on pressure evolution curves in PC parts. Mouldings with Holding Pressure of 7, 22, 36 and 51MPa and Mould Temperature at 80°C	40
Figure 33- Influence of the holding pressure on the pressure evolution curves in PP parts. Mouldings with Holding Pressure of 7, 22, 36 and 51MPa with Mould Temperature at 25°C	41
Figure 34- Influence of the holding pressure on the pressure evolution curves in PP parts. Mouldings with Holding Pressure of 7, 22, 36 and 51MPa with Mould Temperature at 40°C	41
Figure 35- Effect of fibre weight fraction (0,2; 0,3) on the pressure evolution curves. PP mouldings with Holding Pressure of 36MPa with Mould Temperature at 25°C	42

<u>Figure 36– Effect of fibre weight fraction (0,2, 0,3) on the pressure evolution curves. PP mouldings with Holding Pressure of 36MPa with Mould Temperature at 40°C</u>	42
<u>Figure 37– Influence of the holding pressure on the Temperature evolution at the middle of fill in PC parts. Mouldings with Holding Pressure of 7 and 51MPa and Mould Temperature at 80°C</u>	44
<u>Figure 38– Influence of the holding pressure on the Temperature evolution curves in PC parts. Mouldings with Holding Pressure of 7 and 51MPa and Mould Temperature at 80°C</u>	44
<u>Figure 39– Influence of the holding pressure on the Temperature evolution, at the middle of fill. PP mouldings with Holding Pressure of 7 and 51MPa with Mould Temperature at 25°C</u>	45
<u>Figure 40– Influence of the holding pressure on the Temperature evolution. PP mouldings with Holding Pressure of 7 and 51MPa, and with Mould Temperature at 25°C</u>	45
<u>Figure 41– Influence of the holding pressure on the Temperature evolution at middle of fill. PP mouldings with Holding Pressure of 7 and 51MPa with Mould Temperature at 40°C</u>	46
<u>Figure 42– Influence of the holding pressure on the Temperature evolution curves in PP parts. Mouldings with Holding Pressure of 7 and 51MPa with Mould Temperature at 40°C</u>	46
<u>Figure 43– Influence of the holding pressure on the Temperature evolution at middle of fill. PP with 20% GF mouldings with Holding Pressure of 7 and 51MPa with Mould Temperature at 25°C</u>	47
<u>Figure 44– Influence of the holding pressure on the Temperature evolution curves in PP20%GF parts. Mouldings with Holding Pressure of 7 and 51MPa with Mould Temperature at 25°C</u>	47

<u>Figure 45– Influence of the holding pressure on the Temperature evolution at middle of fill. PP with 20% GF mouldings with Holding Pressure of 7 and 51MPa with Mould Temperature at 40°C</u>	<u>48</u>
<u>Figure 46– Influence of the holding pressure on the Temperature evolution curves in PP20%GF parts. Mouldings with Holding Pressure of 7 and 51MPa with Mould Temperature at 40°C</u>	<u>49</u>
<u>Figure 47– Influence of the holding pressure on the Temperature evolution in the middle of fill. PP with 30% GF mouldings with Holding Pressure of 7 and 94MPa with Mould Temperature at 25°C.....</u>	<u>50</u>
<u>Figure 48– Influence of the holding pressure on the Temperature evolution curves in PP30%GF parts. Mouldings with Holding Pressure of 7 and 94MPa with Mould Temperature at 25°C</u>	<u>50</u>
<u>Figure 49– Influence of the holding pressure on the Temperature evolution at the middle of fill. PP with 30% of GF mouldings with Holding Pressure of 7 and 94MPa with Mould Temperature at 40°C.....</u>	<u>51</u>
<u>Figure 50– Influence of the holding pressure on the Temperature evolution at middle of fill. PP with 30% GF mouldings with Holding Pressure of 7 and 94MPa with Mould Temperature at 40°C</u>	<u>51</u>
<u>Figure 51– Effect of the Holding Pressure on the as-mould shrinkage across flow direction of PC with Mould Temperature of 80°C.</u>	<u>53</u>
<u>Figure 52– Effect of the Holding Pressure on the as-mould shrinkage across flow direction of PP with Mould Temperature of 25°C.....</u>	<u>53</u>
<u>Figure 53– Effect of the Holding Pressure on the as-mould thickness shrinkage of PC with Mould Temperature of 80°C.....</u>	<u>54</u>
<u>Figure 54– Effect of the Holding Pressure on the as-mould thickness shrinkage of PP with Mould Temperature of 25°C.....</u>	<u>54</u>
<u>Figure 55– Effect of the Holding Pressure on the as-mould shrinkage across flow direction on MF (Middle of Fill) of PP with Mould Temperature of 25 and 40°C.....</u>	<u>55</u>

<u>Figure 56</u> – <i>Effect of the Holding Pressure on the as-mould thickness shrinkage of PP with Mould Temperature of 25 and 40°C</i>	55
<u>Figure 57</u> – <i>Effect of the Holding Pressure on the as-mould shrinkage across flow direction with Mould Temperature of 25°C for PP with 20% of Glass Fibre</i>	56
<u>Figure 58</u> – <i>Effect of the Holding Pressure on the as-mould shrinkage across flow direction with Mould Temperature of 25°C for PP with 30% of Glass Fibre</i>	57
<u>Figure 59</u> – <i>Effect of the Holding Pressure on the as-mould thickness shrinkage with Mould Temperature of 25°C for PP with 20% of Glass Fibre</i>	57
<u>Figure 60</u> – <i>Effect of the Holding Pressure on the as-mould thickness shrinkage with Mould Temperature of 25°C for PP with 30% of Glass Fibre</i>	58
<u>Figure 61</u> – <i>Effect of the Holding Pressure on the as-mould shrinkage across flow direction on MF (Middle of Fill) with Mould Temperature of 25 and 40°C, for PP with 20% of Glass Fibre</i>	59
<u>Figure 62</u> – <i>Effect of the Holding Pressure on the as-mould shrinkage across flow direction on MF (Middle of Fill) with Mould Temperature of 25 and 40°C for PP with 30% of Glass Fibre</i>	59
<u>Figure 63</u> – <i>Effect of the Holding Pressure on the as-mould thickness shrinkage on MF (Middle of Fill) with Mould Temperature of 25 and 40°C for PP with 20% of Glass Fibre</i>	60
<u>Figure 64</u> – <i>Effect of the Holding Pressure on the as-mould thickness shrinkage on MF (Middle of Fill) with Mould Temperature of 25 and 40°C for PP with 30% of Glass Fibre</i>	60
<u>Figure 65</u> – <i>Effect of Holding Pressures on Experimental Angle Deformation in different positions for PC with Mould Temperature of 80°C</i>	61
<u>Figure 66</u> – <i>Effect of Holding Pressures on Experimental Angle Deformation in different positions for PP with Mould Temperature at: a) 25°C b) 40°C</i>	62

<u>Figure 67– Effect of Holding Pressures on Experimental Angle deformation in different positions for PP with 20% of Glass Fibre with Mould Temperature of: a) 25°C b) 40°C</u>	<u>63</u>
<u>Figure 68- Effect of Holding Pressures on Experimental Angle deformation in different positions for PP with 30% of Glass Fibre with Mould Temperature of: a) 25°C b) 40°C</u>	<u>63</u>
<u>Figure 69– Comparison of experimental and predicted Angle Deformation in different positions for PC</u>	<u>64</u>
<u>Figure 70– Comparison of experimental and predicted Angle Deformation in different positions for PP with Mould Temperature at: a) 25°C b) 40°C</u>	<u>65</u>
<u>Figure 71– Comparison of experimental and predicted Angle Deformation in different positions for PP with 20% of Glass Fibre with Mould Temperature at: a) 25°C b) 40°C</u>	<u>65</u>
<u>Figure 72– Comparison of experimental and predicted Angle Deformation in different positions for PP with 30% of Glass Fibre with Mould Temperature at: a) 25°C b) 40°C</u>	<u>66</u>
<u>Figure 73– Effect of Holding Pressure on fibre orientation with Mould Temperature at 25°C for position 30mm from the gate: a) Hp=7MPa b) Hp=36MPa</u>	<u>68</u>
<u>Figure 74– Effect of Holding Pressure on fibre orientation with Mould Temperature at 25°C for position 120mm from the gate: a) Hp=7MPa b) Hp=36MPa</u>	<u>68</u>
<u>Figure A1.1.1– Effect of fibre weight fraction (0,2; 0,3) on the pressure evolution curves. PP mouldings with Holding Pressure of 7MPa with Mould Temperature at 25°C</u>	<u>83</u>
<u>Figure A1.1.2– Effect of fibre weight fraction (0,2, 0,3) on the pressure evolution curves. PP mouldings with Holding Pressure of 7MPa with Mould Temperature at 40°C</u>	<u>83</u>

<u>Figure A2.1.1– Influence of the holding pressure on the Temperature evolution at the middle of fill in PC parts. Mouldings with Holding Pressure of 22 and 36MPa and Mould Temperature at 80°C</u>	<u>85</u>
<u>Figure A2.1.2– Influence of the holding pressure on the Temperature evolution curves in PC parts. Mouldings with Holding Pressure of 22 and 36MPa and Mould Temperature at 80°C</u>	<u>85</u>
<u>Figure A2.2.1– Influence of the holding pressure on the Temperature evolution, at the middle of fill. PP mouldings with Holding Pressure of 22 and 36MPa with Mould Temperature at 25°C</u>	<u>86</u>
<u>Figure A2.2.2– Influence of the holding pressure on the Temperature evolution. PP mouldings with Holding Pressure of 22 and 36MPa, and with Mould Temperature at 25°C</u>	<u>86</u>
<u>Figure A2.2.3– Influence of the holding pressure on the Temperature evolution at middle of fill. PP mouldings with Holding Pressure of 22 and 36MPa with Mould Temperature at 40°C</u>	<u>87</u>
<u>Figure A2.2.4– Influence of the holding pressure on the Temperature evolution curves in PP parts. Mouldings with Holding Pressure of 22 and 36MPa with Mould Temperature at 40°C</u>	<u>87</u>
<u>Figure A2.3.1– Influence of the holding pressure on the Temperature evolution at middle of fill. PP with 20% GF mouldings with Holding Pressure of 22MPa with Mould Temperature at 25°C</u>	<u>88</u>
<u>Figure A2.3.2– Influence of the holding pressure on the Temperature evolution curves in PP20%GF parts. Mouldings with Holding Pressure of 22MPa with Mould Temperature at 25°C</u>	<u>88</u>
<u>Figure A2.3.3– Influence of the holding pressure on the Temperature evolution at middle of fill. PP with 20% GF mouldings with Holding Pressure of 22MPa with Mould Temperature at 40°C</u>	<u>89</u>

<u>Figure A2.3.4– Influence of the holding pressure on the Temperature evolution curves in PP20%GF parts. Mouldings with Holding Pressure of 22MPa with Mould Temperature at 40°C</u>	<u>89</u>
<u>Figure A2.4.1– Influence of the holding pressure on the Temperature evolution at middle of fill. PP with 30% GF mouldings with Holding Pressure of 36 and 51MPa with Mould Temperature at 25°C.....</u>	<u>90</u>
<u>Figure A2.4.2– Influence of the holding pressure on the Temperature evolution curves in PP30%GF parts. Mouldings with Holding Pressure of 36 and 51MPa with Mould Temperature at 25°C</u>	<u>90</u>
<u>Figure A2.4.3– Influence of the holding pressure on the Temperature evolution at middle of fill. PP with 30% GF mouldings with Holding Pressure of 36 and 51MPa with Mould Temperature at 40°C.....</u>	<u>91</u>
<u>Figure A2.4.4– Influence of the holding pressure on the Temperature evolution curves in PP30%GF parts. Mouldings with Holding Pressure of 36 and 51MPa with Mould Temperature at 40°C</u>	<u>91</u>

LIST OF TABLES

<u>Table 1- Typical properties of PP Hifax BA238G.....</u>	<u>23</u>
<u>Table 2- Typical properties of PC Lexan 123R.....</u>	<u>23</u>
<u>Table 3- Typical properties of PP with 20% of Glass Fibre Hostacom G2 N01.....</u>	<u>24</u>
<u>Table 4- Typical properties of PP with 30% of Glass Fibre Hostacom G3 N01.....</u>	<u>25</u>
<u>Table.5- Experimental processing conditions.....</u>	<u>29</u>

1. Introduction

Plastics industry is one of the world's faster growing industries. The two major processing methods are injection moulding and extrusion.

It is well known that injection moulding is one of the most efficient manufacturing techniques. It is used for thermosets and thermoplastics, and represents 32% of all plastic consumption in the world [1]. The injection moulding process has to meet the increasing demand for a high quality product, being at the same time economically priced.

In the simplest although most frequent case, the injection mould consist of two halves, which are directly mounted to the plates of a moulding machine [2] as illustrated on figure 1.

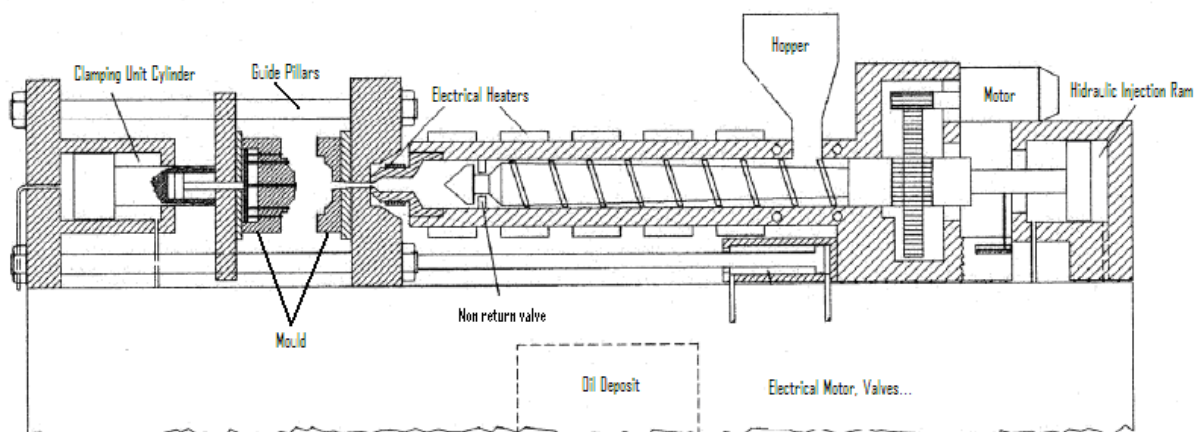


Figure 1- Injection machine scheme (adapted from [3])

These two basic elements, the stationary injection and the movable ejection half can be found in every mould regardless of its design. They could also be called male and female half [2]. The injection moulding operating sequence starts with a pre-determined quantity of moulding material that drops from the feed hopper into the barrel [4]. On this way, the plastic passes through heat barrel zones (heat by conduction), while the rotation of the screw results in a continuous rearrangement of the plastic particles in the flights of the screw. Shear and heat transfer from the barrel wall causes a largely homogeneous heating of the material. The conveying action of the screw builds up pressure in front of its tip. This pressure pushes back the screw. As soon as there is enough supply of melt in the space between tip and nozzle for one shot, the rotation of

the screw stops. At that time the nozzle has been pushed against the sprue bushing of the mould and the mould is clamping, then a sudden controlled pressure surge in the hydraulic cylinder pushes the screw forward and pumps the melt into the mould cavity (**Stage 1- Injection** in figure 2) [5]. Because of the very large temperatures difference between plasticating unit and mould connection is often maintained only as long as needed, that is as long as the melt has still the ability to flow. After the cavity has been filled, the melt starts to solidify [2]. When thermoplastics are processed by injection moulding, the dimensions of the moulded part change as the part cools, since, in the process, the polymer experiences a complicated thermo mechanical history due to a variation on the pressure profile, temperature, non-uniform cooling, etc. As a result deviations of the dimensions of the moulding from the dimensions of the cavity cannot be avoided. These deviations from the nominal size are summarized under the term *Shrinkage*.

The volumetric contraction due to material solidifying can be compensated by further melt supply (holding pressure). Therefore the pressure in the melt has to be maintained until the solidification is terminated (**Stage 2- Holding Pressure and plastication** in figure 2). Since plastication takes a certain amount of time, the screw already starts rotating now and material is fed, metered into the screw and melted, and transported to the front of its tip. Space is generated by pushing the screw coaxially backward, frequently against back pressure. When the moulding is solidified, the injection unit separates from the mould so that material in the nozzle does not cool down likewise. The clamping unit remains closed until the moulding is adequately stable to be ejected. (**Stage 3- Ejection** in figure 2) [2].

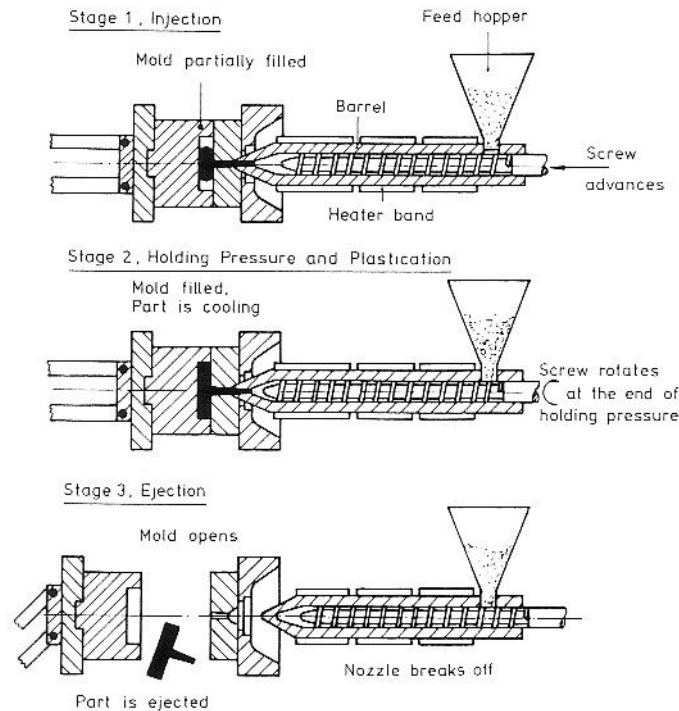


Figure 2- The three stages of injection moulding: injection, plastication (feeding), ejection [5]

During the material solidification thermal and pressure-induced stresses build up in the shell, which eventually give rise to residual stresses in the finished part, as a consequence warpage take place resulting in distortion. There are many mechanisms that can cause imbalance in stresses, such as, the complexity of part geometry, shrinkage variations, differences in cavity pressure, non-uniform cooling, anisotropy etc.

This effects becomes more present, and moulders require greater accuracy, a consistent optimization strategy for machines set-up and production control. The aim is to achieve maximum automatic inspection and quality control of all manufacture parts to obtain parts with the identical tolerances demanded.

Thermoplastics reinforced with short glass fibres have been increasingly used to produce engineering parts for structural applications. The use of short fibres has the advantage of achieving substantial stiffening without compromising significantly the processability of the materials. The fibre reinforced composite materials show lower as-moulded shrinkage compared with unfilled material, because the fibres have much lower thermal expansion coefficients than the matrix polymer, therefore diluting the effects of the shrinkage of the polymer. In fibre composite materials the shrinkage variation results mainly from the anisotropy of the polymeric matrix and the fibre orientation field. Processing conditions and the fibre content, influence the fibre

orientation distribution. The prediction of the composite shrinkage depends on the accuracy of the prediction of the orientation field. It is well known that shrinkage is lower in the fibre direction and larger in the transverse direction; as a result the mould designer must be able to predict the shrinkage in the various directions, if dimensional accuracy is required for the mouldings.

Software Modelling of polymers transformation (CAE – Computer Aided Engineering) allows to understand better the different processes like injection moulding. It constitutes an important tool to predict and to resolve eventual problems that could appear in the process, like the optimization of the cooling system, to avoid *Shrinkage* and *Warping*, to support decisions of conception reducing the need of experimentation during the development of new products or tools, representing an economy of time and costs in the conception and production of parts and / or respective tools of production (mould).

2. State of the Art

2.1. The thermo-mechanical environment

The flow of the polymer melt into a cold mould impression is a typical example of an unsteady, non-isothermal, three-dimensional flow of a compressible, viscoelastic and fluids.

During this process each particle in the material is subjected to a different mechanical and thermal history. When the melt flows through the gate into the impression, a frozen layer of solidified material is formed due to the cold mould walls [6].

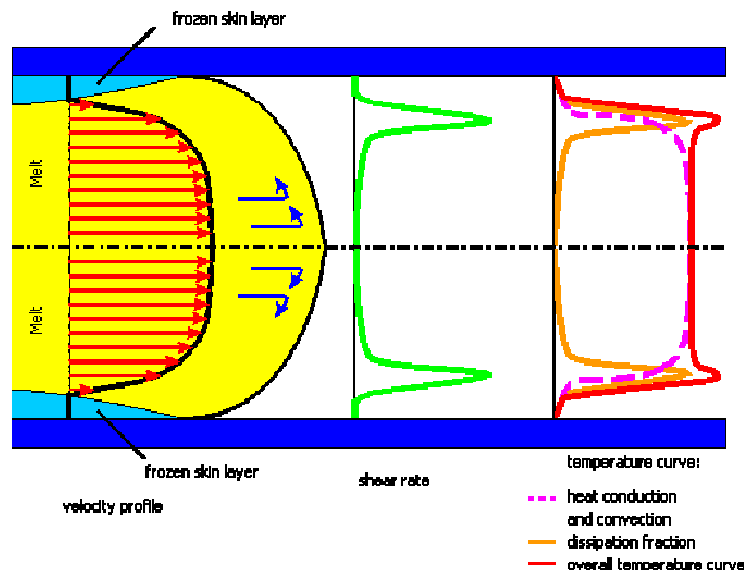


Figure 3- Velocity, shear rate and temperature profiles through thickness [6]

As schematized in the figure 3, the shear rate is maximum near the interface between the frozen skin layer and the melt, and null at the centre. The figure also shows typical profiles of the temperature resulting from the contributions of temperature profiles resulting from the heat generated by conduction and convection, and by viscous dissipation [6].

All these variables that are shown in the figure 3, together with the pressure evolution inside the mould impression, define the thermo-mechanical environment that constrain the overall morphology development and affecting the final properties in the product [e.g. 10, 11, 12]

If the thermo-mechanical history variables (pressure, temperature, flow and cooling rate), can be monitored directly or indirectly in the impression, the moulded product properties can be accurately and consistently predicted [6].

For example the pressure at the impression has been considered the most important parameter to establish a correlation with the dimensions and weight of the moulded part [13], and it is considered a finger print of the process [14]. The figure 4 shows a typical pressure evolution inside the mould impression and its main features.

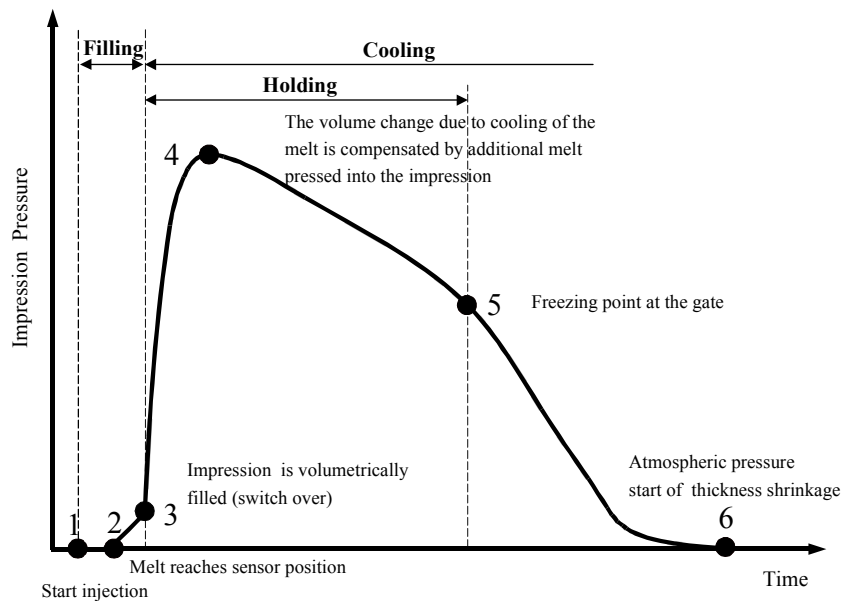


Figure 4- Typical pressure evolution inside the mould impression [6]

Any changes in the injection moulding process due to temperature, flow rate, holding pressure and time, cause changes in this profile. The figure 5 shows the effect of changes of these variables in the pressure evolution profile inside the impression as a net result of the simple variation of a moulding variable [6].

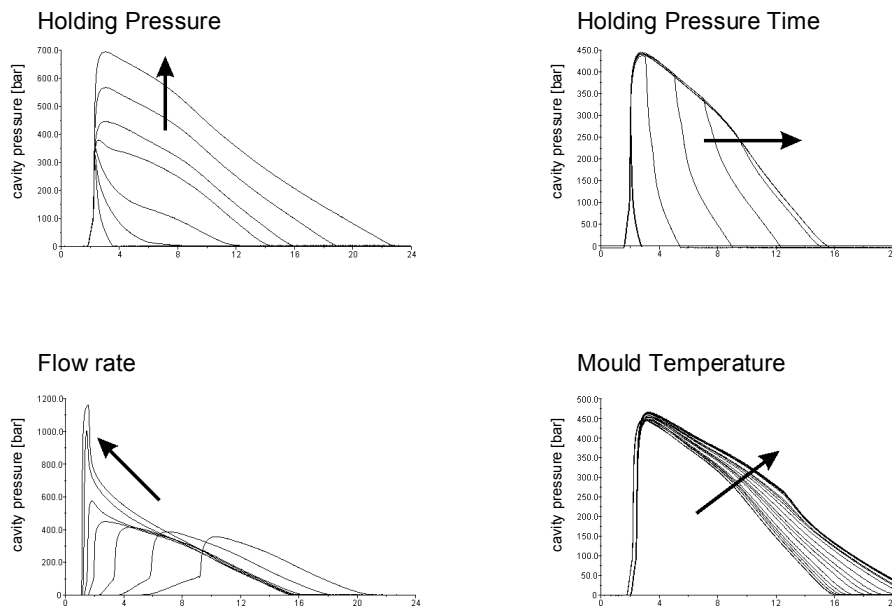


Figure 5- The influence of some injection moulding variables in the pressure evolution profile inside the impression (adapted from [14])

2.2. Shrinkage and warpage behaviour

Injection moulding can make discrete parts that can have complex and variable cross-sections as well as a wide variety of surface textures and characteristics using almost all thermoplastics.

The product quality of injection moulded plastic parts is the result of a complex combination of many factors including materials used, processing parameters, part and mould designs which can affect the shrinkage behaviour of the injection part.

Shrinkage is defined as the reduction in the size of part as compared to the size of the mould. Uniform shrinkage does not cause part deformation and change in shape, but it simply becomes smaller. The shrinkage varies in the space and it is usually quoted at room temperature just after the part has been ejected from the mould:

$$Sh_i = \frac{D_{imp} - D_{part}}{D_{imp}}$$

Where:

D_{imp} is the dimension in the impression in the i direction

D_{part} is the corresponding part dimension

As suggested by Titomanlio, G. *et al* [7] polymers materials normally shrink in thickness direction in order of the different profiles of temperature, while in-plane shrinkage is restricted by the already solidified layers. The limitation of these two theories can be changed by combine the thermodynamic analysis with a thermo-mechanical one.

The cooling rate is high near the mould wall where the orientation caused by the stresses induced by the flow is not able to relax. The interior will cool down more slowly due to the insulation effect of the already solidified polymer. The resulting high thermal gradient and the constrained shrinkage introduce residual stresses in the mouldings [e.g. 8].

To predict the moment shrinkage starts inside the mould before ejection Pantani, R. *et al* [9] measure by strain gages the shrinkage curves in different moulding conditions, analysing them by means of a simple thermo-mechanical model. The advantage of this model is that interactions between the polymer and the mould are easily accounted for, description of main features of shrinkage on the basis of a simple force balance inside the mould. Results showed that the model satisfactorily predicts the moment shrinkage starts inside the mould and revealed the existence of a restraining force not due to pressure, which appeared gradually in a few seconds from the instance of first solidification.

Himasekhar, K. *et al.* [15], Wu, Scott S. *et al.* [16] and, Kikuchi, Hiroyuki *et al.* [17], mentioned that the warpage always results from differential (non-uniform) shrinkage. Because of that non-uniformity, the part will shrink differently at different planar and thickness locations. This causes warpage. Those variations in shrinkage will lead in stresses that are able to overcome the mechanical strength of the part, which results in distortion.

Residual stresses are a process induced stresses that persists in the finished moulded product after of their removal of their original driving force. Those stresses result from the fabrication processes due to the inhomogeneous cooling between the core and the skin. Residual stresses are normally balanced, which means that across thickness the tensile and compression stresses will cancel [8].

A solidified polymer plate can be considered as consisting of a large number of layers, each in a different stress situation. If the layers could be cut free, some of them therefore would expand and others would contract. If the plate is not loaded, all individual stresses contributions will balance out and the product seems to be stress free. Residual stresses however, can be of the same order as the rupture stress

(loading) applied to the product. A high quality product therefore must have a low level of residual stresses [8].

Two interpretations for stress formation in injection moulded products exist: thermal stresses and pressure induced stresses. The residual thermal stresses arise when a piece of material is cooled inhomogeneously and when the cooling moreover causes it to stiffen. The inhomogeneity of the cooling process is responsible for the thermal stresses; the change of the elastic properties during solidification causes to persist after the cooling has been completed. This is best illustrated by considering the surface layers and the core region of the specimen separately. When the surface cools, is free to contract and does not contribute to stress formation. In subsequent steps, as the core layer contracts, the solidified surface layer hinders contraction of the core, eventually resulting in a parabolic stress profile with compressive stresses in the surface and tensile stresses in the core [8], as it can be seen on figure 6.

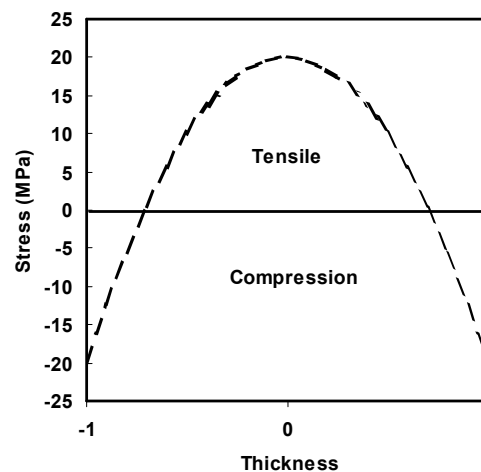


Figure 6- Example of a thermal residual stress distribution after free quenching [8]

The interpretation of pressure induced stresses starts with the idea that layers frozen-in at elevated pressures tend to expand when released from the mold. Since in injection molding the pressure varies during solidification all layers solidify at different pressure and also undergo to thermal contraction (figure 7b). Since layers are forced to agree on the same length, in absence of external forces, some layers will be in compression and some other in expansion (figure 7c).

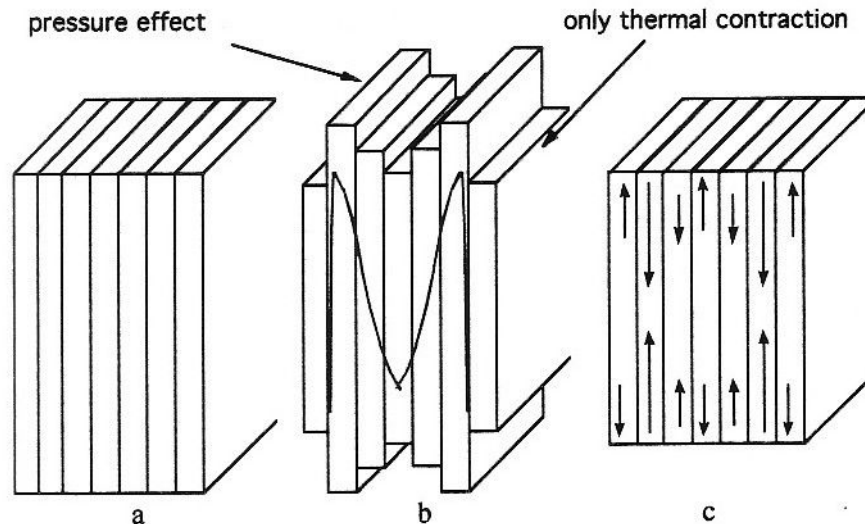


Figure 7- Molded plate: a) plate before solidification; b) plate solidified under a pressure profile in absence of mechanical equilibrium between layers; c) final stress distribution due to mechanical equilibrium between layers [18].

In the study of Titimanlio, G. *et al.* [19] used a simple elastic model to study the effect of in-mould shrinkage on final product dimensions and residual stress distributions. Mentioned the possibility of the shrinkage occur inside the mould. It was conclude that in-mould length shrinkage may had a certain effect on the residual stress distribution and final product length and also reported that friction between polymer surface and mould wall were dominant and avoid length shrinkage until pressure drops to a few MPa.

A moulding part cannot shrink uniformly in all three directions (over its length, width and thickness). Only over the thickness of the part does virtually unimpeded shrinkage take place. Most of the volume shrinkage, therefore, is »used up« in the shrinkage of the wall thickness of the moulded part. Even if the mould does not impede shrinkage in any way, the fact that the layers of the moulding freeze from the outside towards the inside means that shrinkage is obstructed over the length and width of the part [20].

2.3. Factors that influence shrinkage/warpage

Shrinkage occurs due to the thermal contraction (change in volume with a change in temperature) and the compressibility (change in volume with a change in pressure) resulting in a volume change.

For this reason, the mould builder has to predict the difference between the dimensions of the mould cavity and those of the moulded part. In many cases, this is not an easy

task, since shrinkage is influenced by a large number of parameters [20], as material properties (including the amount and type of filler and reinforcement, the molecular weight, the level and orientation, and the rate of crystallization in semi-crystalline polymers), the part and mould geometries (wall thickness), moulding conditions, gate design and mould restrictions [13, 21]. Beside that, Sanschagrín, B. *et al.* [22], included also the aspect ratio of the reinforcement, and conclude that this parameter is more important than the moulding parameters.

2.3.1. Molecular structure

Amorphous vs semi crystalline materials

All polymers suffer a considerable specific volume reduction when the processing temperature changes to the environment temperature. This variation -Volumetric Shrinkage- it's more relevant in semi-crystalline polymers than in amorphous materials. Amorphous materials have a randomly ordered molecular structure which does not have a sharp melt point but instead softens gradually as the temperature rises. These materials change viscosity when heated, but don't shows easy flowing as semi-crystalline materials. When amorphous polymers are heated, the intertwined chains become more mobile/active, and disentanglement and chain slippage occur, resulting in a gradual softening and ultimately flow. As the level of molecular activity increases, the material becomes more fluid, since the attractive forces between the polymer molecules decrease as the average distance between the polymer chains increase. After the molten, amorphous polymer is shaped or formed, the polymer is cooled, and regains its rigidity as the molecular mobility is reduced [23]. They are isotropic in flow, shrinking uniformly in the direction of flow and transverse to flow. As a result, amorphous materials typically exhibit lower mould shrinkage and fewer tendencies to warp than the semi-crystalline materials. Although semi-crystalline materials have a highly ordered molecular structure, with sharp melt points. They do not gradually soften with a temperature increase but, rather, remain hard until a given quantity of heat is absorbed and then rapidly change into a low viscosity liquid. These materials are anisotropic in flow, shrinking less in the direction of flow vs. transverse to flow. The crystallization occurs during cooling and is time and temperature dependent. The cooling rate has a major influence on nucleation and nucleus growth and hence on the structure that develops. The more slowly cooling takes place (through high cavity surface temperatures), the higher the degree of crystallization – and the greater the level of shrinkage.

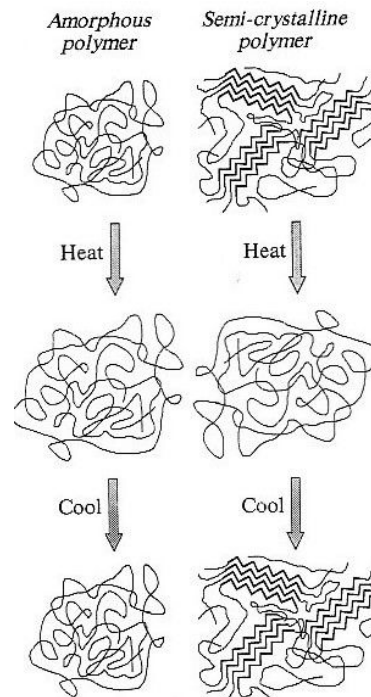


Figure 8- Polymer molecular structure: Amorphous and semi crystalline materials [23]

However according to Timm, W., Marty *et al.* [24] neat semi crystalline materials were normally expected to had more mould shrinkage but in his study they appear to be less sensitive to shear stress and related to orientation induced warpage and shrinkage in contrast , amorphous materials seem to be more sensitive. In contradiction Seyler, R. *et al.* [25] reported that amorphous and semi crystalline materials produce variations in warpage, although semi crystalline materials have higher shrinkages, which will increase the potential for high stresses and warpage. Amorphous materials generally shrink less. Therefore, the variation in shrinkage is fewer, which results in a smaller warpage. The higher shrinkage values create more of an opportunity for variation in shrinkage, which causes warpage.

Reinforced materials

The glass fibres constitute an additional internal restraint, which impedes thermal contraction in the direction of the glass fibres as it can be verify in Zöllner, Olaf *et al.* [20] report. He concluded that through the use of glass fibres, it is possible to reduce shrinkage by 50 to 80 % in the longitudinal fibre direction. Adding more than 20 to 25 % glass fibre has no further effect on the shrinkage behaviour of semi crystalline thermoplastics. According to Seyler, R. *et al.* [25], a neat material will shrink more in the direction of flow and a fibre-filled material will shrink more perpendicular to flow. It was also reported that direction and magnitude of orientation developed during mould filling and packing, have an effect on the shrinkage of a plastic material, which leads to

warpage. Besides that, neat and fibre filled materials react different to these orientation effects, leading to different warpage. This study on warpage sensitivity showed that the material displaying the most warpage due to orientation was the glass filled polypropylene. This material warped almost twice as much as the other materials tested like neat polypropylene, nylon and ABS. When shrinkage is anisotropic across the part and part thickness, the internal stresses created can lead to warpage. Fan, Zhiliang *et al.* [26] studied the 3D technique to warpage analysis and reported that the difference between parallel and perpendicular shrinkage and anisotropic material properties relating to the fibre orientation distribution are one of the main causes of part warpage for fibre filled thermoplastics. Fahy, E., J. *et al.* [27], studied the warpage in reinforced polymers and mentioned that in fibre reinforced injection moulded thin plastic parts, the most dominant cause of part distortion during cooling is in-plane thermal contraction anisotropy. As well, Zöllner, O. *et al.* [22], reported that in the case of glass fibre-filled thermoplastics the orientation of these fillers considerably affects the deformation. Further the opinion of Kech, A. and Hosdez, V. [28] is basically the same since for them, the reasons for warpage are orientations that lead to anisotropic thermal and shrinkage properties, thermal conditions and process parameters. The contradiction between unfilled and fibre reinforced thermoplastics is that isotropic materials are more influence by cooling then fibre orientation. As well Kikuchi, Hiroyuki *et al.* [17] deduced that the primary cause of warpage for a reinforced material is the orientation of the fibre but the main cause of the warpage for a unreinforced material is the non-uniform distribution of temperature and pressure during the injection moulding, in addition it was found that the material anisotropy parameter it's very important for characterizing and for controlling warpage.

Jansen, K., M., B. *et al.* [29] also reported that length shrinkage of a fibre filled material were much smaller than width shrinkage and was not very sensitive to variations in packing pressure, and that the length shrinkage steadily decreases with increasing concentration while width shrinkage was much less affected.

Injection moulding processing conditions

Reducing shrinkage and warpage is one of the objectives to improve the quality of injection-moulded parts. In addition to part design and material properties, process conditions are the most important factor in determining the part quality.

It is well known that process conditions affect many properties of plastic parts including shrinkage (figure 9):

- *Holding pressure*: Controls the compensating flow of material as it is cooling and shrinking. The higher the holding pressure, the lower the mould shrinkage.
- *Pressure holding time*: Controls how long compensation flow is provided. If hold time is too short, part will not be properly packed and will shrink more.
- *Mould temperature*: Can affect how much internal stress there is and amount of crystallization. The moulding shrinkage increases with the mould temperature.
- *Injection velocity*: The injection velocity has almost no influence on overall shrinkage. This parameter affects the amount of orientation of the polymer molecules [20].
- *Melt temperature*: Melt temperature affects the viscosity of the material, therefore, affecting how well it can be packed. An elevated melt temperature increases the potential for thermal contraction in the resin (increased shrinkage) and, secondly, it leads to a reduction in the melt viscosity and hence to better packing and, ultimately, to a reduction in shrinkage [20].
- *Demoulding time*: Controls how long the part stays in its shape in the mould before ejection. A longer time can allow the part to become more rigid and resist warpage or linear shrinkage. It can also contribute to the crystallization of the material.

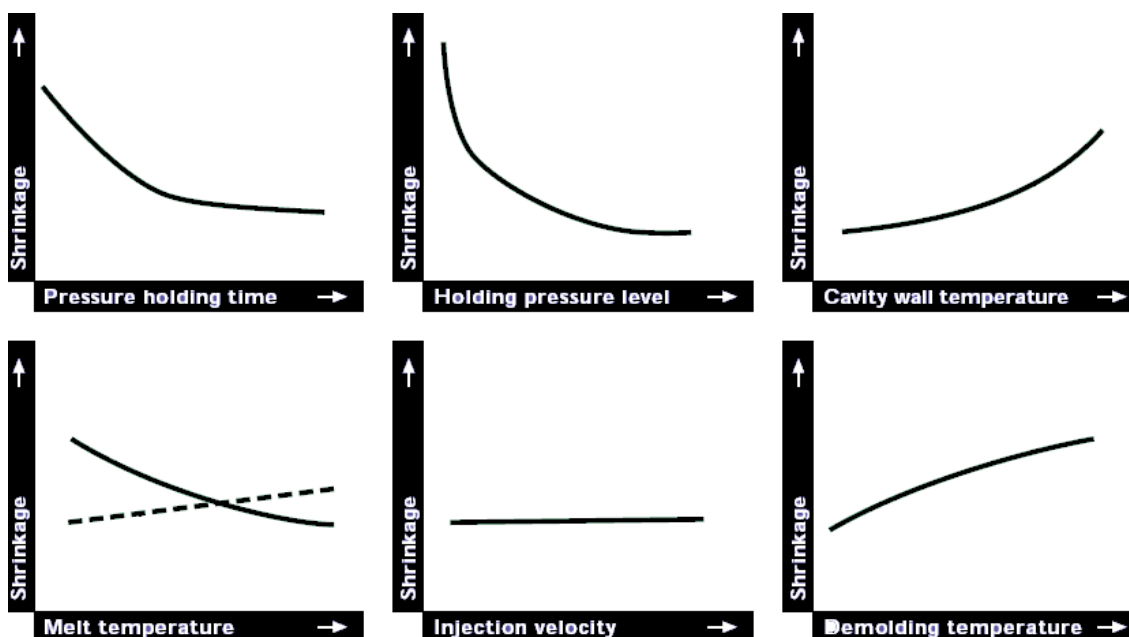


Figure 9- Influence of processing parameters on shrinkage behaviour (adapted from [20])

Several studies were carry out to analyse the effect of processing variables on the as-moulded shrinkage [1, 30-40]. These studies concluded that the Holding pressure is the most significant injection moulding parameter.

In contrast Pramujati, Bamban *et al.* [41] and Healy, Anna *et al.* [42] reported that the melt temperature was the key variable. On the other hand authors as Shiarnng Jou, Wern *et al.* [43] and Wuebken, G. *et al.* [44] found that the effects of mould temperature and melt temperature are statistically significant and the mould temperature is the most important factor. Friel, P. *et al.* [45] also conclude that the processing behaviour of a plastic is highly influenced by the mould surface temperature as a result the optimization of the mould temperature control system is a worthwhile and important as improving the machines, moulds and plastics. Furthermore Chang, Tao, C. *et al.* [46] studied the optimal conditions for reducing shrinkage identified by the Taguchi method and observed that mould temperature, melt temperature, holding pressure and holding time were the most significant factors to the shrinkage behaviour. More recent theories as Mamat, A. *et al.* [1] and Jasen, K., M., B. *et al.* [31] suggested that the holding time was second in importance for its effect on shrinkage while others conclude differently for instance Stebick, M. *et al.* [30] reported that the second most significant variable was determined to be the melt temperature.

Holding pressure, melt temperature and holding time parameters tend to reduce shrinkage when they increase as mentioned on Jasen, K., M., B. *et al.* [32] paper. Mamat, A. *et al.* [1] and Bushko, Wit C. *et al.* [38] concluded that the melt temperature and mould temperature exhibit a smaller influence on shrinkage. As well Jasen, K., M., B., Van Dijk, D., J. and Husselman, M., H. *et al.* [32], Patel, Prabir *et al.* [33] and Pierick, D. *et al.* [39] reported that the mould temperature and injection velocity do not had large effect on shrinkage. In contrast, Bain, Jr, M., F. *et al.* [47] reported that cavity pressure, melt temperature and mould temperature had a large impact on the shrinkage. Wang, T. James *et al.* [40] conclude that, higher packing can deliver more material into the cavity reducing in this way shrinkage, however, higher packing pressure can also create large pressure gradient in the cavity. The pressure difference can enhance the non uniform shrinkage effect and increase warpage.

Furthermore, Akkerman, R. *et al.* [36] conclude that the mould temperature had a slight but relevant effect, a higher mould temperature causes a somewhat larger shrinkage. With the same opinion Gibson, Patrick M. *et al.* [48] showed that higher mould wall temperatures lead to slower cooling rates, increasing the crystallinity and therefore increasing the shrinkage. Of particular interest is the study on warpage in unfilled

amorphous materials as a function of mould temperature difference and holding pressure, by Jansen, K. M. B. *et al.* [49], the experiments showed that warpage increased linearly with the applied temperature difference between mould halves. Not expected was that at low holding pressures the plates curved towards the hot side, whereas at high holding pressures they warped towards the cold side.

In addition, Pierick, D. *et al.* [39] reported that melt temperature becomes increasingly more important as the distance from the gate increases. Other authors as Stebick, M. *et al.* [30] reported that the shrinkage was higher with the hotter melt. Cooling time, mould temperature and filling rate did not have a marked effect on the final shrinkage. On the other hand Cox, W., Howard *et al.* [50], observed that for polypropylene the shrinkage in length direction increases substantially as the fill time increases. In ABS, there is an overall decrease in the shrinkage values in both length and thickness as the fill time is increased, and for nylon the shrinkage in the thickness direction decreases slightly at long fill times.

The Patel, Prabir *et al.* [33] and Boudreaux, E. *et al.* [51] conclude that the shrinkage in the direction of the flow was significantly greater than in the transverse direction. This result is typically observed in unfilled polymers. Moreover, Kumazawa, H. *et al.* [35] conclude that the shrinkage in the thickness direction is three times larger than in the other directions in short holding pressure time. As well, Bushko, Wit C. *et al.* [38], reported that the processing parameters affect the through-thickness shrinkage more than the in-plane shrinkage.

2.3.2. Moulded part geometry

In a few cases the geometry was considered as a variable [37].

In most studies rectangular geometry were considered [1, 9, 17, 21, 29, 39], [31-35] and [51-53], exceptions are for instance the disk parts [17, 25, 27, 37, 54, 55] and flat panels [36].

Fahy, E., J. *et al.* [27] used a circular disk moulding to analyse the in-plane expansion anisotropy because of its simplicity and use in appraising the tendency of different materials to induce warpage. Seyler, R. *et al.* [25] also used disks to illustrate warpage based on orientational effects and found that thinner sections produced more shear stresses, which lead to more orientation and created a higher warpage.

Geometry may affect shrinkage in two ways. First geometry may affect flow and hence cause orientation effects (of amorphous phase, crystalline phase or filled particles) resulting in shrinkage anisotropy. Second geometrical constraints affect the shrinkage boundary conditions. These effects are discussed by Jasen, K., M., B. *et al.* [31], they conclude that the presence of a geometrical constraint in the mould reduces final shrinkage.

Thickness

Polymers have a very low thermal conductivity, compared with metals, cooling from the melt proceeds unevenly, the surface cools more rapidly than the interior. This leads to variations in the structure and crystallinity through the section thickness and can result in the formation of voids or holes due excessive internal shrinkage.

As a general rule the shrinkage increase with the increasing part thickness. Thicker plaques cool more slowly, and slower cooling rates allow the molecules to adopt a regular pattern, forming larger crystalline areas and a higher degree of crystallinity. The higher degree of crystallinity results in higher shrinkage [48]. As already been said, parts with thick wall sections are most difficult to cool (longer to cool) and require additional packing. When parts have both thick and thin sections (figure 10), the location of the gate into the thick section is preferred because it enables packing of the thick section, even if the thinner sections have solidified. The different cooling and packing requirements of the thick and thin sections lead to shrinkage related internal stresses in the wall thickness transition regions. These internal stresses can lead to short or long term warpage. Tapered transitions can be used to avoid high stress concentration, providing gradual flow transitions during mould filling [23].

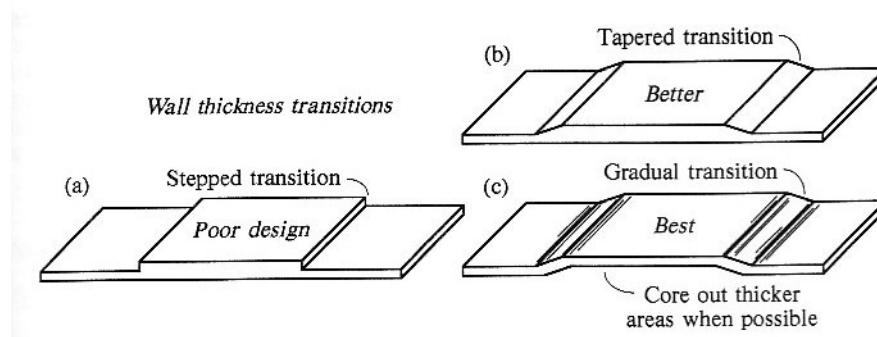


Figure 10- Part geometries: (a) Stepped transition (b) Tapered transition (c) Gradual transition [23]

According to Seyler, R. *et al.* [25], generally thinner parts result in more shear stresses, which more orientation in the flow direction. Additionally, this increases the magnitude of orientation leading in more internal stresses and higher possibility for warpage. As thickness is increased, extensional flow induced orientation will have more of an effect. There will be less orientation in the direction of flow, a lower magnitude of orientation, and thereby a reduced amount of warpage. Another study based on the effects of processing conditions, nominal wall thickness and flow length on the shrinkage [48] showed that the shrinkage increases with increasing part thickness.

Ribs

Ribs can have a pronounced influence on moulded part shrinkage and, in particular, on the uniformity of shrinkage. Ribs should be made thinner than the wall to which they are attached. Ribs generally shrink less (i.e. they »remain longer«) than the other moulded part dimensions [20], the result can be a warped part (figure 11). Martinho, P. [56] carry out a study based on warpage in injection moulded parts and reported that the introduction of ribs on the part decrease warpage, although in some conditions it was verified a small angular variation leading in different deformations.

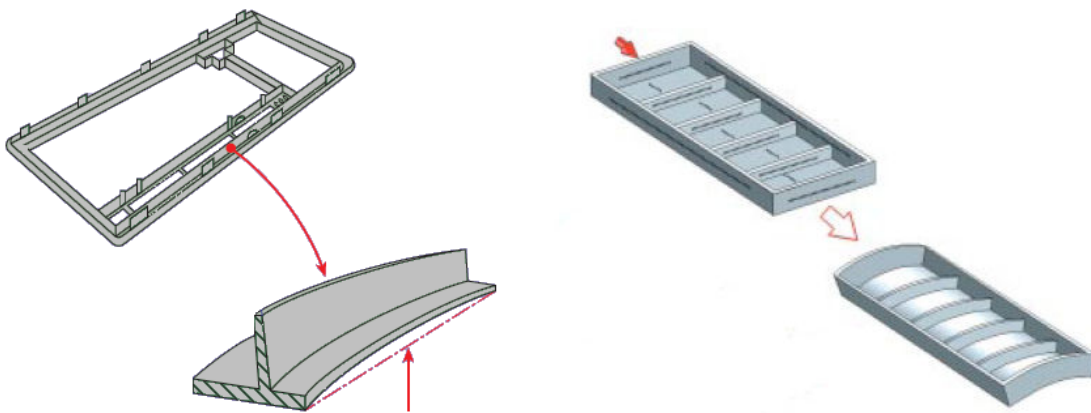


Figure 11- Warpage of a ribbed component [20]

Corner parts

The phenomenon of corner warpage is similarly attributable to shrinkage. The uneven cooling behaviour in the corners causes the inside of the corner to shrink to a greater extent. This leads to stresses and forces which produce corner warpage [20] (figure 13). According to Jansen, K.M.B. *et al.* [49], the angle deflection of corner products was seen to depend in a similar way on temperature difference and holding pressure. It turned out that corners with larger radius were more susceptible to changes in the wall

temperature difference than products with smaller radiused corner. Ammar, Amine *et al.* [57] studied the corner deformation induced by shrinkage anisotropy and showed that the may cause of corner deformation is the asymmetric cooling and anisotropy of in plane shrinkage. During the cooling process in injection moulding, heat fluxes in the mould are lower in inner corners and then the cooling becomes asymmetric (figure 12). Therefore the corner angle of the part becomes smaller than the nominal mould one. On the other hand, due to the large fibre-length/part thickness ratio, most fibres are oriented in the planar direction leading to higher thermal expansion coefficients in the thickness direction as compared to those in the surface direction. When the part cools, a decrease of the enclosed angle in a corner occurs after the moulding is ejected from the mould.

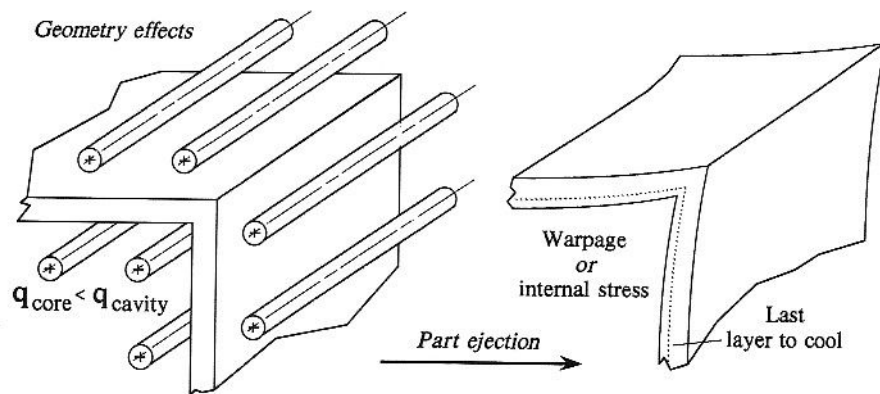


Figure 12- Corner warpage due to differential cooling [23]

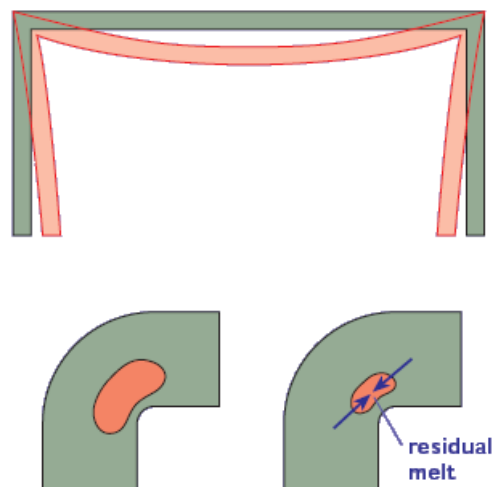


Figure 13- Corner warpage due to uneven thermal behaviour [20]

2.4. Modelling of shrinkage/warpage

Simulation software's have been developed to simulate the processing of the polymer from a melt at the start of injection to a solidified product at the time of ejection. The aim of these codes is to predict and understand the causes of shrinkage and warpage to minimize this effect in future products.

Azevedo, Maurício *et al.* [58] used the Moldflow software to perform cooling analysis with three different injection moulds, with different moulding conditions, in order to investigate the parameters settings for mould temperature. The analysis of the simulation results showed that the cooling water temperature was the most significant parameters to the mould temperature.

Stitz, S. *et al.* [59] used a software (SWIS and MFWARP by moldflow) to predict the shrinkage and warpage. It was reported that simulation results and experimental trends agree well, however quantitatively, the simulation overestimate the warpage. Other studies were made by Zou, Q. *et al.* [60] applied a simulation analysis program as Moldflow (MF/FLOW, MF/COLL, MF/WARP) to predict the amount of warpage, residual stresses and to identify which factors were causing warpage. It was mentioned that the warpage analysis programs is a very useful tool, since it was possible reduced warpage and improved the residual stress and the differential cooling. As well, Zöllner, O. *et al.* [22] based their study on a computation program (Moldflow) to pre-calculate the moulded article deformation of injection moulded glass fibre-reinforced components and the results were very satisfactory.

Other authors as Shijun, Ni [61], also used simulation software from moldflow to predict the part deformation using the different gating options and conclude that the predicted part shrinkage and warpage were in good agreement with the measurements made on the injection moulded frame. In another study [62] he used a systematic simulation approach to minimize warpage and the final analysis results were very good.

Commercial codes like Moldflow and C-Mold calculate shrinkage in a post processing step from the thermal stress distribution. They ignore pressure-induced stresses and as well the solidification pressure term. This can be a possible cause of large discrepancies between predicted and measured shrinkages [21, 63].

Himasekhar, K. *et al.* [15] developed in their study an integrated system (three-layer integrated approach) for shrinkage and warpage predictions that consist of several programs to perform mould-cooling analysis, unified filling/post filling/residual-stress

analysis and equilibrium stress analysis interfaced with a finite-element stress analysis program.

According to, Fan, Z. *et al.* [26] it was used a 3D simulation technique (Moldflow) to warpage analysis and the results were very satisfactory. The accurate prediction of warpage is an important practical problem that should be done by finite element simulation of polymer flow, residual stress formation and parts deformation using midplane shell models, surface shell models, true 3D or hybrid (combination of shells and true 3D) models. True 3D is the most accurate and theoretically sound way to perform flow and warpage analysis, but usually requires significant computational resources [64].

Wu, Scott S. *et al.* [16] and Ito, H. *et al.* [53] used in their study the CAE flow simulation tool to better understand the inside causes of warpage, but it was found that sometimes there are limitations in the simulation software especially for crystalline materials (because of the inhomogeneity of the crystallinity and residual stress) and fibre reinforced plastics. Matsuoka, T. *et al.* [65] also developed injection moulding programs for CAE, those programs were integrated to predict warpage by using a common geometric model of three dimensional thin walled moulded parts, for this kind of study it was used a glass fibre reinforced polypropylene and the results were that the predicted warpage was in good agreement with experimental one.

Shrinkage at a given part dimension is dependent on well known factors, for Bernhardt, E., C. *et al.* [66] the traditional analytical methods did not provide practical means to give these factors full consideration on a routine basis, on the other hand computer modelling (CSE-computerized shrinkage evaluation) package made it possible.

Healy, Anna *et al.* [42], used a predictive model control (MPC), improved by using computational-fluid-dynamics (CFD) simulations, to control the melt temperature. As well Dubay, Rickey [67] developed the same predictive model control and implemented for controlling the cavity pressure during filling.

3. Experimental work

3.1. Part geometry

In this work, a rectangular moulding with a curved end was used. The moulding has the following nominal dimensions, 1,5mm on thickness, 40mm on width and about 134mm on length as it can be seen by figure 14. The purpose of the curved end on the part is to study angle deformations in injection moulding parts.

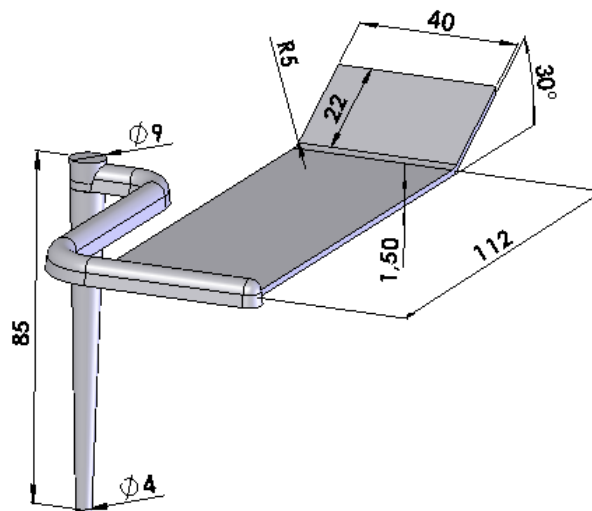


Figure 14- Moulding geometry and nominal dimensions

3.2. Material

Four materials were used for the production of the mouldings: PP Hifax BA238G, PC Lexan 123R, PP Hostacom G2 N01 and PP Hostacom G3 N01

PP Hifax BA238G

The PP from Montell, is a Polypropylene Copolymer suitable for injection moulding with very high impact strength and good UV resistance designed for outdoor applications.

Some relevant physical, mechanical and thermal of *PP Hifax BA238G* as quoted by Basell manufacturer, are presented in table 1.

Table 1- Typical properties of PP Hifax BA238G

<i>Typical Properties</i>	<i>Method</i>	Value Unit
Physical		
Density (Method A)	ISO 1183	0,9 g/cm ³
Melt flow rate (MFR) (230°C/2.16Kg)	ISO 1133	12 g/10min
Mechanical		
Tensile Stress at Break	ISO 527-1, -2	13MPa
Tensile Stress at Yield	ISO 527-1, -2	17MPa
Tensile Strain at Break	ISO 527-1, -2	>100%
Tensile Strain at Yield	ISO 527-1, -2	5%
Flexural modulus	ISO 178	900MPa
Thermal		
Heat deflection temperature B (0.45 MPa) Unannealed	ISO 75B-1, -2	70°C

PC Lexan 123R

The PC from General Electric Plastics, is a polycarbonate plastic material. Lexan resin is an amorphous engineering thermoplastic with high mechanical, optical, electrical and thermal properties. Has low viscosity, U.V. stabilized grade and contains a release agent to ensure easy processing and is available in transparent, translucent, and opaque colours.

Some relevant physical, mechanical and thermal of *PC Lexan 123R* as quoted by General Electric Plastics manufacturer, are presented in table 2.

Table 2- Typical properties of PC Lexan 123R

<i>Typical Properties</i>	<i>Method</i>	Value Unit
Physical		
Density (Method A)	ISO 1183	1.2g/cm ³
Melt flow rate (MFR) (300°C/1.2Kg)	ISO 1133	25.2g/10min
Melt Volume Rate, MVR at 300°C/1.2 kg	ISO 1133	21cm ³ /10min
Mechanical		
Tensile Stress, break, 50 mm/min	ISO 527	65MPa
Tensile Stress, yield, 50 mm/min	ISO 527	63MPa

Tensile Strain, break, 50 mm/min	ISO 527	100%
Tensile Strain, yield, 50 mm/min	ISO 178	90MPa
Flexural Modulus, 2 mm/min	ISO 178	2300MPa
Thermal		
Thermal Conductivity	ISO 8302	0,2W/m-°C
Vicat Softening Temp, Rate B/50	ISO 306	140°C
Vicat Softening Temp, Rate B/120	ISO 306	141°C
HDT/Be, 0.45MPa Edgew 120*10*4 sp=100mm	ISO 75/Be	133°C
HDT/Ae, 1.8 MPa Edgew 120*10*4 sp=100mm	ISO 75/Ae	122°C

PP Hostacom G2 N01

PP from Basell, is a polypropylene homopolymer plastic material with 20% glass flake filler.

Some relevant physical, mechanical and thermal of *PP with 20% of Glass Fibre Hostacom G2 N01* as quoted by General Electric Plastics manufacturer, are presented in table 3.

Table 3- Typical properties of PP with 20% of Glass Fibre Hostacom G2 N01

<i>Typical Properties</i>	<i>Method</i>	<i>Value Unit</i>
Physical		
Density	ISO 1183	1,04g/cm ³
Melt Flow Rate (MFR) (230°C/5.0 kg)	ISO 1133	7,5g/10min
Melt Volume-Flow Rate (MVR) (230°C/5.0 kg)	ISO 1133	8,50cm ³ /10min
Mechanical		
Tensile Stress at Yield (50 mm/min)	ISO 527-1, -2	33MPa
Tensile Strain at Break (50 mm/min)	ISO 527-1, -2	15%
Tensile Strain at Yield (50 mm/min)	ISO 527-1, -2	8,0%
Flexural Modulus	ISO 178	Secant: 2900MPa
Flexural Strength (3.5 %)	ISO 178	40MPa
Thermal		
HDT B (0.45 MPa) Unannealed	ISO 75B-1, -2	120°C

HDT A (1.80 MPa) Unannealed	ISO 75A-1, -2	75°C
--	---------------	------

PP Hostacom G3 N01

The PP from Basell, is a polypropylene homopolymer plastic material with 30% glass fibre.

Some relevant physical, mechanical and thermal of *PP with 30% of Glass Fibre Hostacom G3 N01* as quoted by General Electric Plastics manufacturer, are presented in table 4.

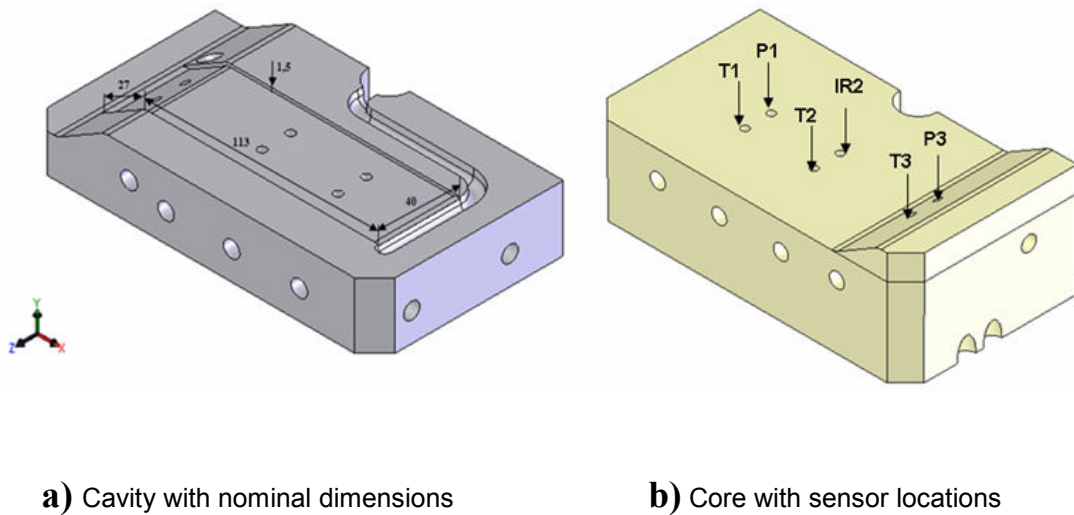
Table 4- Typical properties of PP with 30% of Glass Fibre Hostacom G3 N01

<i>Typical Properties</i>	<i>Method</i>	<i>Value Unit</i>
Physical		
Density	ISO 1183	1,14g/cm ³
Melt Flow Rate (MFR) (230°C/5.0 kg)	ISO 1133	5,7g/10min
Melt Volume Flow Rate (MVR) (230°C/5.0 kg)	ISO 1133	5cm ³ /10min
Melt Flow Rate (MFR) (230°C/2.16 kg)	ISO 1133	1,14g/10min
Melt Volume-Flow Rate (MVR) (230°C/2.16 kg)	ISO 1133	1cm ³ /10min
Mechanical		
Tensile Stress at Break (50 mm/min)	ISO 527-1, -2	85MPa
Tensile Strain at Break (50 mm/min)	ISO 527-1, -2	3%
Flexural Modulus	ISO 178	Secant: 5500MPa
Flexural Strength (3.5 %)	ISO 178	120MPa
Thermal		
HDT B (0.45 MPa) Unannealed	ISO 75B-1, -2	155°C
HDT A (1.80 MPa) Unannealed	ISO 75A-1, -2	140°C
Vicat Softening Temperature (B50 (50°C/h 50N))	ISO 306	130°C
Vicat Softening Temperature (A50 (50°C/h 10N))	ISO 306	160°C

3.3. Mould

Two mouldings blocks (figure 15) were manufactured and assemble in an existent structure as it can be seen in figure 16. Both inserts have straight cooling channels and the main difference is the layout of the cooling channels. In the design of the block

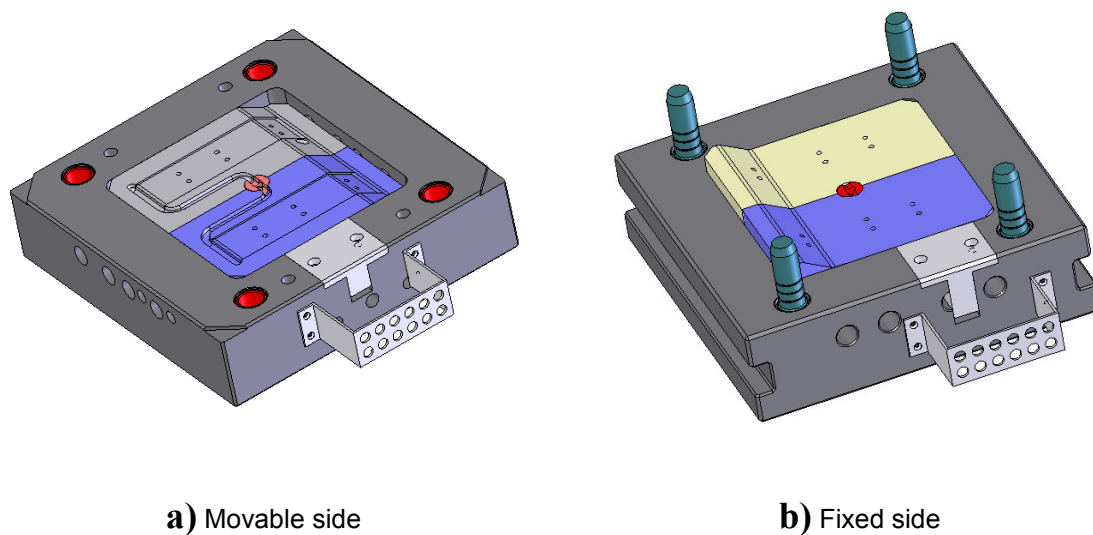
mouldings was considered 24 places capable to locate the sensors. However in this study it was decided to use one of the pair of mouldings blocks and to locate the sensors as indicated in the figure 15. The core contains two pressure sensors (P1 and P2), three thermocouples (T1, T2, T3) and one Infrared sensor (IR2)



a) Cavity with nominal dimensions

b) Core with sensor locations

Figure 15- Moulding blocks



a) Movable side

b) Fixed side

Figure 16- Mould structure

3.3.1. Cooling channels layout optimization

The layout of the cooling channels was optimized by researchers of Ecole des Mines d'Albi (in scope of Eurotooling project) using a home made code that uses boundary element method. [68]

Part quality and cycle time during injection moulding depend on heat transfer within the mould and the polymer part. Numerical simulation methods are widely used as a help to mould cooling conception. [68] The objective was to minimize the average temperature and the difference of temperature at the surface of the cavity. The optimization of the cooling channels positions, have a great importance on the final results since the study is based on shrinkage and warpage behaviour. Through the figure 17 could be seen the decrease of the temperature difference (about 4°C) after the optimization.

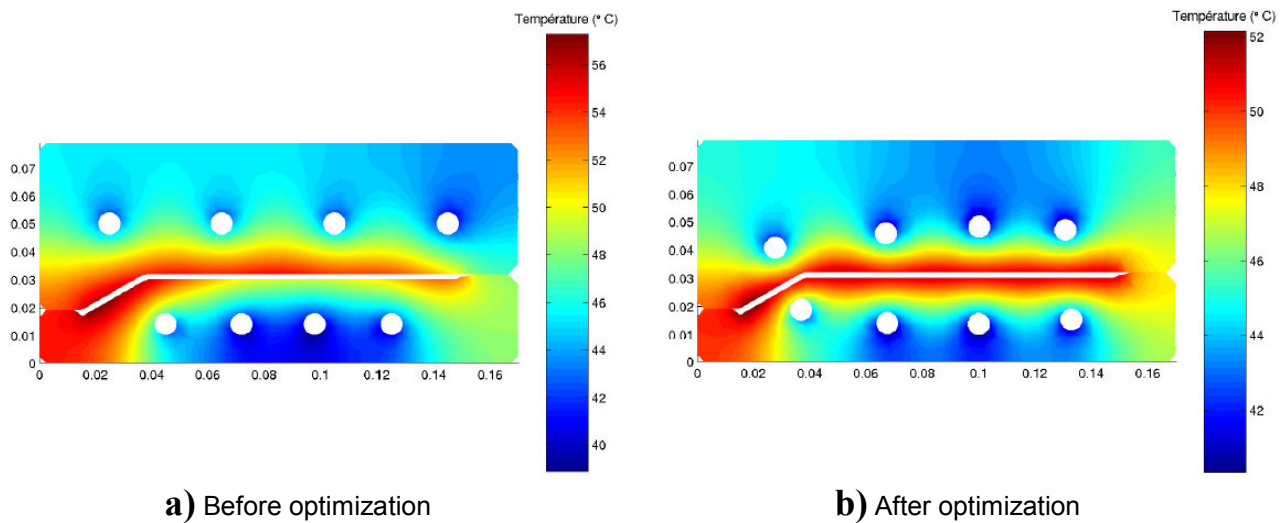


Figure 17- Optimization results

3.4. Acquisition system and sensors

The cavity pressure and temperature measurements, during the cycle time were done through the data acquisition system, Priamus Toll Box. The system contains two portable measuring units, to connect 6 pressure and 4 temperature sensors. The objective is to acquire the pressure and temperature evolutions in different processing cycles. These curves are like a finger impression representing a specific processing parameters.

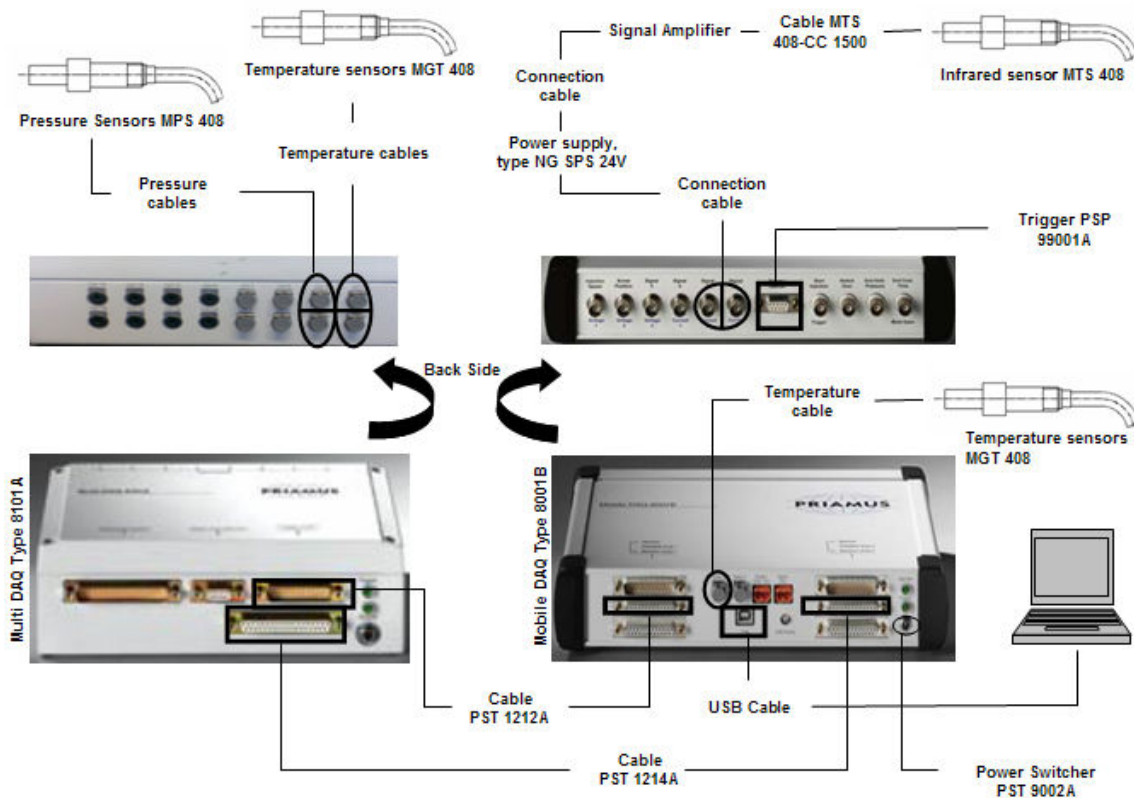


Figure 18- Acquisition System

In this work were used (figure 18):

- Two piezoelectric quartz pressure sensor (MPS 408) with standard dimensions and unified sensitivity, usually the output for this kind of sensors is 9.4 pC/bar;
- Three standard thermocouple (MGT 408) with 2 measuring spots to detect the temperature gradient in the wall of the mould. It's a sensor very useful to detect problems with the temperature control of the mould in production and development, the output for this kind of sensors, type K (Ni-Cr-Type) is $42\mu\text{V}/^\circ\text{C}$ around 100°C and $43\mu\text{V}/^\circ\text{C}$ around 500°C ;
- One Infrared temperature sensor (MTS 408) with short response time, of about 15msec. It is a sensor able to measure the melt temperature in the cavity and the direct measurement of the cooling-down of the plastic part being moulded. The IR-output is $25\text{ mV}/^\circ\text{C}$.

3.5. Injection moulding machine

The injection machine used to obtain the moulded parts is an Engel 200/45 with clamping force of 45 tones, screw diameter of 30mm that makes possible the use of 162MPa (Maximum Injection pressure).



Figure 19- Injection moulding machine

3.6. Processing conditions

The processing conditions were held as constant as possible with the only change of holding pressure and mould temperature in each material. The experimental processing conditions can be found in table 5.

Table.5- Experimental processing conditions

	PC	PP	PP20%	PP30%
Inject. Temp. (°C)	300	180	250	250
Mould Temp. (°C)	80	25, 40	25, 40	25, 40
Holding Pressure (MPa)	[7-51]	[7-51]	[7-36]	[7-94]
Holding time (s)	10	10	10	10
Cooling time (s)	15	12	12	12
Injection Speed (mm/s)	50	70	50	50
Injection Flow Rate (cm³/s)	35	50	35	35

3.7. Shrinkage and warpage measurements procedure

3.7.1. Thickness and width shrinkage

For each process condition the dimensions of three consecutive parts were measured. The parts were kept in a room with constant temperature of $\pm 23^{\circ}\text{C}$, and the measurements were made approximately 24 hours after ejection.

The Width and Thickness dimensions were measured in sensors position 1 (near gate), 2 (Middle of Fill) and 3 (End of Fill) with a digital calliper (precision $\pm 1 \mu\text{m}$) and a micrometer (precision $\pm 1 \mu\text{m}$) respectively.

Shrinkage was calculated as $(L_0 - L)/L_0$ where L_0 is the original dimension of the mould, and L is the dimension of the sample. The shrinkage was statistically characterised by average and standard deviation.

3.7.2. Angle deformation

3.7.2.1. Experimental methodology

Through the process of Reverse Engineering, it is possible to extract the digital shape of any physical object and use that data to, troubleshoot, reproduce, study, analyze, inspect or use in other downstream applications. This digital data can be delivered in the form of just plain xyz points, also commonly called a point cloud.

The strategy used to study the experimental angle deformation was consisted in a 3D Scanning, reproducing the critical angular zone in different positions 6, 16, 26 and 35mm as it can be seen on figure 20. The aim is to convert the physic model in virtual model.

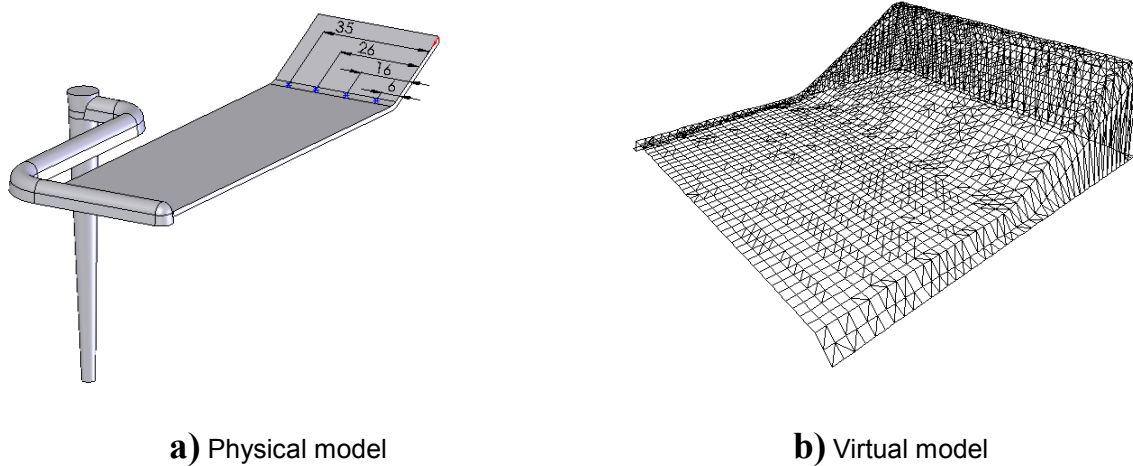
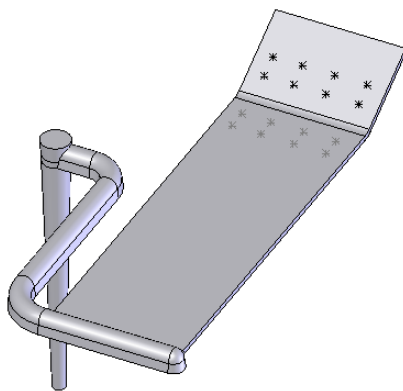


Figure 20- Experimental angle deformation

The basic steps were:

1- Sixteen coordinates of points in total were taken through the virtual model (figure 20b), near of specific points (6, 16, 26 and 35mm) for all processing conditions;



$$P_i = (x_i, y_i, z_i)$$

$$i = 1, \dots, 16$$

Figure 21- Measure points

2- Straight lines were created with the specified points;

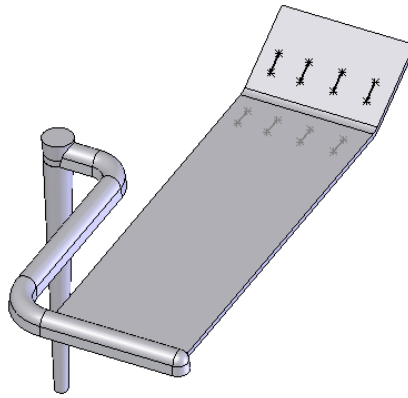


Figure 22- Lines for the angle measurements

The equation of the lines is obtained by the following equation :

$$\frac{y - y_2}{x - x_2} = \frac{y_1 - y_2}{x_1 - x_2}$$

3- With the lines slopes, the respective angles were calculated;

$$\alpha = \left(\frac{m_1 - m_0}{1 + m_0 m_1} \right) \quad \alpha_{1\dots 4} = 180 + \alpha$$

with :

$$m = \frac{y_1 - y_0}{x_1 - x_0}$$

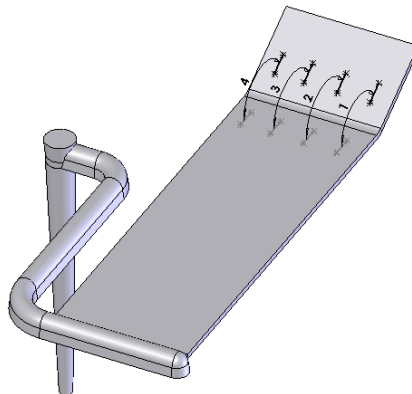


Figure 23- Angles (1 to 4) to measure

4- The difference between the angular measurements of the cavity insert and the parts will give the angle deformation.

3.7.2.1. Simulation methodology

In a perfect world, an analysis of the part including; flow, cooling, and warp are done in the design stage before the tool is built. Practically this does not always happen, and even if it does, the tool and process settings used in production are not the same as what was analysed. It is necessary to validate all the parameters as possible and adjustment to the analysis model and process settings to be the same between MPI and production.

The experimental results were compared with predictions made by commercial software as Moldflow.

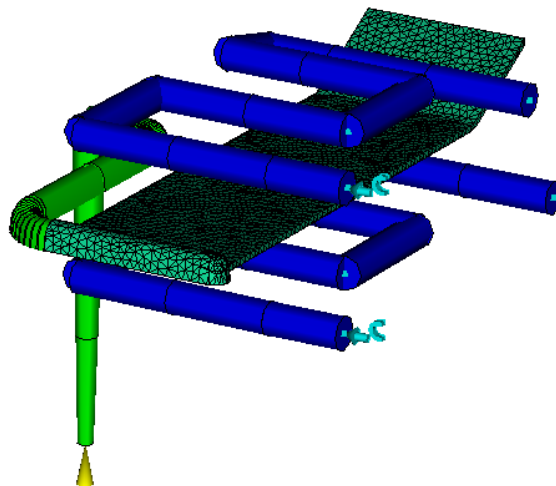
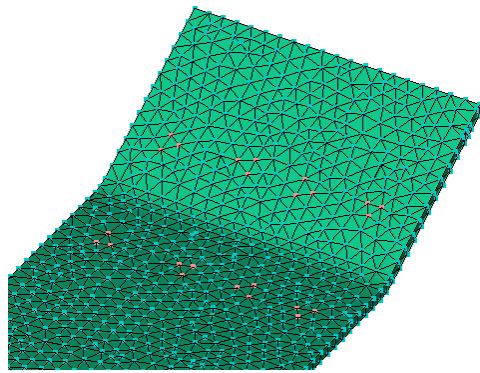


Figure 24- Mesh model

The basic steps were:

1- Twenty four coordinates in total were taken through the Moldflow model (figure 21b), near of specific points (6, 16, 26 and 35mm), before part deformation and after part deformation, for all processing conditions;



a)

$$P_i = (x_i, y_i, z_i)$$

$$i = 1, \dots, 24$$

b)

Figure 25- Coordinates: **a)** On Moldflow model (before and after deformation) **b)** Equation

2- Eight planes were created with the specified points;

$$Ax + By + Cz + D = 0$$

in which :

$$\vec{n} = (A, B, C) \text{ vector normal to the plane}$$

D gives the perpendicular distance from the origin to the plane

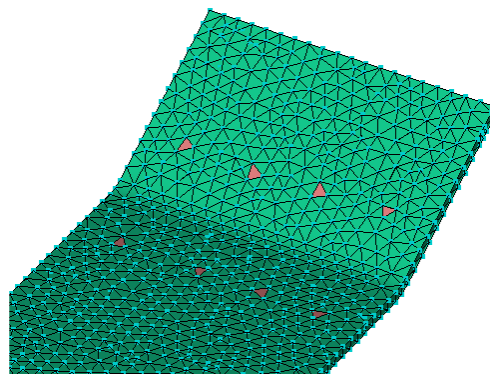


Figure 26- Planes on Moldflow model (before and after deformation)

3- The respective angles between planes were calculated;

The sharp angle between to planes is the sharp angle between the normal directions of the planes

$$\cos \theta = \frac{n_1 \times n_2}{|n_1 \times n_2|}$$

n_1 and n_2 are normal vectors

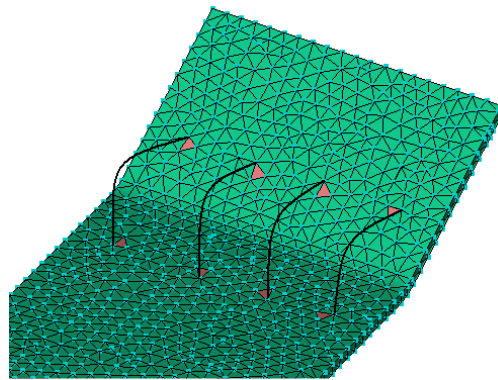


Figure 27- Angles between planes on Moldflow model (before and after deformation)

4- The difference between the angular measurements before deformation and the angular measurements after deformation of the models will give the angle deformation.

3.7.4. Fibre orientation

The polypropylene reinforced with 20% of Glass Fibre, were used to assess the fibre orientation. One moulding for each process conditions of holding pressure of 7 and 36MPa with mould temperature at 25°C was selected. The mouldings were cut in two positions along the flow path 30mm (LA1/LA2), and 120mm (LC1/LC2) from the gate, as demonstrated through figure 28.

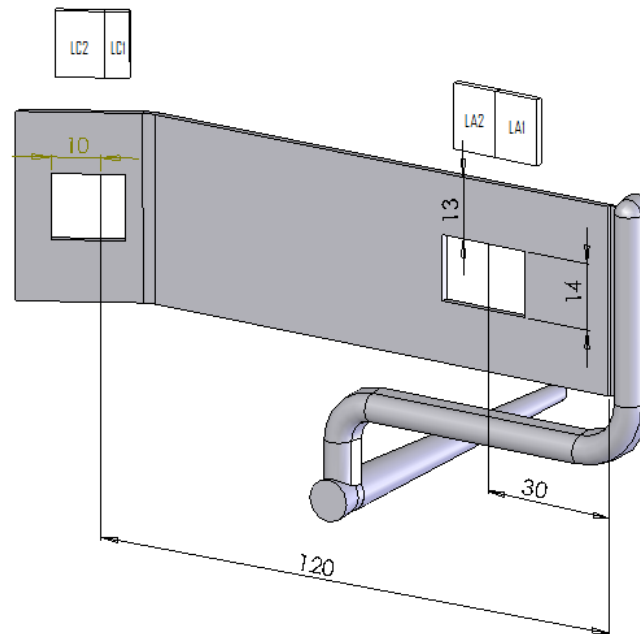


Figure 28- Positions of the Specimens used to study the fibre orientation

The cross sections were cut on the plane perpendicular to the surface of the plate in the flow direction. The preparation of the specimens consisted in putting the specimens in a resin mould to facilitate the handling during the polishing step (figure 29). Then, polish the top surface using a sequence of abrasives with progressively decreasing grind sizes (500, 1000, 2400, 4000) to obtain a uniform planar surface.

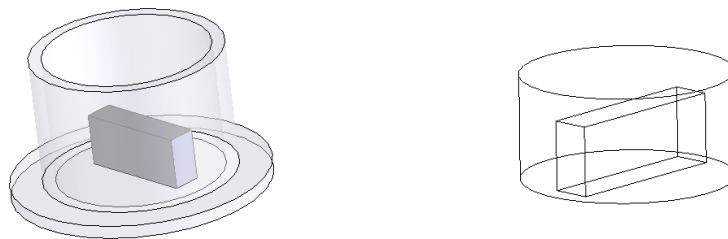
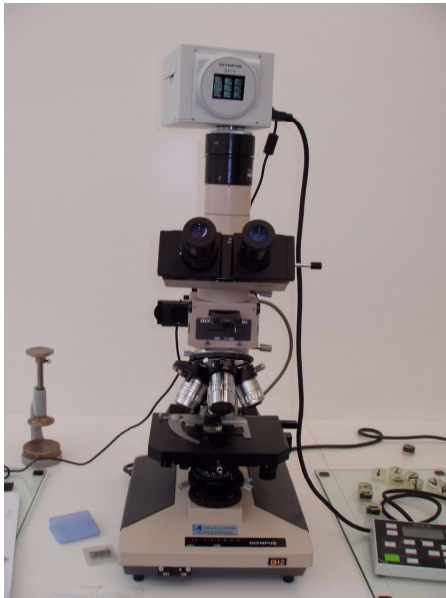


Figure 29- Specimens for polishing

After specimen's preparation, the images were obtained by reflection microscopy and acquire, using the Quantimet 500 program (figure 30).



a) OLYMPUS BH2 reflection microscopy



b) Quantimet 500 program

Figure 30- Equipments

The measurements were made through the thickness in three columns in order to evaluate the sampling error.

The fibre orientation was measured, using the method proposed by Bay and Tucker [69]. In order to determine the state of orientation of the fibres it is necessary to obtain specimens from representative regions of the products with a statistical significance. The measurements were made in 11 layers across thickness. The sections of the fibres will appear in the images (figure 31) as circles, ellipses or rectangles, according to the direction of penetration in the matrix.

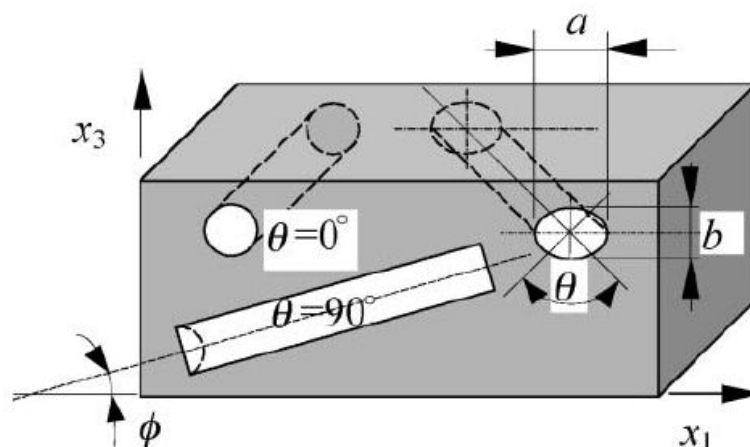


Figure 31- Possible forms of fibre sections in a polishing surface: ϕ is the out of orientation angle [70].

From the geometry and alignment of those entities it is possible to calculate the distribution of fibre orientation in terms of the in-sectioning-plane angle, ϕ and out-of-sectioning-plane angle, θ [70, 71]. The out of plane orientation angle, θ , is derived from the major and minor axes of the ellipse, a and b , as

$$\theta = \arccos \left(\frac{b}{a} \right)$$

The in-plane orientation is determined by the angles defined by the major axis of the ellipse and the pre-selected reference axes (figure 31) [70]. These angles, θ and ϕ , can be determined by digitizing the coordinates of the endpoints of the major and minor axes of the ellipses, either manually or by image analysis tools [70]. The relevant components of the unit vector \mathbf{p} for the calculation of the orientation tensor of the specimens cut in the 1-3 sectioning plane, are

$$p_1 = \sin \theta \cos \phi$$

$$p_2 = \cos \theta$$

$$p_3 = \sin \theta \sin \phi$$

The elements of the second-order tensors that describe the fibre orientation can be calculated from the values of the vectors p_i using

$$\langle a_{ij} \rangle = \frac{\sum_n (p_i)_n (p_j)_n F_n}{\sum_n F_n}$$

The parameter F_n is a weighting function that corrects the bias resulting from the lower probability of the fibre lying parallel to the section plane appear in the image [70].

4. Experimental results and discussion

4.1. Cavity pressure evolution

For the efficient measurement of mould cavity pressure, moulds must be equipped with sensors. The mould cavity pressure is generally recognized to be a meaningful indicator of the quality of the moulding and stability of the process. The freezing of gates or parts of the mould, which prevents the holding pressure to fill critical sections, can be detected by measuring this pressure.

The pressure evolution during the injection process is presented in this chapter. The cavity pressure evolution was obtained, to provide more information about the influence of the pressure on part shrinkage.

4.1.1. Pressure evolution for PC

The recorded Pressure evolution curves for PC with different Holding Pressures for P1 and P3 are shown in **figure 32**.

It can be seen that the cavity pressure is zero from the closing of the mould until the material reach the sensor P1 (**figure 32a**) and sensor P3 (**figure 32b**). It can be notice that, for holding pressure smaller than 22MPa, the pressure in the mould cavity, reach zero between 3 and 4 s. At this time, the thickness shrinkage starts and the moulding detach from the impression wall. For higher holding pressures the cavity pressure tend to reach a residual, non-zero value, since the over packing of the polymer at the moment of the gate freeze-off is so high that thermal contraction due to cooling is not able to offset the pressure effect and the moulding remains in contact with the wall impression.

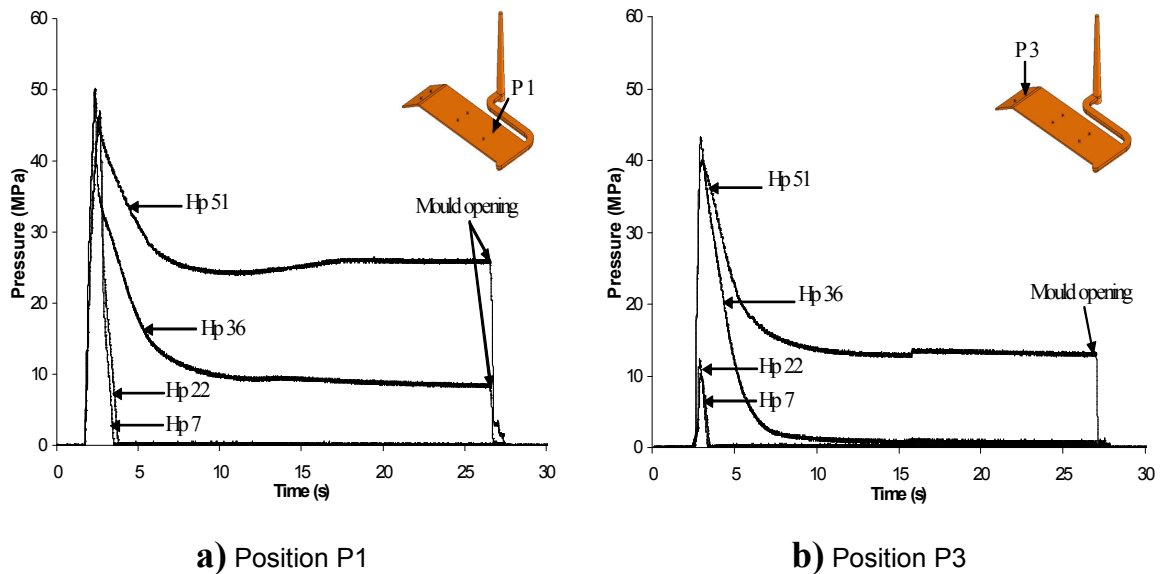


Figure 32– Influence of the Holding Pressure on pressure evolution curves in PC parts. Mouldings with Holding Pressure of 7, 22, 36 and 51MPa and Mould Temperature at 80°C

4.1.2. Pressure evolution for PP

The recorded Pressure evolution curves for PP with different Holding Pressures (7, 22, 36 and 51MPa) for P1 and P3 are shown in **figure 33 and 34**.

Experimental pressure curves of PP, with increasing holding pressures and mould temperatures, are depicted. As it can be seen, low holding pressures causes a sudden drop in cavity pressures and become zero earlier (onset of thickness shrinkage). In contrast with PC samples showed on **figure 32**, no residual pressures are show in this case. This signifies, that the material wasn't highly packed, inside the impression at the instance of the gate solidification. From **figures 33 and 34** it can be observed that the increase of the mould temperature has a small increase on the maximum cavity pressure.

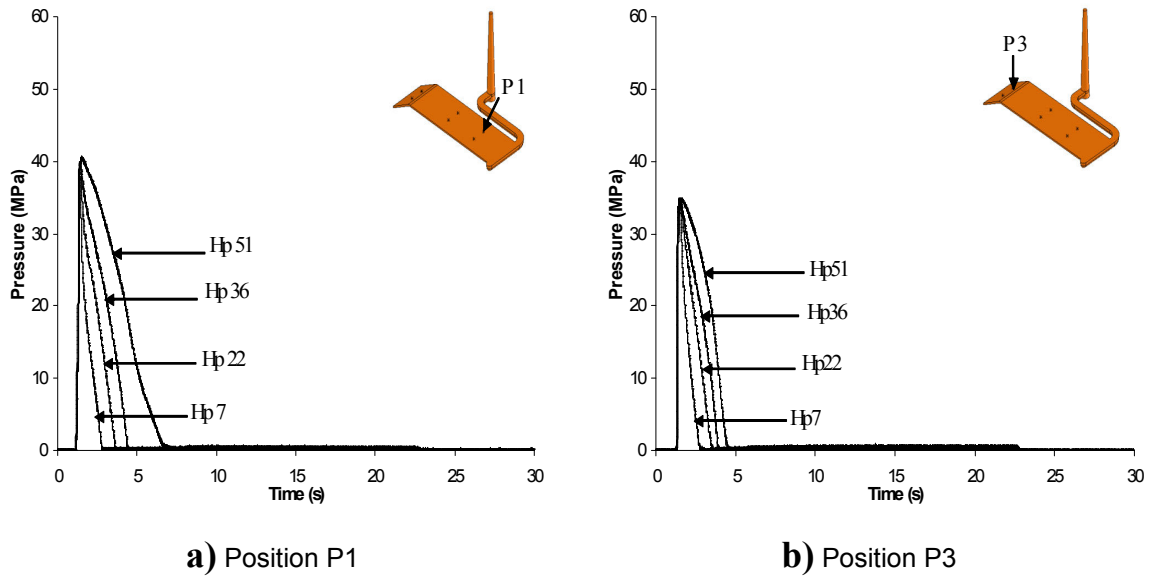


Figure 33– Influence of the holding pressure on the pressure evolution curves in PP parts. Mouldings with Holding Pressure of 7, 22, 36 and 51MPa with Mould Temperature at 25°C

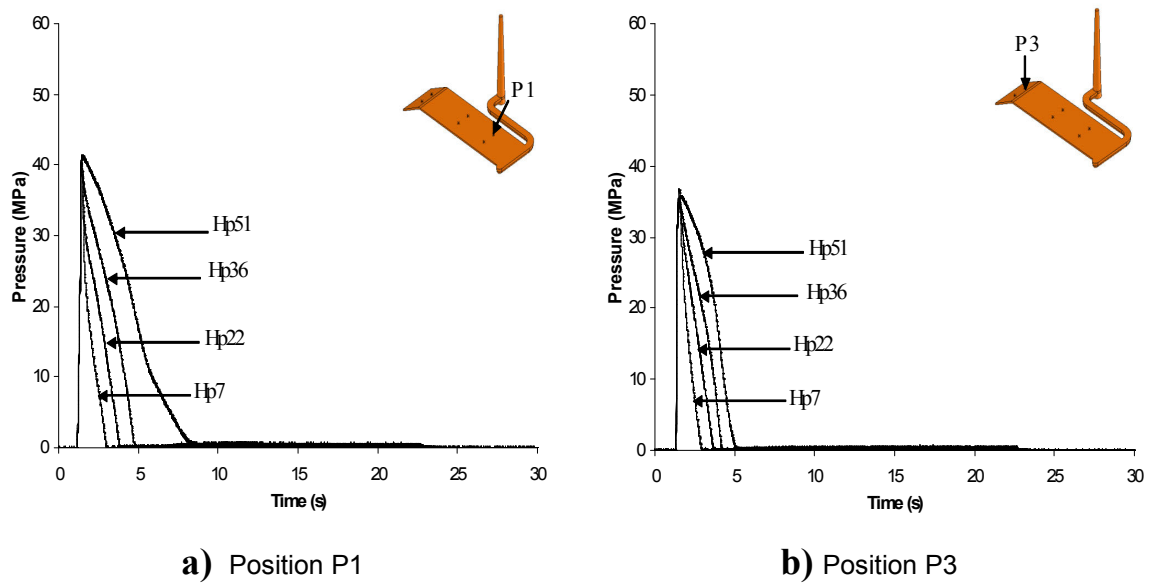


Figure 34– Influence of the holding pressure on the pressure evolution curves in PP parts. Mouldings with Holding Pressure of 7, 22, 36 and 51MPa with Mould Temperature at 40°C

4.1.3. Pressure evolution for reinforced PP

The recorded Pressure evolution curves for PP with different fibre weight fraction with Holding Pressures of 36MPa in positions P1 and P3 for Mould Temperatures of 25 and 40°C, are shown in **figures 35** and **36**, respectively.

It can be observed that the pressure in the cavity decreases with the increase of fibre weight fraction. This behaviour is expected since the incorporation of the fibres increase the viscosity inducing more difficulties on the flow during packing phase. It was also notice, that the Mould Temperature is a process parameter with a small influence on pressure curves.

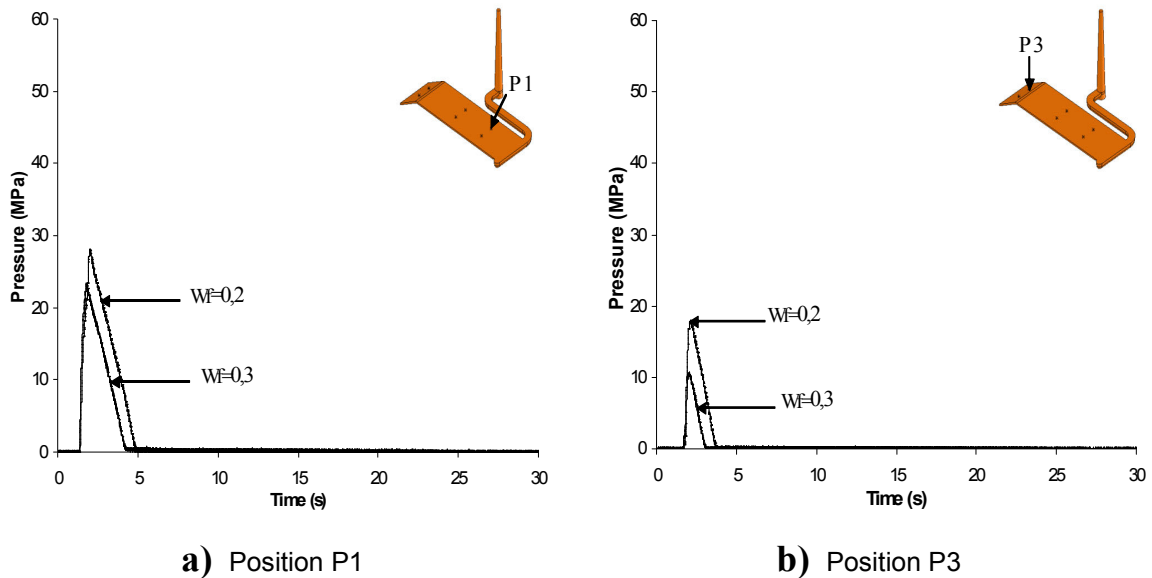


Figure 35– Effect of fibre weight fraction (0,2; 0,3) on the pressure evolution curves. PP mouldings with Holding Pressure of 36MPa with Mould Temperature at 25°C

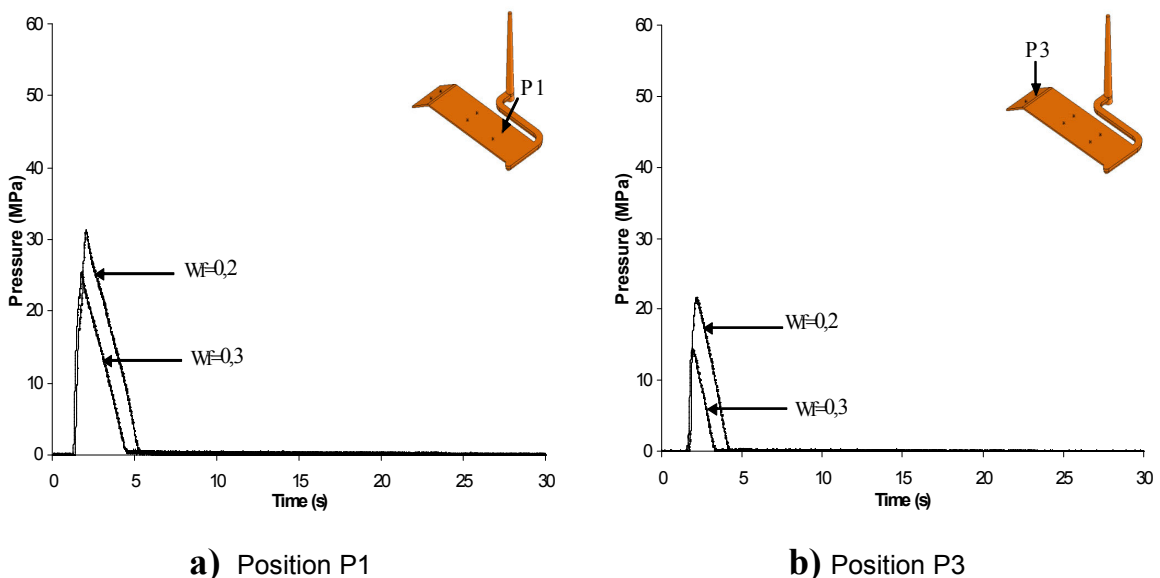


Figure 36– Effect of fibre weight fraction (0,2, 0,3) on the pressure evolution curves. PP mouldings with Holding Pressure of 36MPa with Mould Temperature at 40°C

4.2. Moulding temperature evolution

Modern injection moulding practice requires the measurement of process variables such as melt and mould temperature in order to produce the highest quality polymer parts. Various sensors have been developed to measure the temperature during processing, and knowledge of those parameters has been used to provide more precise control of the process. It is widely known that the viscosity of the melt affects all the processing parameters in plastic injection moulding. The control of melt temperature is considered the most critical factor in injection moulding due to its direct effect on polymer melt viscosity.

The temperature evolution along time in three positions (T1- Temperature sensor located Near Gate, T2- Temperature sensor located Middle of Fill, T3- Temperature sensor located End of Fill and a IR2- Infrared sensor located Middle of Fill) for different materials is presented in this chapter.

4.2.1. Temperature evolution for PC

A plot of the evolution of the surface temperature T1, T2, T3 and IR2 at the cavity along flow path for PC with different Holding Pressures are shown in **figure 37** and **38**.

For the recorded temperature curves obtained, two levels of holding pressure were selected. The surface temperature of the cavity for holding pressure of 7MPa and 51MPa, are close up to 2,5s and then have a sharp decrease becoming equal to the mould temperature (around 80°C). The location of the sensor on **figure 38b**, corresponding to T3, is farther away from the gate and can be notice that the peak of temperature is less than in the others position of sensors (T1 and T2). This expected result is due to the fact that the flow front of the melt does not conserve its initially high temperature. Through the analysis of **figure 32**, can be observed that for the condition of holding pressure of 7MPa the pressure evolution drop around 4s, and the part begins to shrink on thickness direction creating a air gap between the polymer – mould interface. Usually, the air gap leads to an increase of the temperature but in this material (PC), thickness shrinkage is lower relatively to PP material. This effect could be observed on **figure 53**, and as a consequence the air gap produced should be small and the heat is still being conducted. Although in the same figure for condition of holding pressure of 51MPa the pressure tend to reach a residual, non-zero value,

consequently the polymer remains in contact with the wall impression. This effect could be explained observing **figure 53**, whose thickness shrinkage is -7% indicating that the polymer suffered an expansion through that direction.

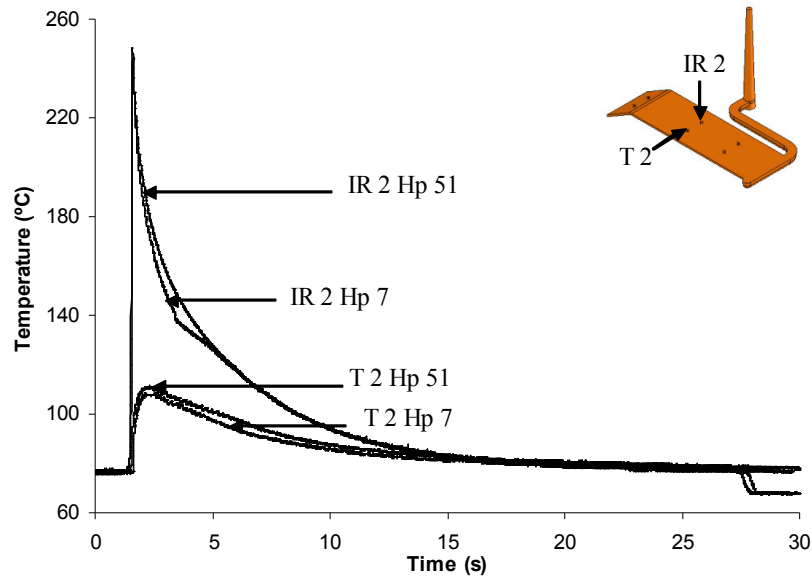


Figure 37– Influence of the holding pressure on the Temperature evolution at the middle of fill in PC parts. Mouldings with Holding Pressure of 7 and 51MPa and Mould Temperature at 80°C

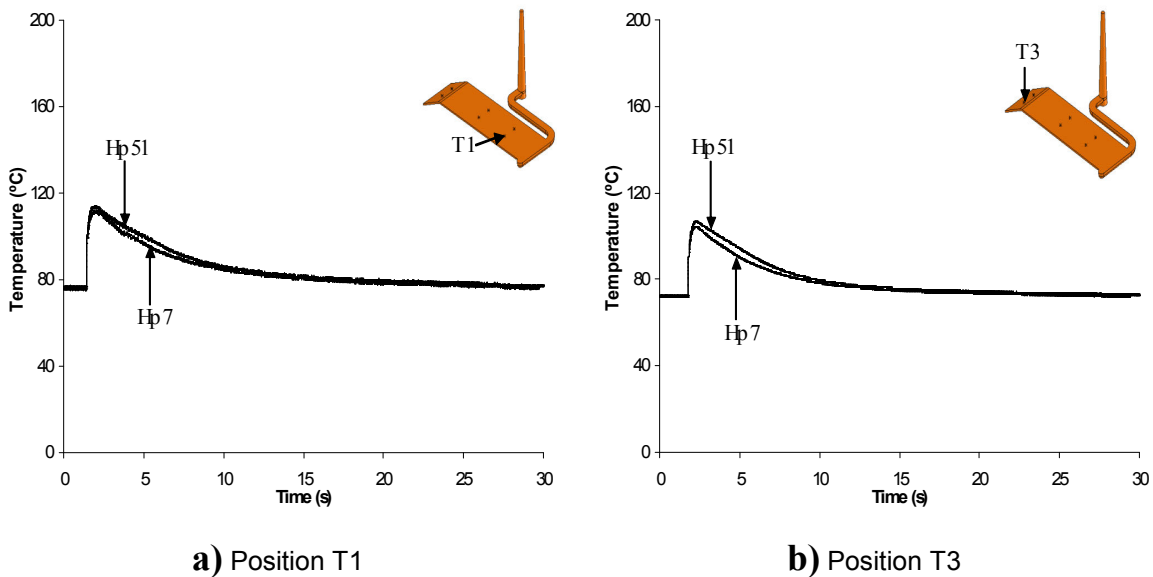


Figure 38– Influence of the holding pressure on the Temperature evolution curves in PC parts. Mouldings with Holding Pressure of 7 and 51MPa and Mould Temperature at 80°C

4.2.2. Temperature evolution for PP

The recorded Temperature curves, for PP with different Holding Pressures are shown in **figure 39 to 42**.

Analysing the infrared curves, for holding pressure of 7MPa after 4s (coincident with minimum pressure value), the temperature slightly increase, corresponding to the moment when part detached from the mould surface, and then falls off, and the temperature difference between the part surface and mould wall becomes smaller.

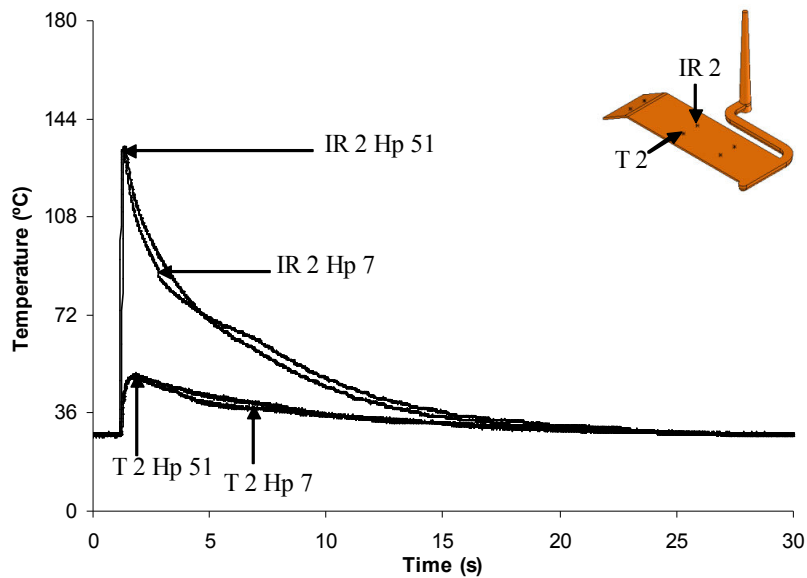
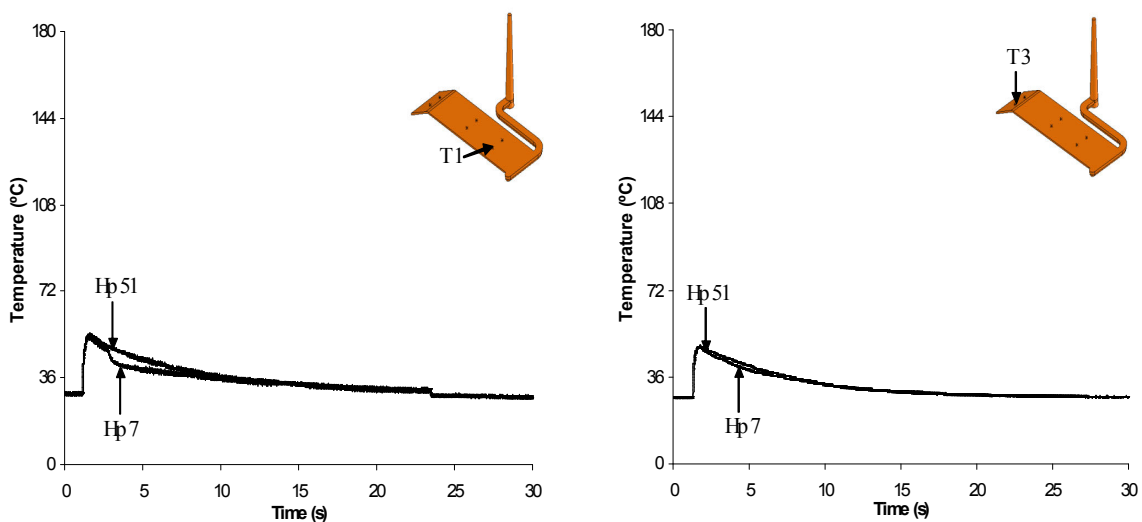


Figure 39– Influence of the holding pressure on the Temperature evolution, at the middle of fill. PP mouldings with Holding Pressure of 7 and 51MPa with Mould Temperature at 25°C

In **figure 40** is show the temperature evolution measure with the thermocouples. It could be observed that the temperature drops rapidly around 3s which is the time that the pressure in the cavity shows its minimum value (figure 33).



a) Position T1

b) Position T3

Figure 40– Influence of the holding pressure on the Temperature evolution. PP mouldings with Holding Pressure of 7 and 51MPa, and with Mould Temperature at 25°C

For a mould temperature of 40°C as show in **figures 41** and **42**, it can be noticed that no influence on temperature evolution is show in comparison with the temperature evolution obtain with mould temperature of 25°C (**figure 39** and **40**)

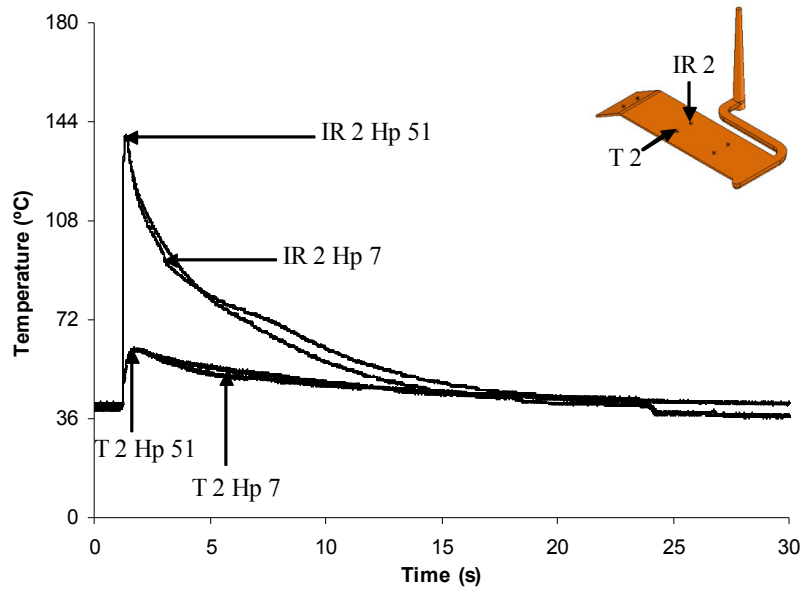


Figure 41– Influence of the holding pressure on the Temperature evolution at middle of fill. PP mouldings with Holding Pressure of 7 and 51MPa with Mould Temperature at 40°C

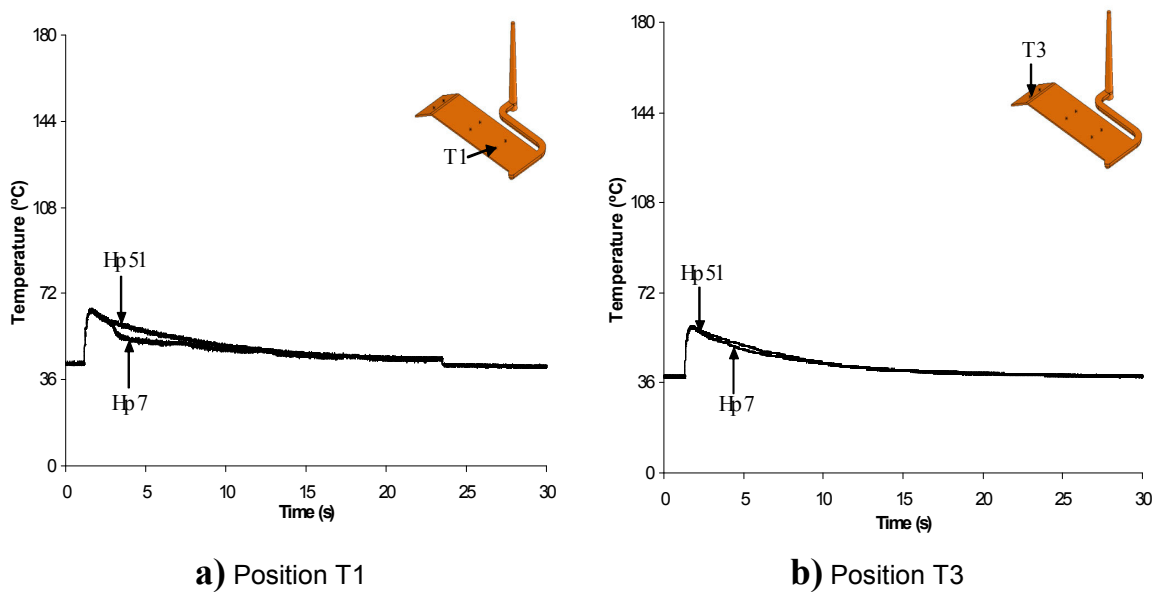


Figure 42– Influence of the holding pressure on the Temperature evolution curves in PP parts. Mouldings with Holding Pressure of 7 and 51MPa with Mould Temperature at 40°C

4.2.3. Temperature evolution for PP20%

A plot of the evolution, of the surface temperature T1, T2, T3 and IR2 at the core along flow path for PP20% with different Holding Pressures (7, 36MPa) are shown in **figure**

43 to 46. As could be observed the maximum temperature value is approximately 180°C. This observation reflects the increase of the injection temperature used to process PP with 20% GF. Also could be seen that the incorporation of Glass Fibres doesn't attenuates the effect of the holding pressure on the temperature evolution.

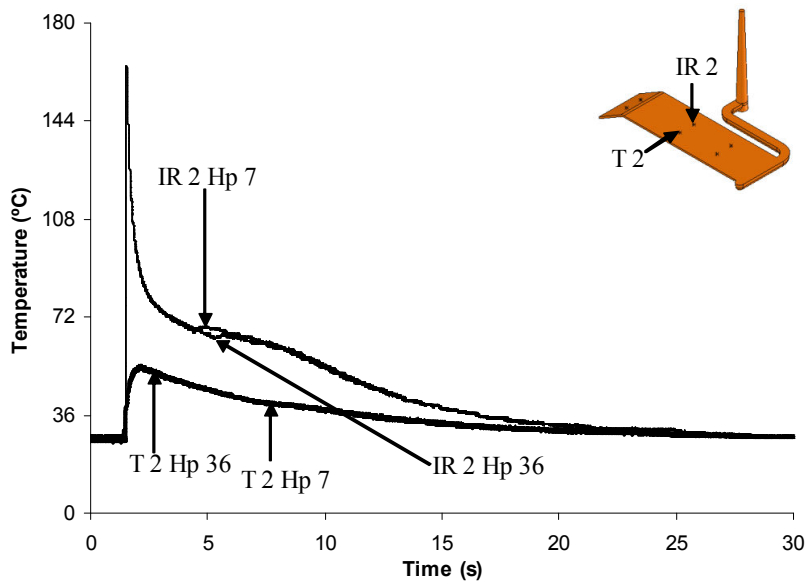


Figure 43– Influence of the holding pressure on the Temperature evolution at middle of fill. PP with 20% GF mouldings with Holding Pressure of 7 and 51MPa with Mould Temperature at 25°C

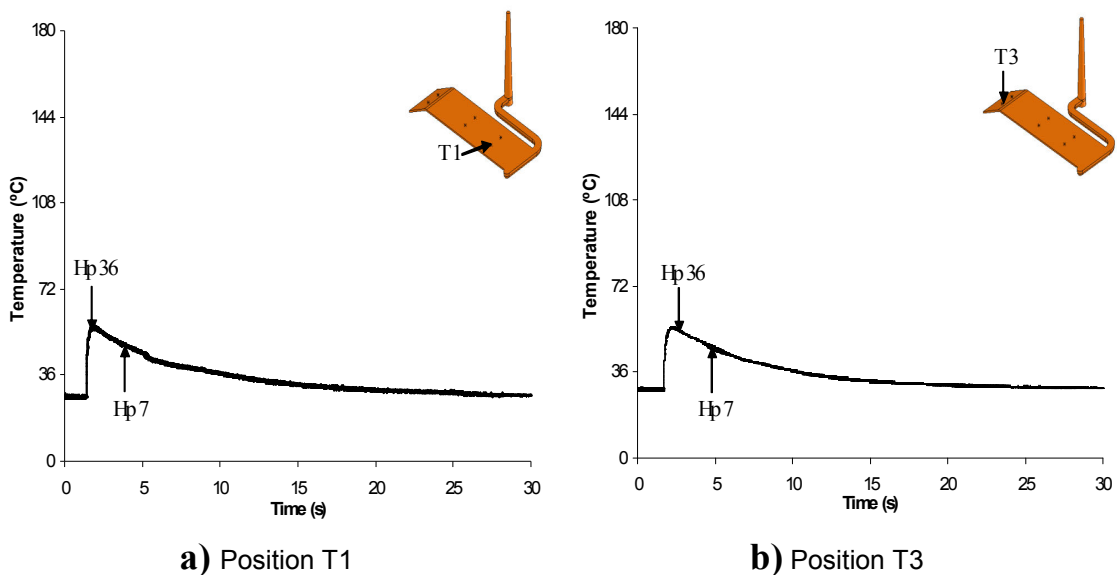


Figure 44– Influence of the holding pressure on the Temperature evolution curves in PP20%GF parts. Mouldings with Holding Pressure of 7 and 51MPa with Mould Temperature at 25°C

As could be seen in **figure 45**, the IR sensor is more sensible to the temperature evolution during the cooling that the thermocouple sensors. Infrared sensors measure temperature from a distance by detecting the amount of thermal electromagnetic radiation emitted from the object being measured. This is one advantage, since it is possible to measure the temperature after part detachment. This effect can be clearly observed through the slightly increase on the temperature curve after 4s of the injection. This separation is more evident on the temperature curve that corresponds to holding pressure of 7MPa, resulting from the thickness shrinkage that is obviously higher for low holding pressures. This behaviour affects the cooling progress and the time of the detachment is delayed. The IR sensors, give us additional information that is not possible with the contact sensors, as the moment when the part detach from the mould walls.

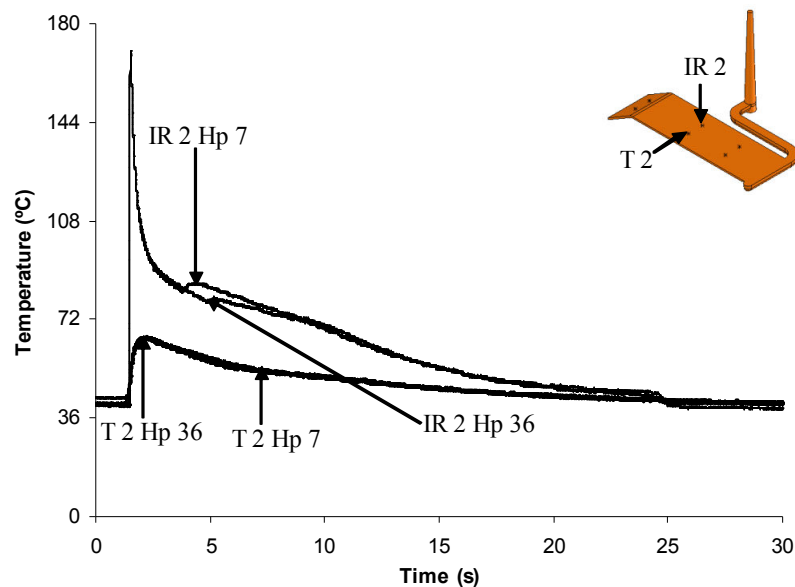


Figure 45– Influence of the holding pressure on the Temperature evolution at middle of fill. PP with 20% GF mouldings with Holding Pressure of 7 and 51MPa with Mould Temperature at 40°C

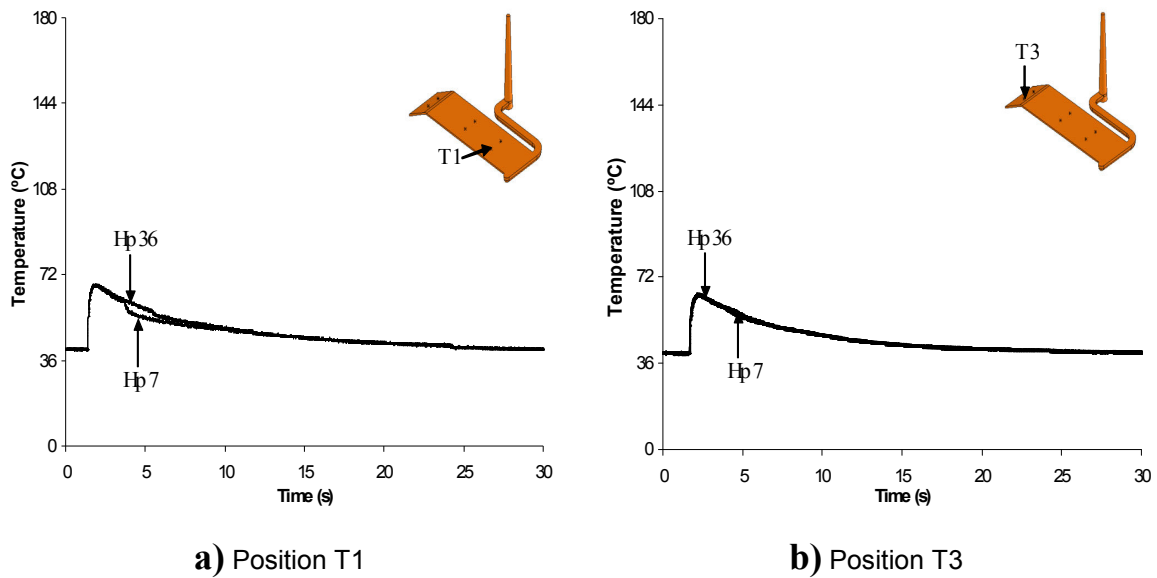


Figure 46– Influence of the holding pressure on the Temperature evolution curves in PP20%GF parts. Mouldings with Holding Pressure of 7 and 51MPa with Mould Temperature at 40°C

4.2.4. Temperature evolution for PP30%

A plot of the evolution of the surface temperature T1, T2, T3 and IR2 at the core along flow path for PP30% with different Holding Pressures (7 and 94MPa) for mould temperature of 25°C are shown in **figure 47** and **48**.

When the fibre weight fraction, of the polymer increases, the viscosity also increases. The pressure loss will increase and the pressure level will be reduced. Consequently thickness shrinkage increase and a air gap will be formed. This effect can be seen through the analysis of **figure 47** and **48**, where the detachment of the part is more evident on the temperature curve that corresponds to holding pressure of 7MPa. Comparing these results with **figures 45** and **46**, the separation of the part, starts earlier for temperature curves corresponding to PP30%, around 2, 3s, since for material PP20% was around 4s.

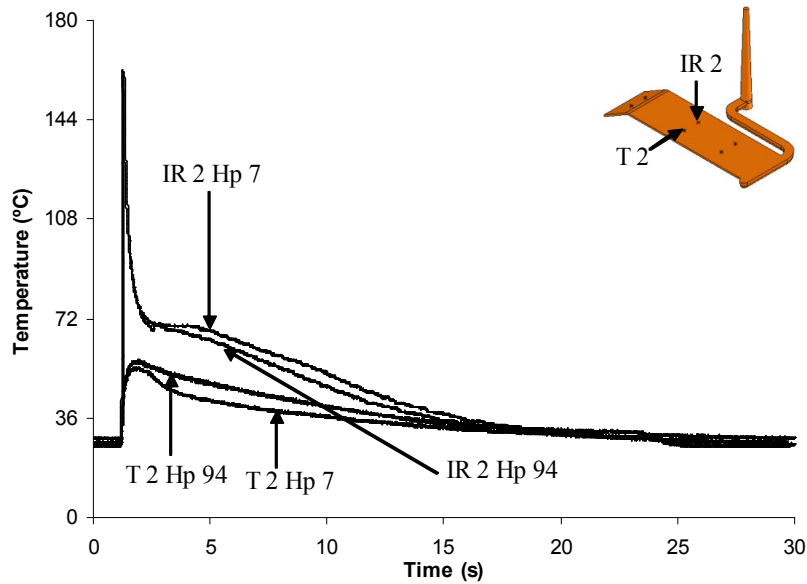


Figure 47– Influence of the holding pressure on the Temperature evolution in the middle of fill. PP with 30% GF mouldings with Holding Pressure of 7 and 94MPa with Mould Temperature at 25°C

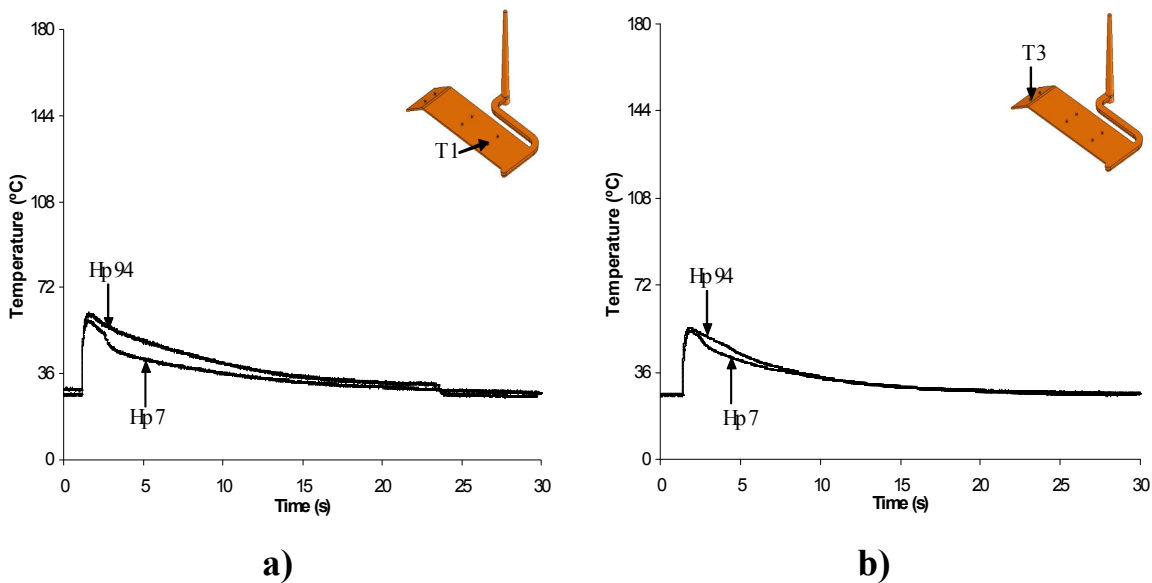


Figure 48– Influence of the holding pressure on the Temperature evolution curves in PP30%GF parts. Mouldings with Holding Pressure of 7 and 94MPa with Mould Temperature at 25°C

The results of temperature evolution along flow path for PP30% with different holding pressures for mould temperature of 40°C are show in **figures 49** and **50**.

When the mould temperature increases, (in this case from 25°C to 40°C), the thickness shrinkage in the mould reduces and a lower air gap is formed. Therefore the mould temperature is an influent parameter on the air gap development during injection moulding. Opposely to the expected, seems that this condition parameter don't have

influence on temperature curves. The time of polymer detach seems to be insensitive to the mould temperature change.

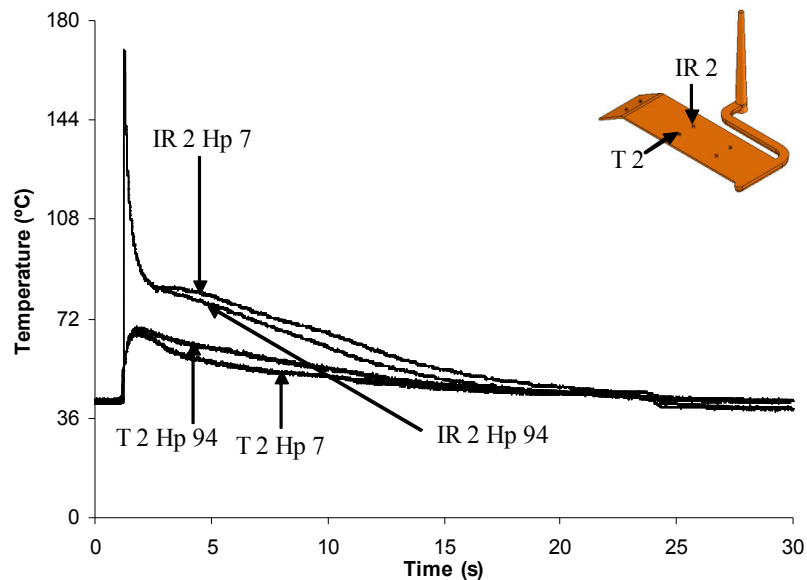


Figure 49– Influence of the holding pressure on the Temperature evolution at the middle of fill. PP with 30% of GF mouldings with Holding Pressure of 7 and 94MPa with Mould Temperature at 40°C

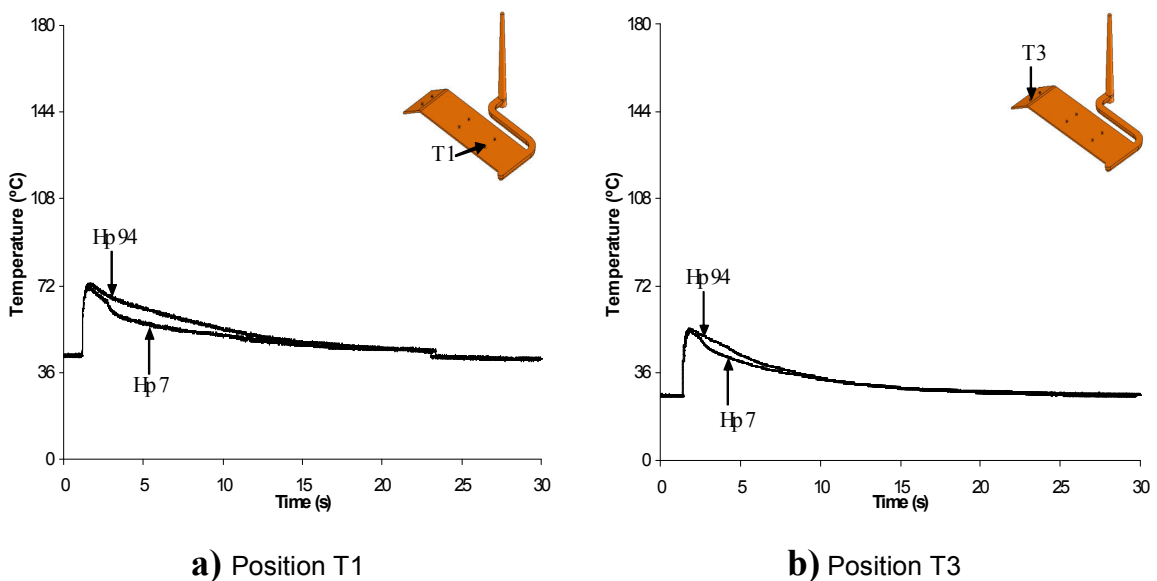


Figure 50– Influence of the holding pressure on the Temperature evolution at middle of fill. PP with 30% GF mouldings with Holding Pressure of 7 and 94MPa with Mould Temperature at 40°C

4.3. As-moulding shrinkage

As-moulded Shrinkage of injection moulded products depends on processing parameters such as Holding Pressure and Mould Temperature. As the melt polymer cools thermal contraction of each solid polymer layer would cause shrinkage.

In this chapter the as-moulding shrinkage was measured in different moulding conditions and analysed to understand the effect of Processing Conditions and the fibre contents.

4.3.1. Unreinforced materials

4.3.1.1. Effect of holding pressure

The results of the as-moulded shrinkage across flow direction, as a function of the holding pressure for PC and PP are shown in **figures 51** and **52**, respectively.

The as-mould Shrinkage across flow direction for PP and PC, increase with the distance to the gate, because of the pressure drop further away from the gate. As it can be seen in **figure 51** and **52**, the as-mould shrinkage also decreases inversely to the pressure applied during the holding phase, having a linear evolution. This effect could be explained since packing becomes more efficient. As show from figures above, semi crystalline PP has the largest mean dimension change and amorphous PC has the lowest shrinkage, as expected.

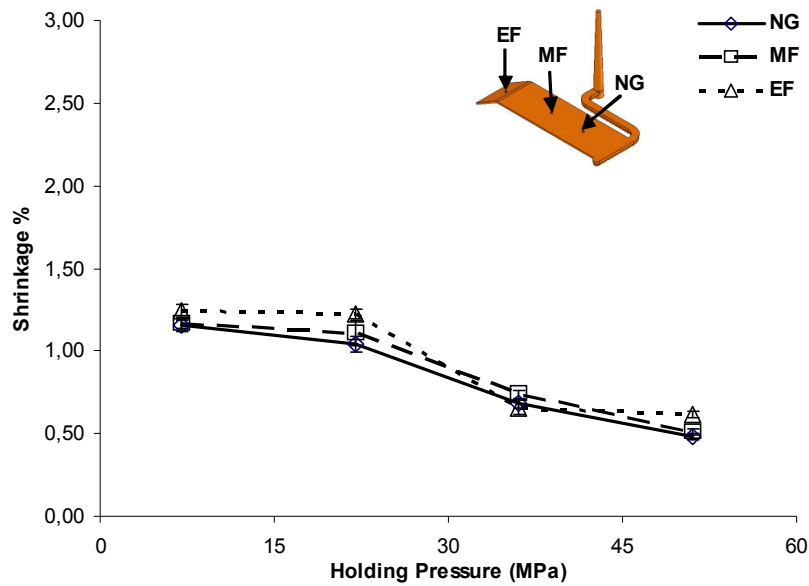


Figure 51– Effect of the Holding Pressure on the as-mould shrinkage across flow direction of PC with Mould Temperature of 80°C.

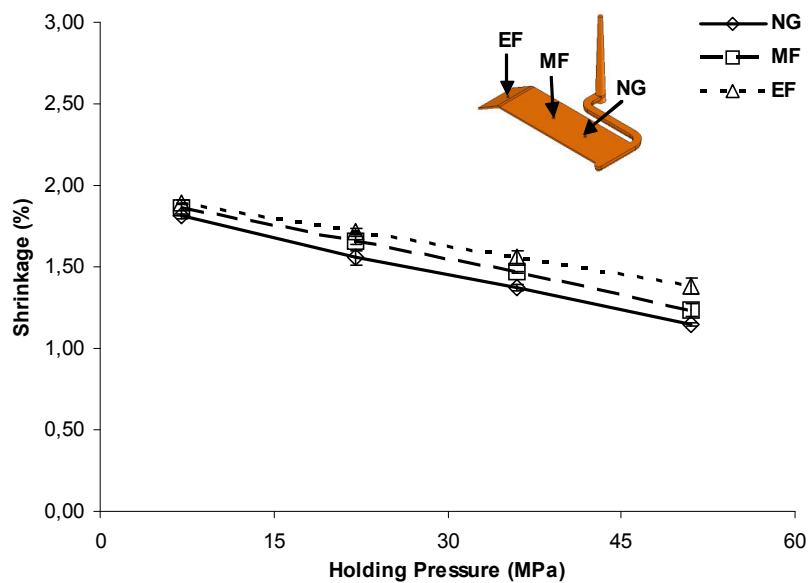


Figure 52– Effect of the Holding Pressure on the as-mould shrinkage across flow direction of PP with Mould Temperature of 25°C.

The results of the as-moulded thickness direction, as a function of the holding pressure for PC and PP are shown in **figures 53** and **54**, respectively.

It can be observed that the as-mould thickness shrinkage for PP decrease with Holding pressure. After a holding pressure of 22MPa, the thickness shrinkage results of both materials turn out to be negative (which means an expansion of the mouldings). This effect is more noticeable on amorphous PC than in the semi crystalline PP. This result

is probably due to the elastic expansion of the compressed polymer material or/and to the mould deformation caused by the injection holding pressure.

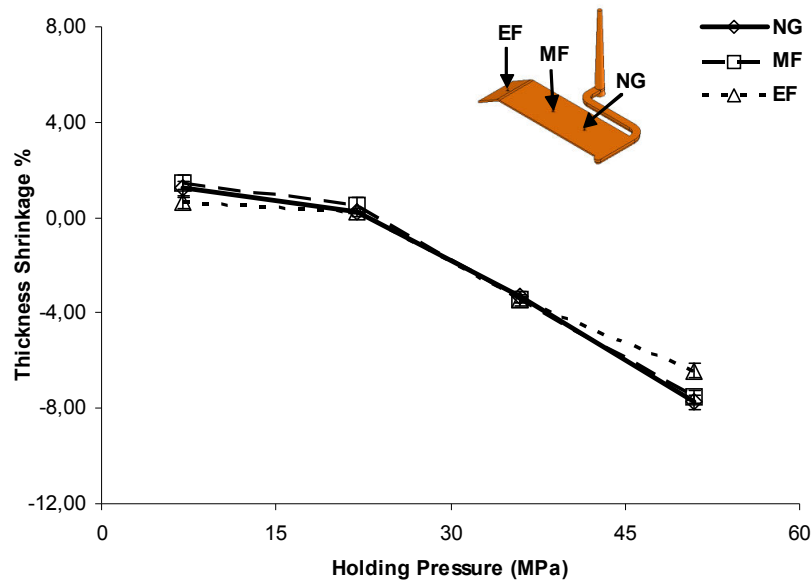


Figure 53– Effect of the Holding Pressure on the as-mould thickness shrinkage of PC with Mould Temperature of 80°C.

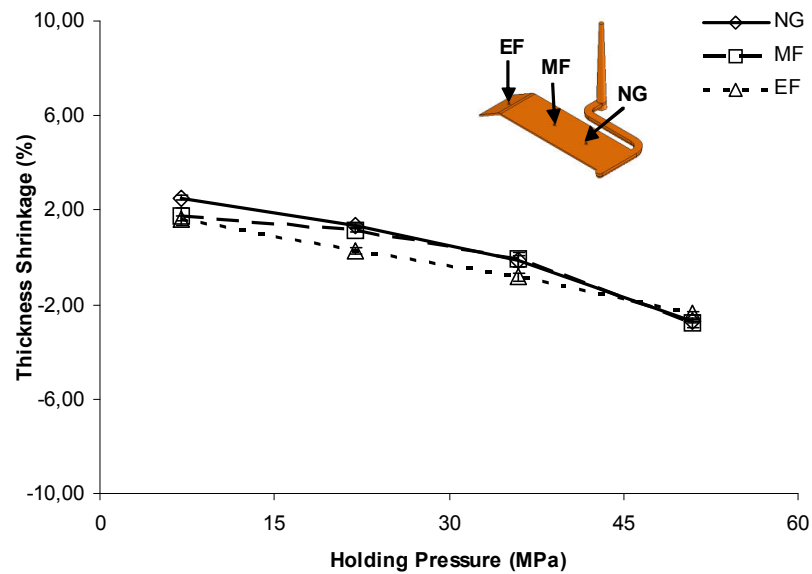


Figure 54– Effect of the Holding Pressure on the as-mould thickness shrinkage of PP with Mould Temperature of 25°C.

4.3.1.2. Effect of mould temperature

The results of the as-moulded shrinkage across flow and thickness direction at **MF**-Middle of Fill, as a function of the holding pressure for PP with Mould Temperatures of 25°C and 40°C, respectively are shown in **figures 55 to 56**.

To assess the effect that the mould temperature has on shrinkage for semi crystalline PP, T_m was varied from 25 to 40°C. Through the analysis of **figure 55**, the as-mould shrinkage across flow direction for both mould temperatures, decreases inversely to the pressure applied during the holding phase. Moreover, the results show that the as-mould shrinkage across flow direction behaviour is similar for the two mould temperatures. Also can be notice from **figure 56** that, for higher mould temperature and holding pressure the thickness shrinkage is negative resulting from the elastic expansion on thickness direction.

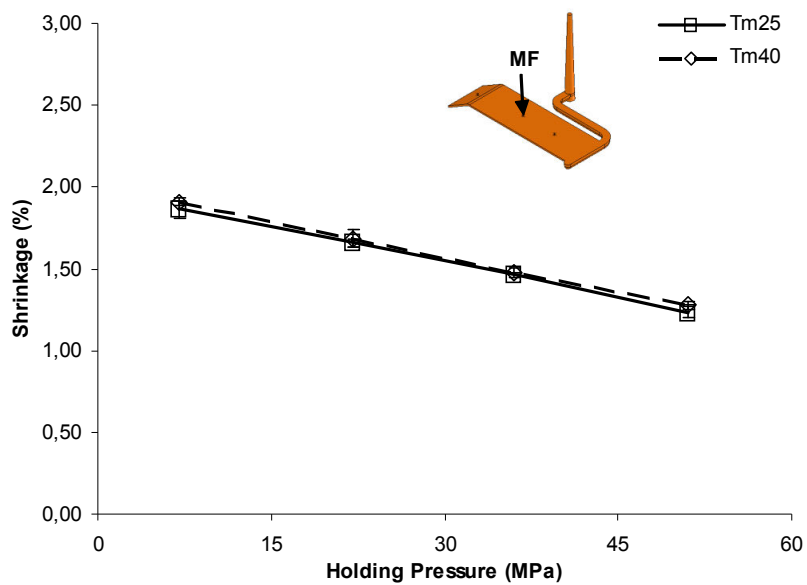


Figure 55– Effect of the Holding Pressure on the as-mould shrinkage across flow direction on MF (Middle of Fill) of PP with Mould Temperature of 25 and 40°C.

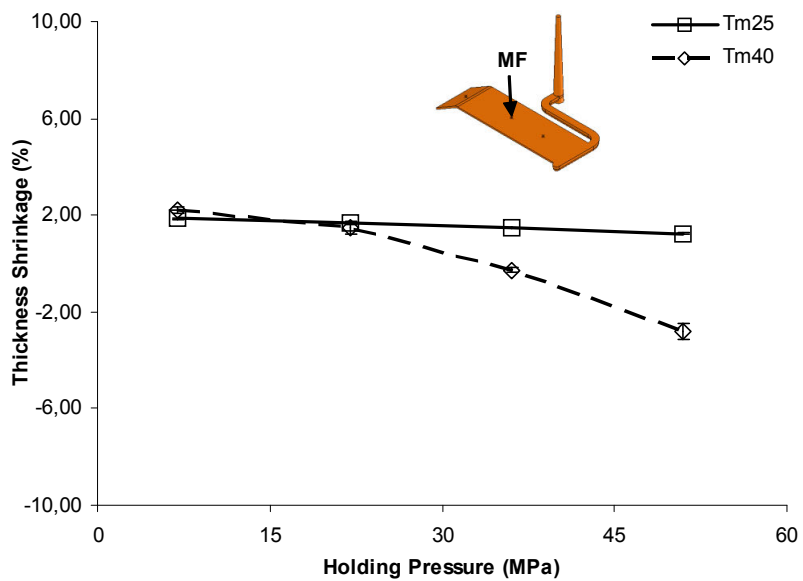


Figure 56– Effect of the Holding Pressure on the as-mould thickness shrinkage of PP with Mould Temperature of 25 and 40°C.

4.3.2. Reinforced materials

4.3.2.1. Effect of holding pressure

The results of the as-moulded shrinkage across flow and thickness direction, as a function of the holding pressure for PP with 20% and 30% of Glass Fibres with Mould Temperature of 25°C, are shown in **figures 57 to 60**.

As can be seen on **figures 57**, for the material with 20% of Glass Fibre, the increase of the holding pressure doesn't affect the shrinkage across the flow. Nevertheless a increase of shrinkage is observed with the distance to the gate that is higher comparing with the PP without fibres (**figure 52**). This behaviour is due to the fact that for PP with 20% of Glass Fibre, the holding pressure doesn't affect significantly the fibre orientation (see **figures 73 and 74**).

Moreover, the effect of holding pressure on shrinkage across flow direction for PP with 30% of Glass Fibre is show in **figure 58**. It can be notice that with the increase of holding pressure the width shrinkage decrease linearly (decrease of about 1,40%). It could also be observed that the part shrink less near gate than in other positions far away from the gate.

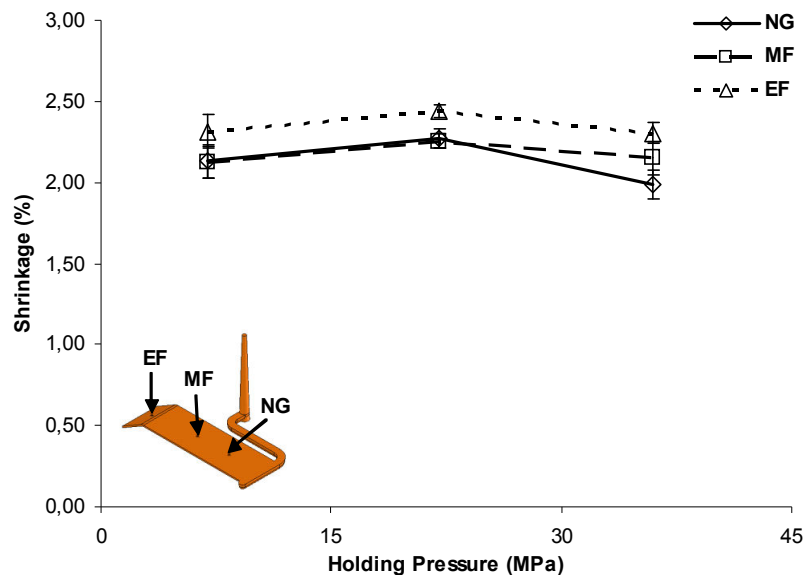


Figure 57– Effect of the Holding Pressure on the as-mould shrinkage across flow direction with Mould Temperature of 25°C for PP with 20% of Glass Fibre

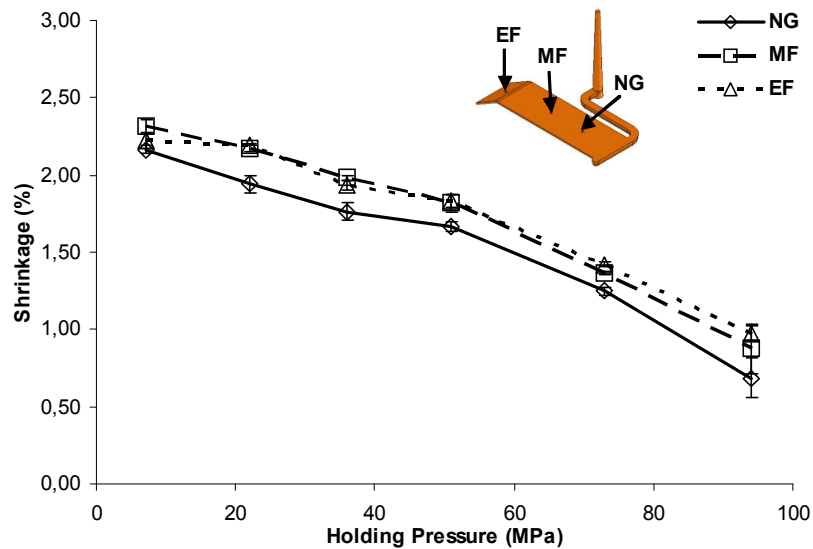


Figure 58– Effect of the Holding Pressure on the as-mould shrinkage across flow direction with Mould Temperature of 25°C for PP with 30% of Glass Fibre

In **figures 59** and **60** could be notice that as-mould thickness shrinkage for PP with 30% of Glass Fibres is slightly greater than for PP with 20% of Glass Fibres. This could be explained by the fact of the anisotropy increases. The thickness shrinkage results of **figure 60**, indicate that the increase of the holding pressure result in a greater thickness shrinkage. This results are probably due to the elastic expansion of the compressed polymer material or/and to the mould deformation caused by the injection pressure.

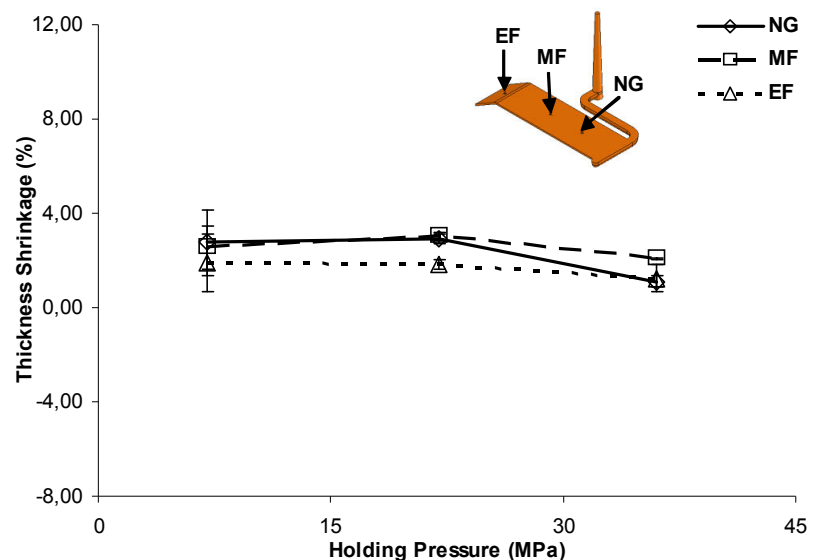


Figure 59– Effect of the Holding Pressure on the as-mould thickness shrinkage with Mould Temperature of 25°C for PP with 20% of Glass Fibre

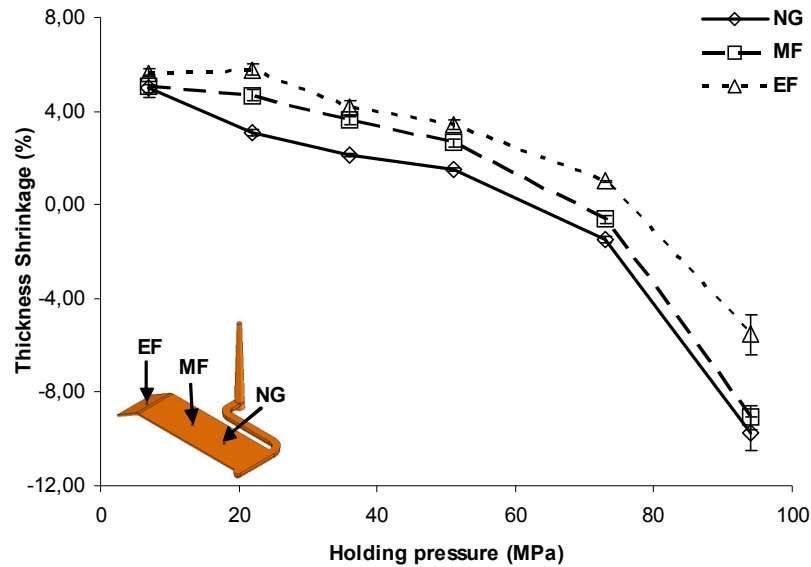


Figure 60– Effect of the Holding Pressure on the as-mould thickness shrinkage with Mould Temperature of 25°C for PP with 30% of Glass Fibre

4.3.2.2. Effect of mould temperature

The results of the as-moulded shrinkage across flow and thickness direction on **MF**-Middle of Fill, as a function of the holding pressure for PP with 20 and 30% of GF with Mould Temperatures of 25°C and 40°C, respectively are shown in **figures 61 to 64**.

Considering the cooling time a fixed parameter, a high mould temperature causes the plastic inside the mould cavity to cool down from a higher temperature environment. As a result the part will be ejected with an upper temperature resulting in larger as-mould shrinkage. This effect could be observed in **figure 61** until a holding pressure of 22MPa. After this value the mould temperature parameter seems to become an insignificant parameter with the increasing of holding pressure. In case of PP with 30% of Glass Fibres the mould temperature changes, seem do not have influence on as-mould shrinkage across flow direction.

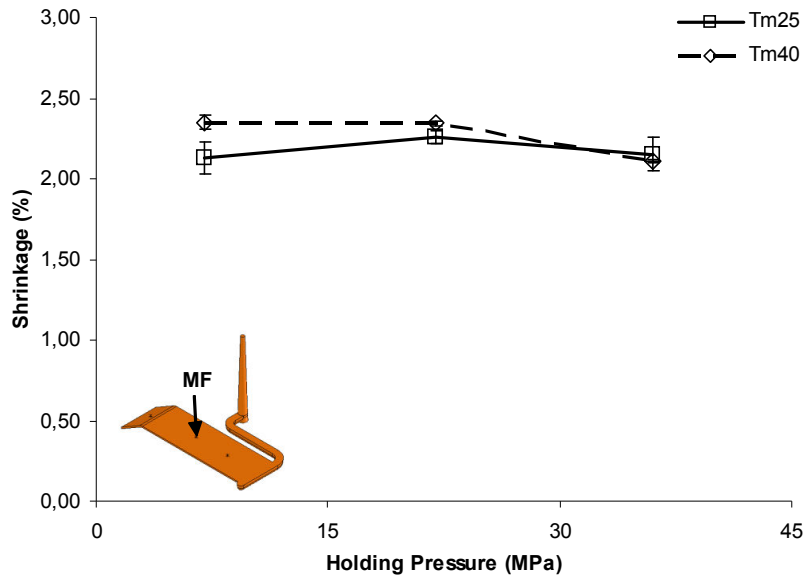


Figure 61– Effect of the Holding Pressure on the as-mould shrinkage across flow direction on MF (Middle of Fill) with Mould Temperature of 25 and 40°C, for PP with 20% of Glass Fibre

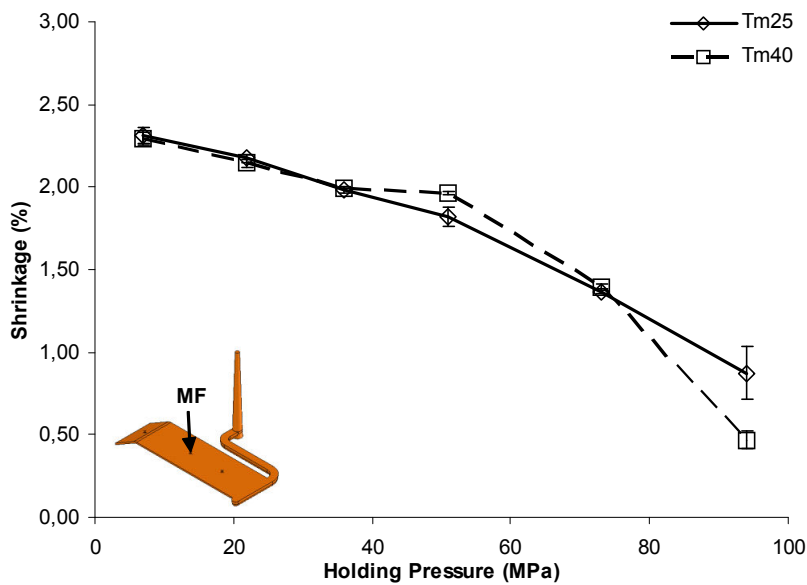


Figure 62– Effect of the Holding Pressure on the as-mould shrinkage across flow direction on MF (Middle of Fill) with Mould Temperature of 25 and 40°C for PP with 30% of Glass Fibre

As observed in **figures 63** and **64**, the affect of mould temperature on as-mould thickness shrinkage is very similar to the case of as-mould shrinkage across flow direction (**figures 61** and **62**).

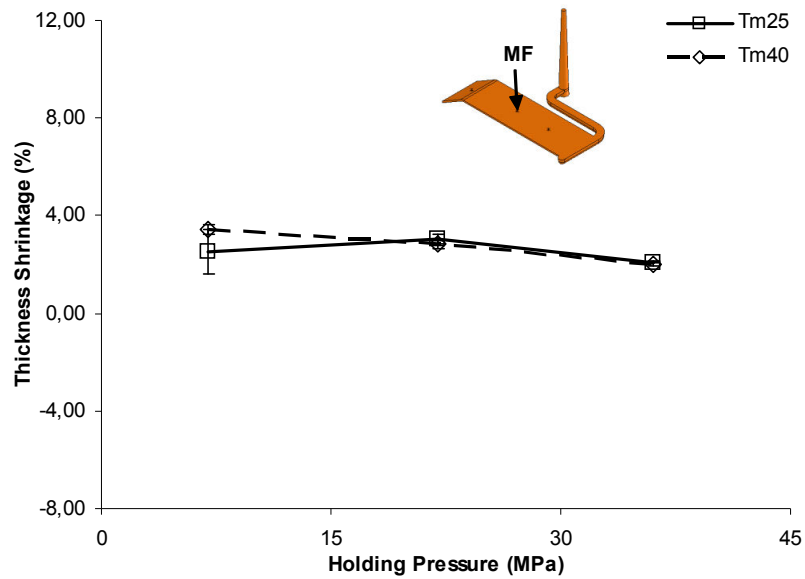


Figure 63– Effect of the Holding Pressure on the as-mould thickness shrinkage on MF (Middle of Fill) with Mould Temperature of 25 and 40°C for PP with 20% of Glass Fibre

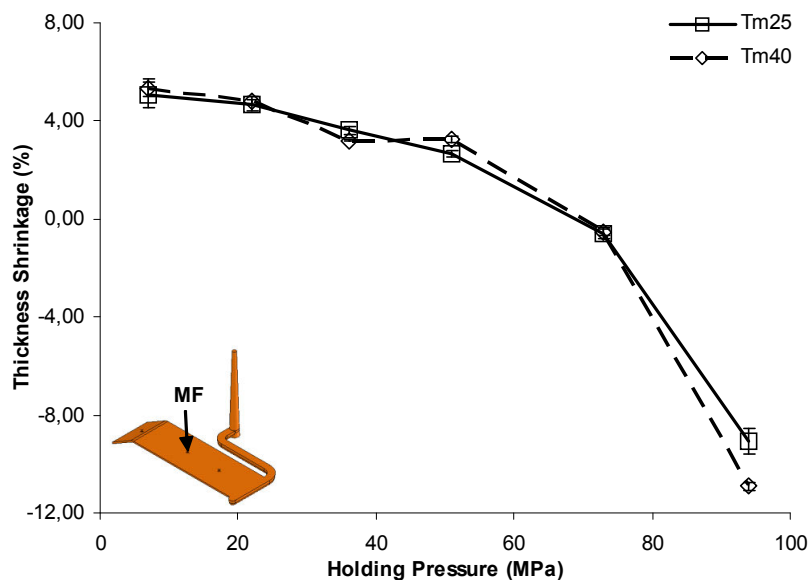


Figure 64– Effect of the Holding Pressure on the as-mould thickness shrinkage on MF (Middle of Fill) with Mould Temperature of 25 and 40°C for PP with 30% of Glass Fibre

4.4- Experimental warpage

Cooling and Solidification start as soon as the melt is in contact with the mould walls. As a consequence, polymer solidification occurs under different pressure levels at different times. Thermal and pressure-induced stresses build up in the shell layer, which give rise to part shrinkage and to stresses after ejection. Shrinkage variations and anisotropy of in-plane shrinkage lead to part deformation and warpage.

In this chapter the effect of Holding Pressure and Mould Temperature on experimental Angle deformation for unreinforced (PP) and reinforced (PP with 20 and 30% of Glass Fibres) materials, are presented and analyze.

4.4.1. Effect of processing conditions

The experimental results of the Angle Deformation (Mould Angle – Part Angle) in different positions (6, 16, 26, 35mm) as a function of the Holding Pressure for PC and for PP, are shown in **figure 65** and **66** respectively.

The experimental results for PC material show that holding pressure affects the warpage behaviour of the moulding parts. The increase of holding pressure decrease the part angle (angular zone in the curved end of the part) being more close to the zero deformation. The experimental results confirm that exists, an optimum holding pressure that could avoid the warpage. As it was verified on **figure 65a)** and **b)** the holding pressures greater than 7MPa, tend to have angles more close to zero angle deformation. The change of mould temperature didn't seem to affect significantly the angle deformation (the profile suffer small changes). It could be observed that for holding pressure of 36MPa the angle deformation through the different positions is approximately zero (optimum processing condition).

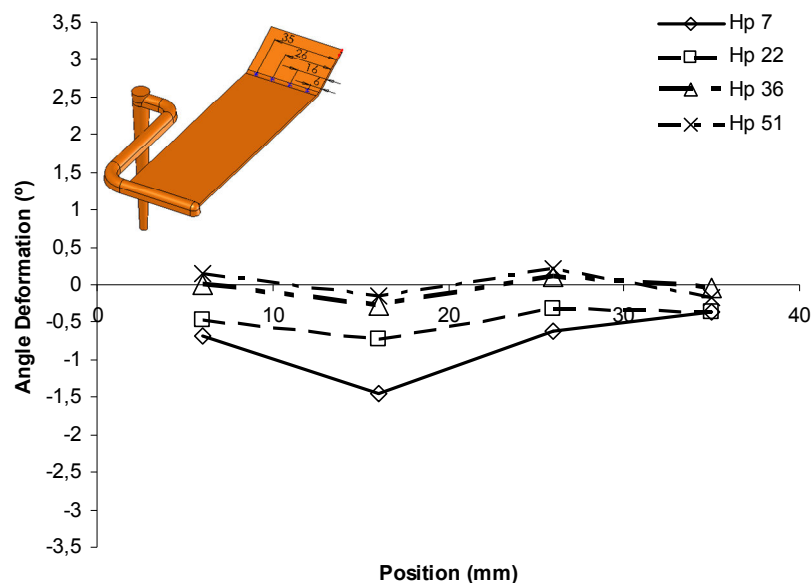


Figure 65– Effect of Holding Pressures on Experimental Angle Deformation in different positions for PC with Mould Temperature of 80°C

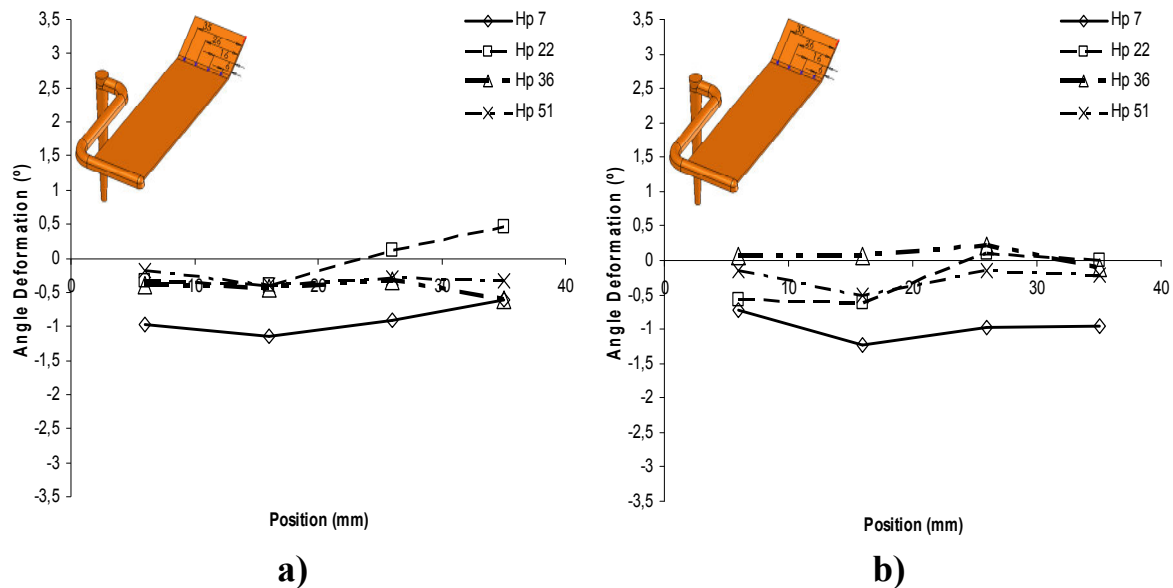


Figure 66– Effect of Holding Pressures on Experimental Angle Deformation in different positions for PP with Mould Temperature at: **a)** 25°C **b)** 40°C

4.4.2. Effect of fibre contents

The results of the Experimental Angle Deformation (Mould Angle – Part Angle) as a function of the Holding Pressure in different Angles positions (6, 16, 26, 35mm) for PP with 20 and 30% of Glass Fibre with mould temperature at 25°C and 40°C, are show in **figure 67** and **68**, respectively.

The experimental results confirm that with the incorporation of Glass Fibres the tendency and profile are significant different from those with unfilled material. Analysing **figure 67a)** and **b)** is notorious that holding pressure and mould temperature seems to have more impact on warpage behaviour of the moulding parts. In, **figure 67a)** can be seen that until holding pressure of 22MPa the part angle as a propensity to close, in proximity to a zero angle deformation. After, applying one superior holding pressure, the angle has an opposite behaviour then expected. Although the increase of mould temperature (**figure 67b)**, turns to have a remarkable change on the curves tendency. The part angle opens with the increase of holding pressure until 22MPa and then starts to close and become near of zero angle deformation.

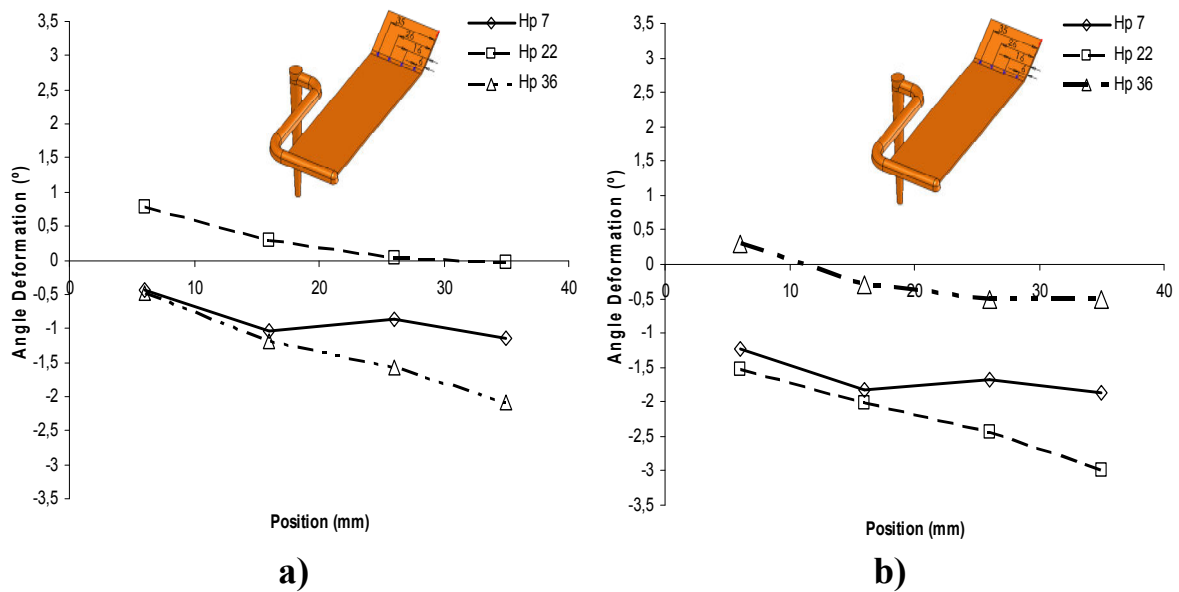


Figure 67– Effect of Holding Pressures on Experimental Angle deformation in different positions for PP with 20% of Glass Fibre with Mould Temperature of: **a)** 25°C **b)** 40°C

There are clear distinctions between results of PP with 30% and PP with 20% of Glass Fibre as it can be seen through **figures 67** and **68**. The results show that a higher holding and lower holding decrease the angle deformation, this result is more notice on **figure 68b**).

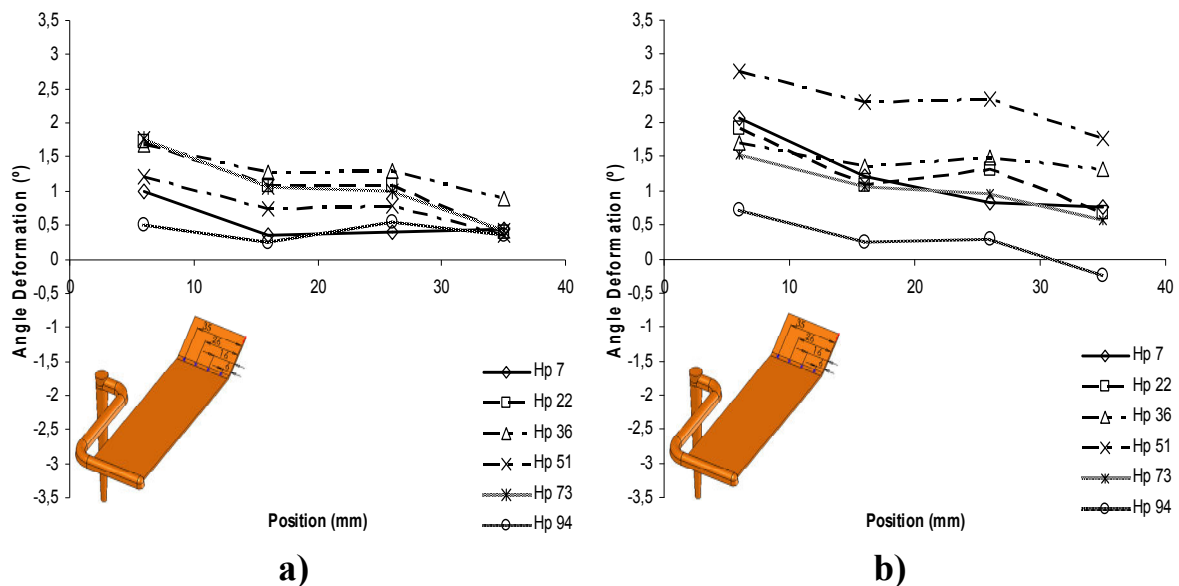


Figure 68- Effect of Holding Pressures on Experimental Angle deformation in different positions for PP with 30% of Glass Fibre with Mould Temperature of: **a)** 25°C **b)** 40°C

4.5- Predicted warpage

Dimensional accuracy of moulded part is one of the main concerns and major challenge since a large number of physical effects can contribute to the final warpage and shrinkage. Understand and predict part warpage is the basis to solve actual industrial issues [72]. For this reason numerical simulation of polymer injection moulding has been widely used in industry as a tool for improving and optimising product and mould design.

In this chapter the predicted angle deformation for unreinforced (PP) and reinforced (PP with 20 and 30% of Glass Fibre) materials, are presented and analyzed.

4.5.1. Effect of processing conditions

The comparison of experimental and predicted results of the Angle Deformation (Mould Angle – Part Angle) in different positions as a function of the extreme Holding Pressures for PC and for PP, are shown in **figure 69** and **70**, respectively.

The predicted angle deformations results under predict the experimental results. As it can be seen on **figure 69**, predicted curves don't have significant variations with the increase of the holding pressure (around zero deformation).

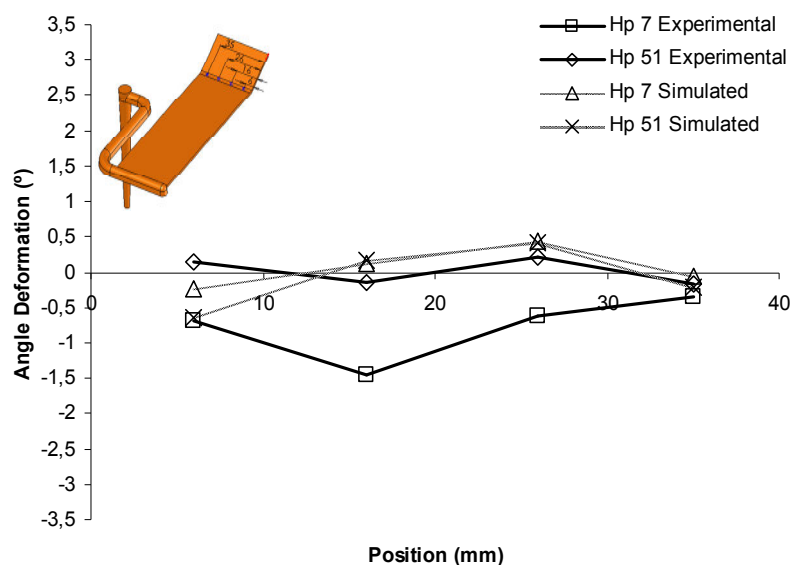


Figure 69– Comparison of experimental and predicted Angle Deformation in different positions for PC

Contrarily to PC predicted results, in the case of PP they seem to be sensitive to holding pressure variations. It can be observed a same tendency observed in the experimental curves, as it could be observed on **figure 70**. It clearly notices the increase of part angle with higher holding pressures. Although, there is no significant differences, in angle deformation with the change of mould temperature from 25 to 40°C.

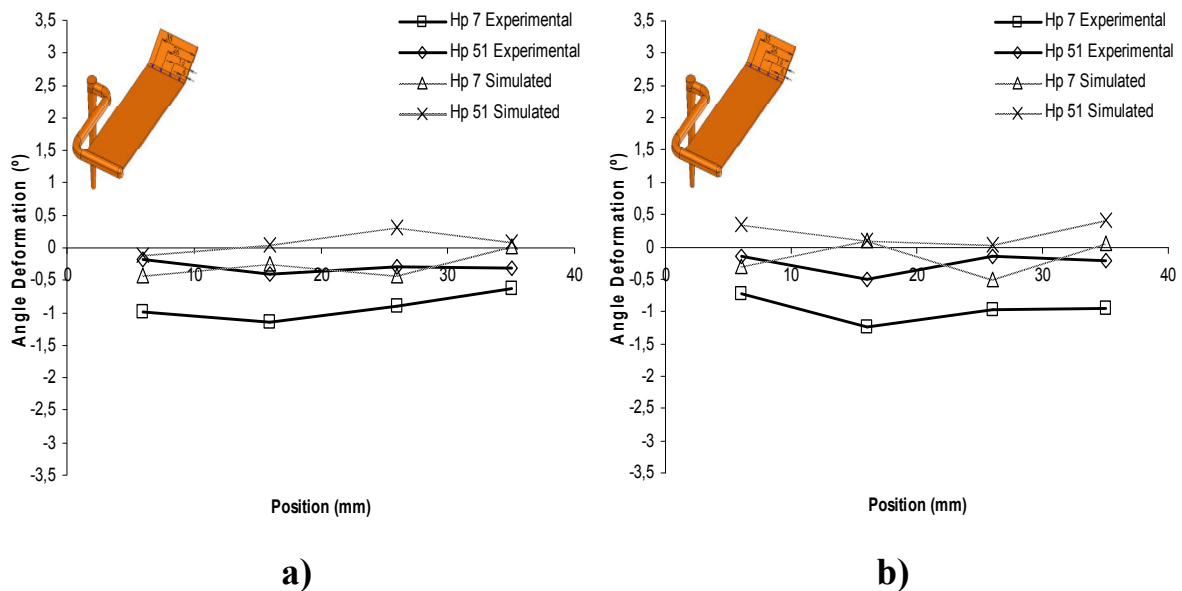


Figure 70– Comparison of experimental and predicted Angle Deformation in different positions for PP with Mould Temperature at: **a) 25°C b) 40°C**

4.5.2. Effect of fibre contents

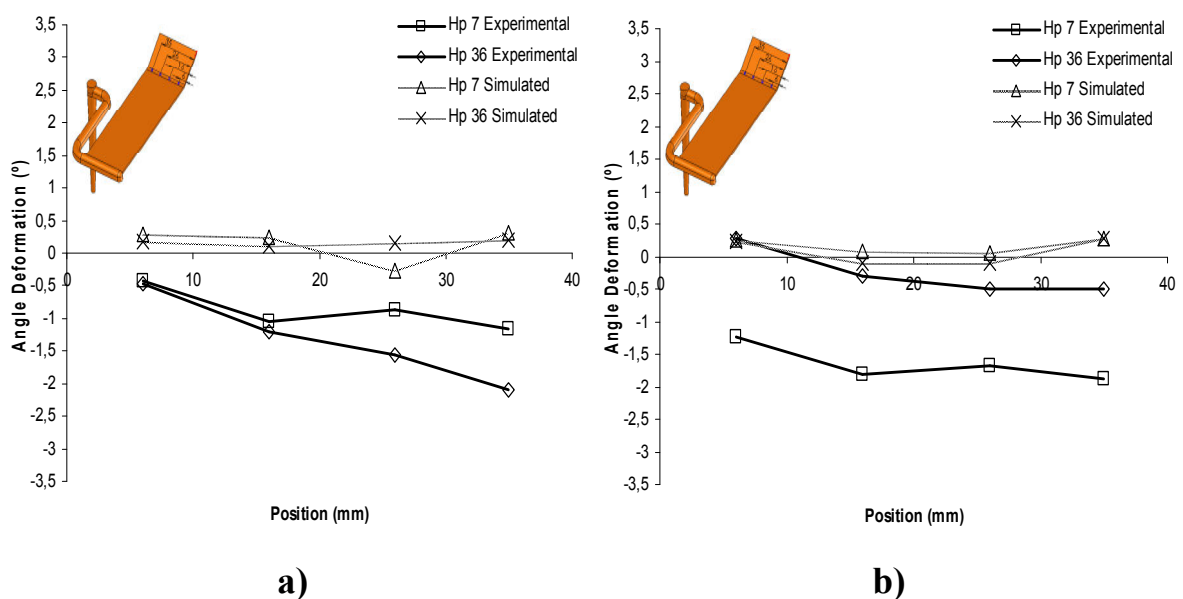


Figure 71– Comparison of experimental and predicted Angle Deformation in different positions for PP with 20% of Glass Fibre with Mould Temperature at: **a) 25°C b) 40°C**

The prediction results of fibre reinforced materials **figure 71**, show that the angle deformation are significantly different from the experimental results. Analysing the predicted results it is observed that angle deformation is around zero, although the experimental results show considerable angle deformation.

Also the predicted results show that the software is not sensitive to the changes on the mould temperature and Glass Fibre contents. However these processing variables affect the experimental angle deformation as could be seen in **figures 71** and **72**.

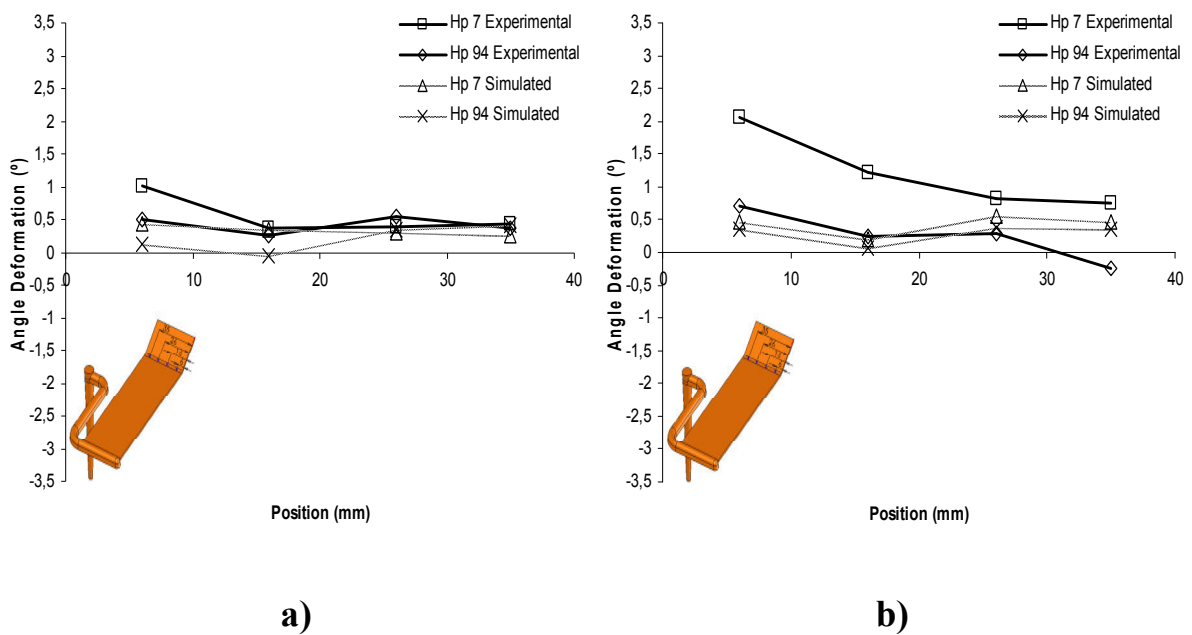


Figure 72– Comparison of experimental and predicted Angle Deformation in different positions for PP with 30% of Glass Fibre with Mould Temperature at: **a)** 25°C **b)** 40°C

4.6- Fibre orientation

Thermoplastics reinforced with short glass fibres have been increasingly used to produce engineering parts for structural applications. The use of short fibres has the advantage of achieving substantial stiffening without compromising significantly the processability of the materials [71].

However, a key aspect of these fibre-reinforced materials is the complicated fibre orientation distribution produced during injection moulding [73]. Typically, a layered structure is found throughout the thickness of the moulding, and the orientation of each layer is highly dependent on the fibre characteristics, the melt flow pattern within the mould, the conditions used in the moulding process [74] and the fibre contents (due to the fibre-fibre interaction). As a result in fibre composite materials the shrinkage

variation results mainly from the anisotropy of the polymeric matrix and the fibre orientation field. The prediction of the composite shrinkage depends on the accuracy of the prediction of the fibre orientation and distribution.

In this chapter the effect of Holding Pressure (7 and 36MPa) on fibre orientation for PP with 20% of Glass Fibre with mould temperature at 25°C, are presented and analyze.

4.6.1. Effect of processing conditions

The experimental results of fibre orientation in different positions along the flow path (30 and 120mm) as a function of the Holding Pressure with mould temperature at 25°C for PP with 20% of Glass Fibre, are shown in **figure 73** and **74**, respectively.

Through the analysis of fibre orientation tensors, it is clear that a_{33} tensor component (correspondent to thickness direction) has small values ($a_{33} \approx 0$). This is in accordance with the expectations, since the flow of polymer composites in injection moulding is laminar, leading to planar fibre orientation states. This fact could be confirmed by the element a_{11} (characterize the fraction of fibres aligned in the flow direction) behaviour where fibre orientation is always predominant in the flow direction ($a_{11} \geq 0.6$). It is also possible to observe that there are two typical regions, one with alignment of the fibres in flow direction near the wall and other with preferential orientation transverse to the flow direction, in the core. In this region the fibre orientation becomes more random ($a_{33} \approx a_{22} \approx 0.5$) when the distance to gate increases. On the other hand the increase of holding pressure didn't seem to have any influence, leading to equal levels of fibre orientation in the three dimensions.

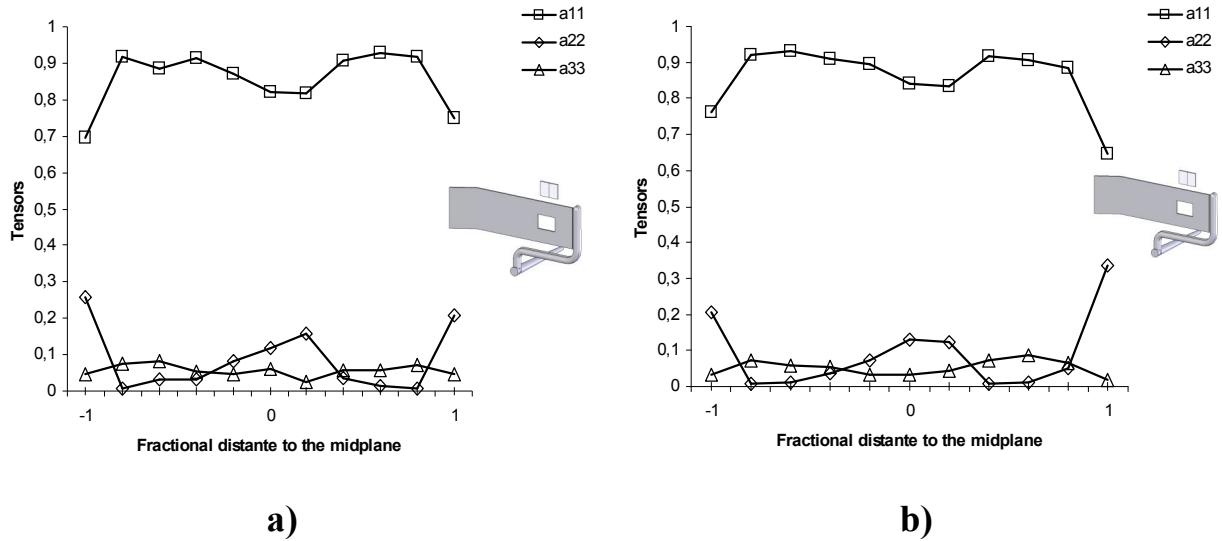


Figure 73– Effect of Holding Pressure on fibre orientation with Mould Temperature at 25°C for position 30mm from the gate: **a)** Hp=7MPa **b)** Hp=36MPa

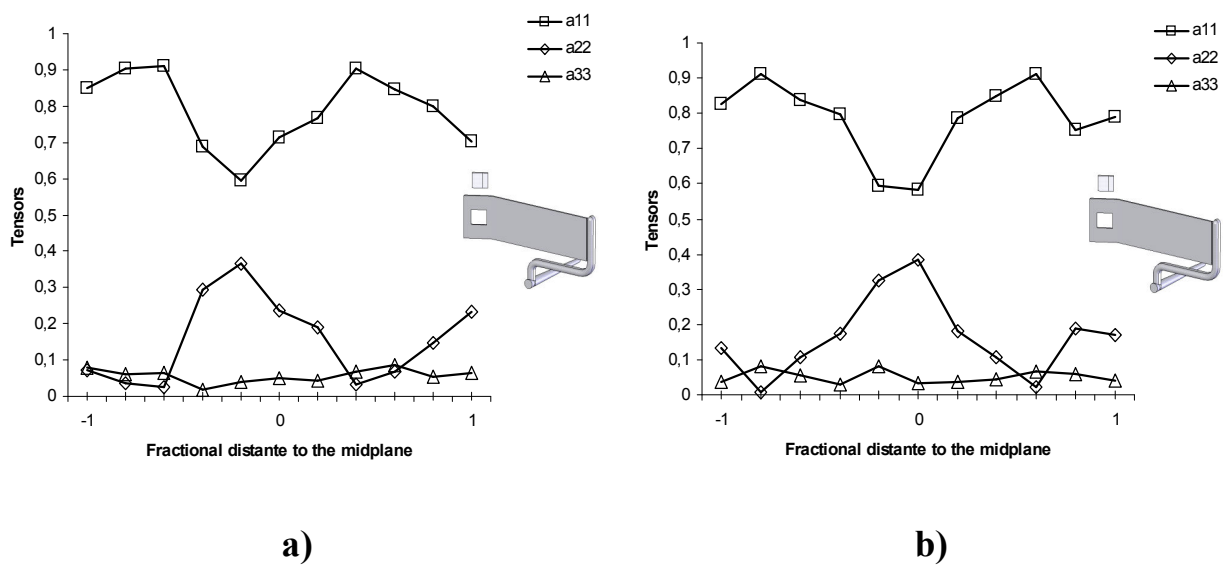


Figure 74– Effect of Holding Pressure on fibre orientation with Mould Temperature at 25°C for position 120mm from the gate: **a)** Hp=7MPa **b)** Hp=36MPa

5. Conclusions

Cavity pressure evolution

- The data acquisition systems can be directly used for monitoring the part quality, ensuring higher reproducibility. The direct measurement provides the facility to understand the behaviour of the flow during the injection moulding. This thesis is one more “piece” to complement all the studies made around this subject.
- Lower holding pressure causes a sudden drop cavity pressure and becomes zero earlier (onset of the thickness shrinkage);
- In contrast with PC samples, the residual pressures are zero for PP, when high holding pressures are applied. This behaviour is due to the lower thickness shrinkage and higher pressure in the cavity;
- The mould temperature seems to have a small influence on the pressure curves;
- The increase of the fibre weight fraction, increase the viscosity of the polymer, having more difficulties to flow during the filling and packing phase, as a consequence the pressure in the cavity decreases, resulting in higher shrinkage.

Moulding temperature evolution

- The objective of this research work was to combine the contact temperature sensor with infrared temperature sensor to evaluate the temperature of the material inside the cavity.
- In contrast with the thermocouples the infrared sensors give temperature evolution of the material during/after the detach of the part (coincident with the minimum pressure value) from the mould wall;
- The temperature measured by the infrared sensor showed that the holding pressures affect the thermal behaviour of the moulding part. Smaller thickness shrinkage (lower gap) creates better heat transfer (is the case of PC);

-
- The mould temperature seems to be a process variable with a small influence on the pressure curves;
 - With the incorporation of Glass Fibres the viscosity increases, the pressure loss increases, resulting in an increase of volume shrinkage.

As-moulding shrinkage

- The as-mould shrinkage across flow direction for unreinforced and reinforced materials, increase with the flow path, due to the lower pressure that occurs away from the gate. This behaviour is more evident on the unreinforced materials;
- As-mould shrinkage across flow direction for unreinforced and for PP with 30% of Glass Fibres, decrease inversely to the holding pressure. Nevertheless, the as-mould shrinkage across flow direction for PP with 20% of Glass Fibres seems to be unaffected by holding pressure;
- The as-mould thickness shrinkage for unreinforced materials, decrease with the flow path however reinforced materials has an inverse behaviour. In both materials the as-mould thickness shrinkage decrease inversely to holding pressure, however it is clear notice an expansion (negative shrinkage) of the mouldings due to the elastic expansion of the compressed polymer material or/and to the mould deformation caused by the injection pressure;
- Semi crystalline material (PP) shows higher shrinkage than amorphous material (PC) and lower than reinforced materials, as expected;
- The addition of Glass Fibres increases the as-mould shrinkage across flow direction and thickness shrinkage being more evident for PP with 30% of Glass Fibres. This could be explained by the increase of the anisotropy;

Warpage

- The holding pressure affects the warpage behaviour of the moulding parts;

-
- The holding pressure and mould temperature have more effect on warpage behaviour of the reinforced materials (once absolute values are greater);
 - For unreinforced materials the increase of holding pressure decrease the angle deformation;
 - The results showed that exist an optimum holding pressure that could avoid the warpage for both reinforced and unreinforced materials.
 - The results of the simulations, shows that the predictions values of angle deformations are significantly different from the experimental results;
 - Contrarily to semi-crystalline unreinforced material predicted results, in the case of amorphous and reinforced materials, they seem to be more insensitive to holding pressure and mould temperature variations;
 - In opposite to unreinforced PP (semi-crystalline material), the predicted angle deformation of PC (amorphous material) and reinforced PP, seems to be insensitive to variations on the holding pressure and mould temperature;
 - A better predictions of fibre orientation and improved models to describe warpage deformation is still needed.

Fibre Orientation

- The degree of orientation on flow direction (a_{11}) decrease with the distance to the gate, but the dominant orientation still in the flow direction;
- The variation of holding pressure didn't seem to have influence on fibre orientation.

6. Further Work

Is our opinion that is still need additional studies, namely:

- The use of more materials in further experiments to expand and validate the conclusion;
- Use another model from Moldflow software, like midplane model than 3D model (used in this thesis), once results seem to be obtained in shorter time than that required from the 3D solid;
- The runner system is one of the most important functional system of the mould since affects the melt filling pattern and determines the final shrinkage and warpage. It is crucial to understand the importance of the runner system, namely the gate, on the shrinkage and the fibre orientation;
- The use of ultrasound techniques, show great promise on the processing monitoring. Cavity pressure sensors results in a mark on the moulded product. For this reason the use of ultrasonic sensors seems to be a good topic for further research;

7. References

- [1] Mamat, A., Trochu, F., Sanschagrin, B. - **Analysis of Shrinkage by dual Kriging for Filled and Unfilled Polypropylene moulded Part** - Polymer Engineering and science, vol.35, n°19 (1995), p. 1511-1520.
- [2] Menges, G., Mohren, P. - **How to Make Injection Molds**. Second Edition, New York: Hanser (1993), p. 89. ISBN 3-446-16305-0.
- [3] Cunha, A. M., Pouzada, A. S. - **Injection Moulding Process** – Guimarães: Universidade do Minho.
- [4] Crawford, R. J. - **Plastics Engineering** - Belfast: Pergamon Press (1987), p. 185. ISBN 0-08-032627-7.
- [5] Johannaber, F. - **Injection Molding Machines: a user's guide**. Third Edition, Munich: Hanser (1994), p. 8-9. ISBN 3-446-17733-7.
- [6] Pontes, A. J. - **Shrinkage and Ejection Forces in Injection Moulded Products** - Guimarães: Universidade do Minho (2002), 248 p., PhD Thesis.
- [7] Titomanlio, G. and Jansen, K. M. B. - **Effect of Pressure History on Shrinkage and Residual Stresses (Injection Moulding with Constrained Shrinkage)** - Polymer Engineering and science, vol.36, n°15 (1996), p. 2029-2039.
- [8] Jansen, K.M.B - **Residual Stresses in Quenched and Injection Moulded Products** - Intern. Polym. Process., vol. 9: n° 1 (1994), p. 82-89.
- [9] Pantani, R., Titomanlio, G. - **Analysis of Shrinkage Development of Injection Moulded PS Samples** - Intern. Polymer Processing XIV, vol.14: n° 2 (1999), p. 183-190.
- [10] Viana, J.C. - **Mechanical Characterisation of Injection Moulded Plates** - Guimarães: Universidade do Minho (1999), 250 p., PhD Thesis.
- [11] Viana, J. C., Cunha, A. M. and Billon, N. - **The tensile Behaviour of an Injection Moulding Propylene-Ethylene Copolymer: Effect of the Local Thermo mechanical Conditions** – Intern. Polymer Processing, n°43 (1997), p. 159-166.

-
- [12] Brito, A. M., Cunha, A. M., Pouzada, A. S. and Crawford, R. J. - **Predicting the Skin-Core Boundary Location in Injection Mouldings** - Intern. Polymer Processing, vol. 6, n°4 (1991), p. 370-377.
- [13] Jensen, R. - **The mould filling process: technical requirements and findings, in Rheinfeld, D. (ed.)**. Injection Moulding Technology, Düsseldorf: VDI-Verlag (1981), p. 173-195. ISBN 3-18-404067-4.
- [14] **Plastics Processing. Injection Molding, Extrusion, Die Casting**. Winterthur: Kistler Instrumente AG (1998).
- [15] Himasekhar, K., Chiang, H. H., Lautenbach, S., Wang, K., K., Santhanam, N.- **Assessment of Shrinkage and Warpage Using an Integrated Analysis of Moulding Dynamics** – Proceedings of 49th annual meeting of the Society of Plastic Engineers. Montreal, 1991, p. 242-249.
- [16] Wu, Scott S.- **CAE Application: Shrinkage and Warpage of an Injection Moulded Part** - Proceedings of 55th annual meeting of the Society of Plastic Engineers. Toronto, 1997.
- [17] Kikuchi, Hiroyuki and Koyama, Kiyohito - **Generalized Warpage Parameter** - Polymer Engineering and science, vol.36, n°10 (1996).
- [18] Pantani, R. - **Analysis of Shrinkage Development in Injection Moulded Samples** - Salerno: università degli Studi di Salerno (1999), 161 p., PhD Thesis.
- [19] Titomanlio, G. and Jansen, K. M. B. - **In-Mold Shrinkage and Stress Prediction in Injection Molding** - Polymer Engineering and science, vol.36, n° 15 (1996), p. 2041-2049.
- [20] Zöllner, Olaf – **The fundamentals of shrinkage of thermoplastics**. Bayer (2001).
- [21] Burke, C., Kazmer, D. - **An experimental Validation of a Shrinkage/Warpage Predictor** - Proceedings of 50th annual meeting of the Society of Plastic Engineers. Detroit, 1992, p. 1354 -1363.

-
- [22] Zöllner, O., and Sagenschneider, U. - **Shrinkage and Deformation of Glass Fibre-Reinforced Thermoplastics may be Calculated** - *Kunststoffe plast Europe* (1994), p. 72-77.
- [23] Malloy, Robert A. - **Plastic Part Design for Injection Molding: An Introduction**. New York: Hansen (1994), p. 2, 64, 77. ISBN 1-56990-129-5.
- [24] Timm, W. Marty and Coutts, J. Michael - **Relationship of Predicted Shear Stress to Molded Plastics Parts** - Proceedings of 61st annual meeting of the Society of Plastic Engineers. Nashville, 2003, p. 3373-3377.
- [25] Seyler, R., Erie, P. and Schenck, A. - **Warpage Index Based on Cooling and Orientational Effects** - Proceedings of 61st annual meeting of the Society of Plastic Engineers. Nashville, 2003, p. 3353-3357.
- [26] Fan, Z., Lin, B., Costa, F., Xiaoshi, J., Zheng, R. and Kennedy, P. - **Three-Dimensional Warpage Simulation for Injection Molding** - Proceedings of 62nd annual meeting of the Society of Plastic Engineers. Chicago, 2004, p. 491-495.
- [27] Fahy, E. J. - **Modelling Warpage in reinforced Polymer Disks** - *Polymer Engineering and science*, vol.38, n° 7 (1998), p 1072-1084.
- [28] Kech, A. and Hosdez, V. - **3D-Simulation of Warpage for Short Fibre Reinforced Thermoplastics** - 21st annual meeting of the polymer processing society. Leipzig, Germany, 2005.
- [29] Jansen, K. M. B. and Van Dijk, D. - **Shrinkage of Injection Moulded Fibre Composites** - 66th annual meeting of the polymer processing society. Sweden, 1997, p. 3-4.
- [30] Stebick, M. - **Anisotropic Shrinkage as Developed by Flow During Injection Moulding** - Proceedings of 48th annual meeting of the Society of Plastic Engineers. Dallas, 1990, p. 1983-1985.
- [31] Jansen, K. M. B., Pantani, R., Titomanlio, G. - **As-Moulded Shrinkage Measurements on Polystyrene Injection Moulded Products** - *Polymer Engineering and science*, vol.38, n°2 (1998), p. 254-264.

-
- [32] Jansen, K. M. B., Van Dijk, D., J. and Husselman, M., H. - **Effect of Processing Conditions on Shrinkage in Injection Moulding** - Polymer Engineering and science, vol.38, n°5 (1998) p. 838-846.
- [33] Patel, Prabir - **Effect of Processing Conditions on the Shrinkage and Crystallinity of Injection-Molded Parts** - Proceedings of 53th annual meeting of the Society of Plastic Engineers. Toronto, 1997.
- [34] Liao, S. J., Chang, D. Y., Chen, H. J., Tsou, L. S., Ho, J. R., Yau, H. T., and Hsieh, W. H. - **Optimal Process Conditions of Shrinkage and Warpage of Thin-Wall Parts** - Polymer Engineering and science, vol.44, n°5 (2004).
- [35] Kumazawa, H. - **Prediction of Anisotropic Shrinkage of an Injection Molded Part** - Proceedings of 52nd annual meeting of the Society of Plastic Engineers. S. Francisco, 1994, p. 817-821.
- [36] Akkerman, R., Dijk, D. J., Klarenbeek, M., Tijl, H. - **Residual Stresses In, And Shrinkage of PE and PS Injection Moulded Symmetrically cooled Flat Panels** - 64th annual meeting of the polymer processing society. Stuttgart, 1995.
- [37] Jansen, K. M. B., Dijk, D. and Hout, D. - **Shrinkage anisotropy in semi-crystalline Materials** - 66th annual meeting of the polymer processing society. Sweden, 1997, p. 3-5.
- [38] Bushko, Wit C. and Stokes, Vijay K. - **Solidification of Thermoviscoelastic Melts. Part II: Effects of Processing Conditions on Shrinkage and Residual Stresses** - Polymer Engineering and science, vol.35, n°4 (1995).
- [39] Pierick, D. and Noller, R. - **The Effect of Processing Conditions on Shrinkage** - Proceedings of 49th annual meeting of the Society of Plastic Engineers, Vol.1. Montreal, 1991, p. 252-258 .
- [40] Wang, James T. and Yoon, K. C. - **Shrinkage and Warpage Analysis of Injection-Molded Parts** - Proceedings of 58th annual meeting of the Society of Plastic Engineers. Orlando, 2000.
- [41] Pramujati, Bambang and Dubay, Rickey - **Process Identification of Barrel Temperature Control in Injection Molding: A MIMO Approach** - Proceedings

-
- of 61st annual meeting of the Society of Plastic Engineers. Nashville, 2003, p. 3560-3563.
- [42] Healy, Anna, Dubay, Rickey and Gerber, Andrew - **Controlling Melt Temperature in Injection Moulding Using an Adaptive CFD Predictive Controller** - - Proceedings of 61st annual meeting of the Society of Plastic Engineers. Nashville, 2003, p 3300-3304.
- [43] Shiarnng Jou, Wern - **Effects of Moulding Conditions Upon the Moulding Shrinkage of Polypropylene** - Proceedings of 52nd annual meeting of the Society of Plastic Engineers. S. Francisco, 1994, p. 745-748.
- [44] Wuebken, G. - **Thermal Considerations in the Design of Injection Moulds** - Soc. Chem. Industrielle, 5th European Plastics and Rubber Conference, Paris (1978).
- [45] Friel, P. - **Influence of Mould Surface Temperature Control on Processing and on the Quality of Injection Mouldings** - Kunststoffe German Plastics 76 (1986) 1.
- [46] Chang, Tao C. - **Shrinkage Behaviour and Optimization of Injection Moulded Parts Studied by the Taguchi Method** - Polymer Engineering and science, vol.41, n°5 (2001).
- [47] Bain, Jr M. F., Janicki, S. L. and Thomas, L. S. - **Mold Shrinkage: Not a Single Data Point** - Proceedings of 50th annual meeting of the Society of Plastic Engineers. Montreal, 1992.
- [48] Gipson, Patrick M., Grelle, Peter F. and Salamon, Brent A. - **The Effects of processing Conditions, Nominal Wall Thickness and Flow Length on the Shrinkage Characteristics of Injection Molded Polypropylene** - Proceedings of 57th annual meeting of the Society of Plastic Engineers. New York, 1999.
- [49] Jansen, K. M. B., Van Dijk, D. J. and Keizer, K. P. - **Warpage of Injection Moulded Plates and Corner Products** – Intern. Polymer Processing XIII (1998) 4.
- [50] Cox, W. Howard and Mentzer, Charles C. - **Injection Moulding: The Effect of Fill Time on Properties** - Polymer Engineering and science, vol.26, n°7 (1986).

-
- [51] Boudreaux, E., and Ford, G. A. - **Effect of Processing Temperatures on the Shrinkage of Polymethylpentene Compounds** - Proceedings of 47th annual meeting of the Society of Plastic Engineers. New York, 1989, p. 360-363.
- [52] Chang, R. Y. and Tsaur, B. D. - **Experimental and Theoretical Studies of Shrinkage, Warpage, and Sink Marks of Crystalline Polymer Injection Moulded Parts** - Polymer Engineering and science, vol.35, n^o15 (1995).
- [53] Ito, H., Kikutani, T., Tada, K., and Koyama, K. - **Modelling and Numerical Simulation of Polymer Crystallization in Injection Molding Process** - 66th annual meeting of the polymer processing society. Sweden, 1997.
- [54] Hebert, L. P., Girard, P., Salloum, G. and Gaudreault, M. - **Effect of Inserts on Shrinkage in Injection Moulded HDPE Disks** - Proceedings of 49th annual meeting of the Society of Plastic Engineers, Vol.1. Montreal, 1991, p. 430-432.
- [55] Marinelli, A., Farah, M. and Bretas, R. - **A New Tool for Monitoring Crystallization Development in Injection Molded Parts** - 19st annual meeting of the polymer processing society. Melbourne, Australia, 2003.
- [56] Martinho, P. M. G. - **Estudo do Empeno em Peças Moldadas por injeção** - Guimarães: Universidade do Minho (2002), 216 p., Master Thesis.
- [57] Ammar, Amine, Leo, Vito and Régnier, Gilles - **Corner Deformation Induced by Shrinkage Anisotropy of Injected Thermoplastics: Experimental Study and Numerical Approach** – 70th annual meeting of the polymer processing society. Montréal, Canadá, 2001, p. 1-12.
- [58] Azevedo, Maurício, Pita, Victor and Mosci, Renato - **Understanding the Effect of Processing Parameters on the Mold Temperature** - Proceedings of 61th annual meeting of the Society of Plastic Engineers. Nashville, 2003, p. 3564-3569.
- [59] Stitz, S. - **Is it Really Possible to Predict Shrinkage and Warpage?** - Kunststoffe German Plastics 81 (1991) 10, p. 880-885.
- [60] Zou, Q. and Horney, J. R. - **Minimize Injection Moulded Plastic Part Warpage by Applying Warpage Analysis in Mold Design** - Proceedings of 52nd annual meeting of the Society of Plastic Engineers. S. Francisco, 1994, p. 1104-1110.

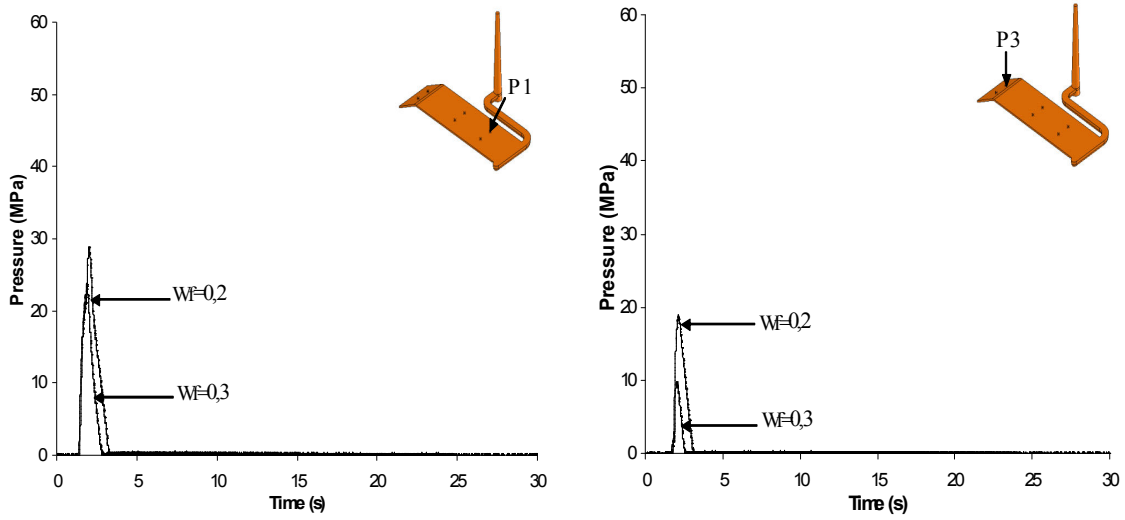
-
- [61] Shijun, Ni - **Effects of Mold Gating on Shrinkage and Warpage of Injection Molded Parts** - Proceedings of 61th annual meeting of the Society of Plastic Engineers. Nashville, 2003, p. 544-548.
- [62] Shijun, Ni - **Minimizing Warpage of an Injection Molded Part by systematic Simulation Analysis** - Proceedings of 62nd annual meeting of the Society of Plastic Engineers. Chicago, 2004, p. 616-620.
- [63] Mentzer, Charles C., Foss, Peter H. and Shay, Robert M. - **Comparison of C-Mold Predictions and Experimental Shrinkages: Fibre-Filled Materials** - Proceedings of 54th annual meeting of the Society of Plastic Engineers. Indianapolis, 1996.
- [64] Bakharev, A., Zheng, R., Fan, Z., costa, F. S., Jin, X. and Kennedy, P. K. - **Corner Effect in Warpage Simulation** – Proceedings of 63rd annual meeting of the Society of Plastic Engineers. Boston, Massachusetts , 1996, p. 511-515.
- [65] Matsuoka, T., Takabatake, J., Koiwai, A., Inoue, Y., Yamamoto, S., and Takahashi, H. –**Integrated Simulation to Predict Warpage of Injection Moulded Parts**- Polymer Engineering and science, Vol.31, N° 14 (1991).
- [66] Bernhardt, E., C. - **Cavity Dimensioning Using Computerized Shrinkage Evaluation Software** - Proceedings of 47th annual meeting of the Society of Plastic Engineers. New York, 1989.
- [67] Dubay, Rickey - **Predictive Control of Cavity Pressure During Injection Filling** - Proceedings of 59th annual meeting of the Society of Plastic Engineers. Dallas, 2001.
- [68] Mathey, Eliette - **Injection Mould Cooling Optimization using Boundary Element Heat Transfer Simulation** - Toulouse: Université Paul Sabatier (2004), PhD Thesis.
- [69] Bay, R. S. and Tucker III, C. L. - **Fibre Orientation in Simple Injection Moldings. Part II: Experimental results** - Polym. Eng. and Sci., vol.32, n°4 (1992).
- [70] Pontes, A. J., Neves, N. M., and Pouzada, A. S. - **The Role of the Interaction Coefficient in the Prediction of the Fibre Orientation in Planar Injection Moldings** - Polymer Composites, vol. 24, n°3 (2003).

-
- [71] Neves, N. M., Pontes, A. J. and Pouzada, A. S. - **Experimental Validation of Morphology Simulation in Glass fibre Reinforced Polycarbonate Discs** - Journal of Reinforced Plastics and Composites, vol.20, n°06 (2001).
- [72] Leo, V., Van Meulebeke, G. and Blanc S. - **Understanding and Measuring Warpage of Moulded Parts** – International Conference on Polymers and Moulds Innovations. Marinha Grande, 2005, p. 1-5.
- [73] O’Dowd, F, Lévesque, M. and Gilchrist, M. D. - **Analysis of Fibre Orientation Effects on Injection Moulded Components** – Proc. IMechE, vol.220, Part B: J. Engineering Manufacture (2006).
- [74] Ho, K. C. and Jeng, M. C. - **Fibre Orientation of Short Glass Fibre Reinforced Polycarbonate Composites Under Various Injection Moulding Conditions** - Plastics Rubber Composites Processing, vol.25 (1996), p. 469-476.

8. Appendix (Extra experimental data)

APPENDIX A1-Moulding pressure evolution

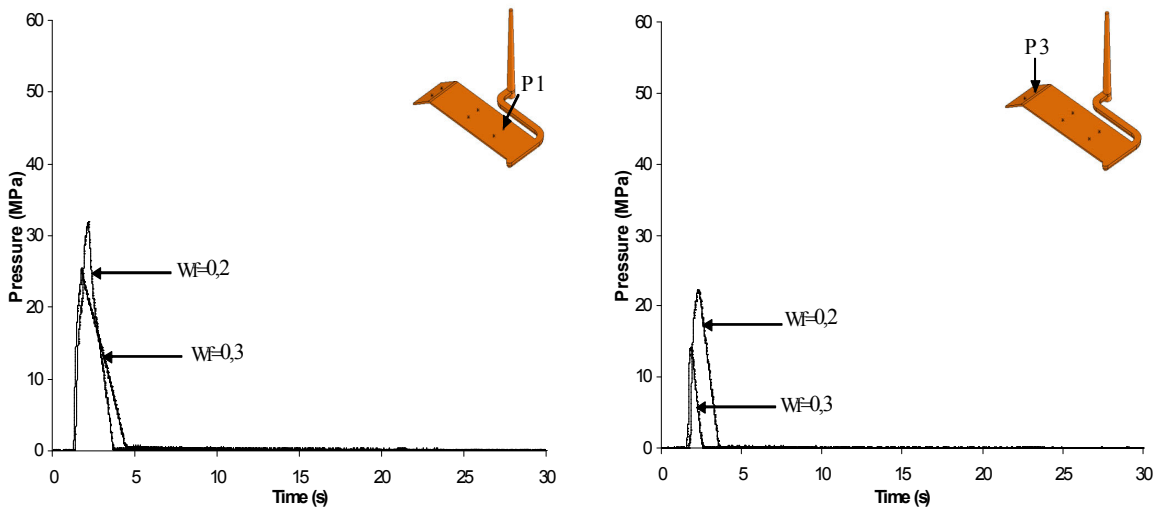
A1.1-Pressure evolution for reinforced PP



a) Position P1

b) Position P3

Figure A1.1.1– Effect of fibre weight fraction (0,2; 0,3) on the pressure evolution curves. PP mouldings with Holding Pressure of 7MPa with Mould Temperature at 25°C



a) Position P1

b) Position P3

Figure A1.1.2– Effect of fibre weight fraction (0,2, 0,3) on the pressure evolution curves. PP mouldings with Holding Pressure of 7MPa with Mould Temperature at 40°C

APPENDIX A2-Moulding temperature evolution

A2.1-Temperature evolution for PC

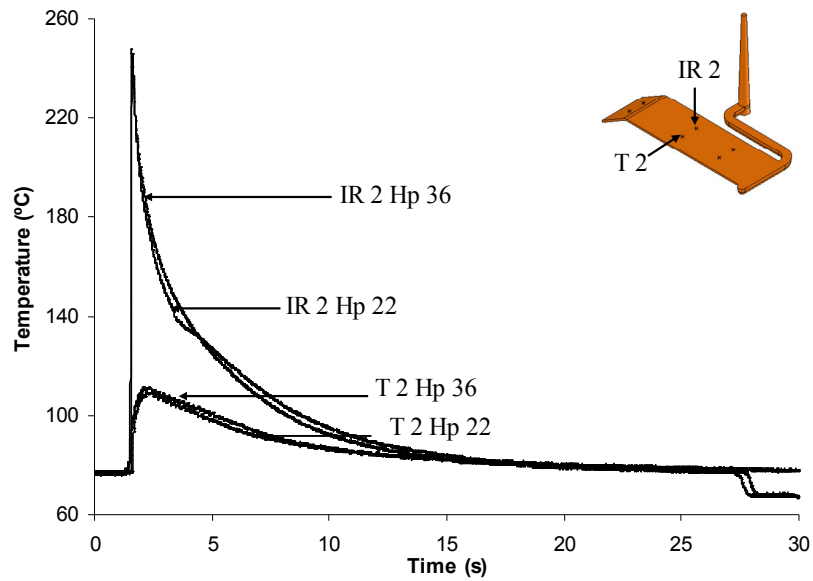


Figure A2.1.1– Influence of the holding pressure on the Temperature evolution at the middle of fill in PC parts. Mouldings with Holding Pressure of 22 and 36MPa and Mould Temperature at 80°C

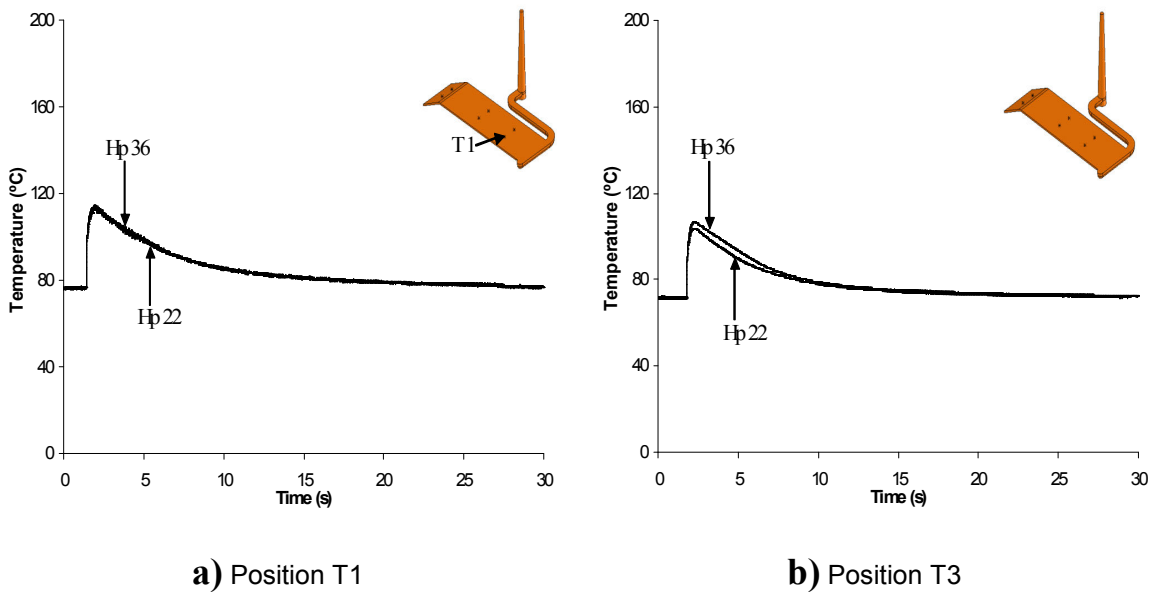


Figure A2.1.2– Influence of the holding pressure on the Temperature evolution curves in PC parts. Mouldings with Holding Pressure of 22 and 36MPa and Mould Temperature at 80°C

A2.2-Temperature evolution for PP

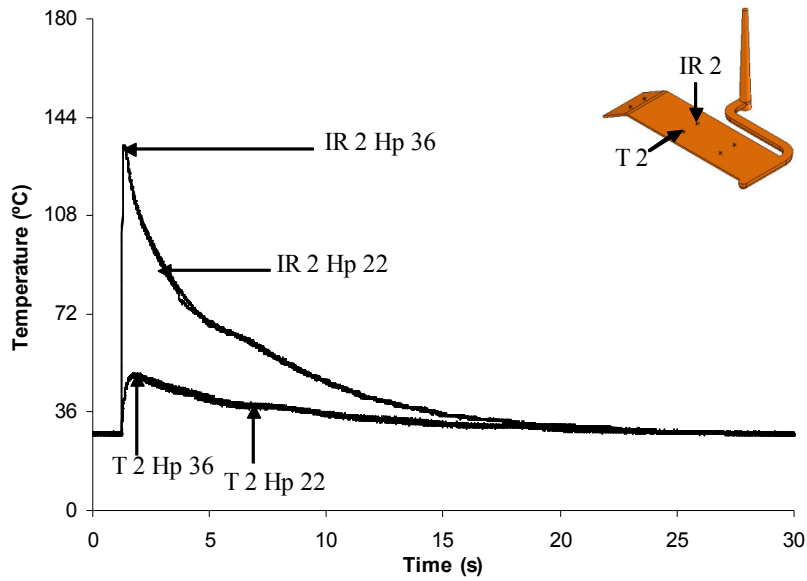


Figure A2.2.1– Influence of the holding pressure on the Temperature evolution, at the middle of fill. PP mouldings with Holding Pressure of 22 and 36MPa with Mould Temperature at 25°C

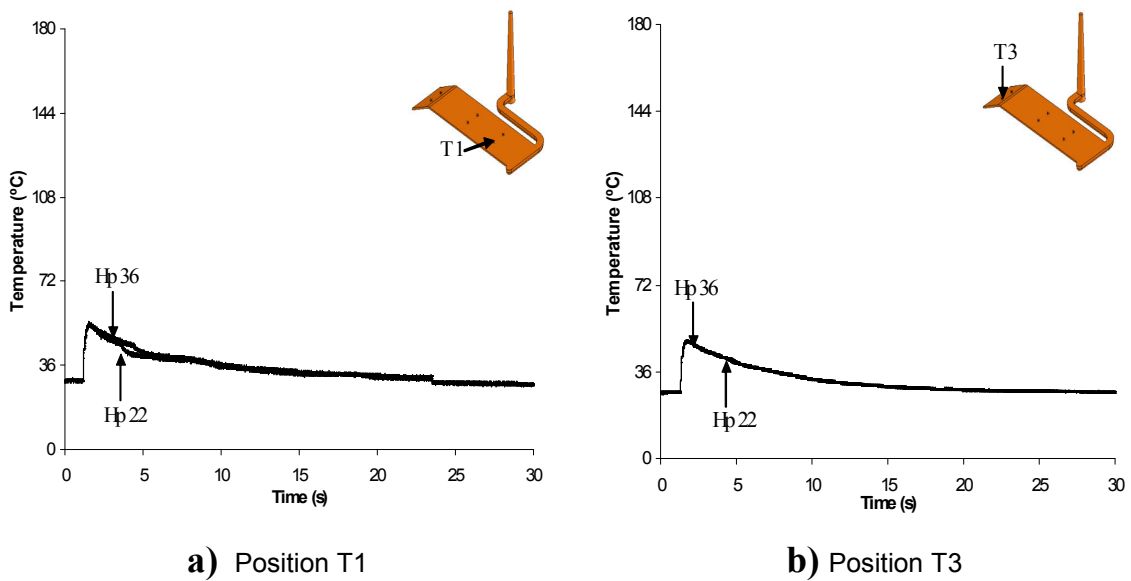


Figure A2.2.2– Influence of the holding pressure on the Temperature evolution. PP mouldings with Holding Pressure of 22 and 36MPa, and with Mould Temperature at 25°C

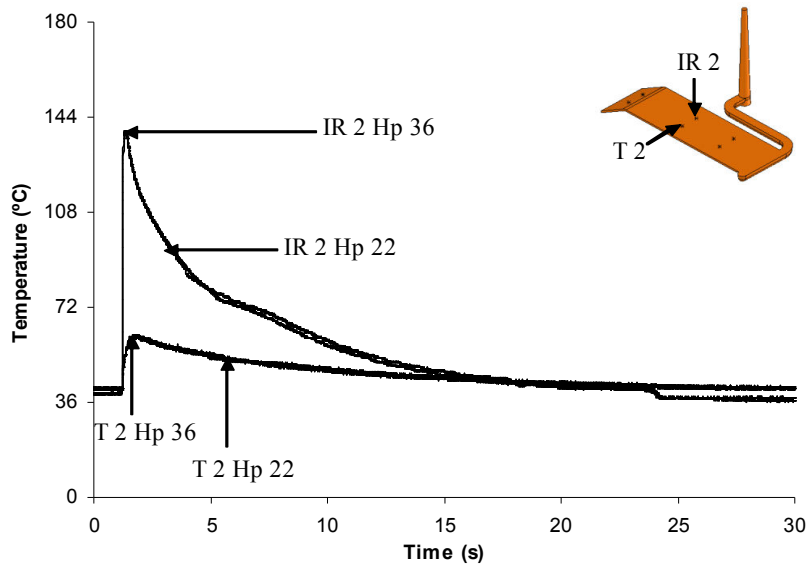
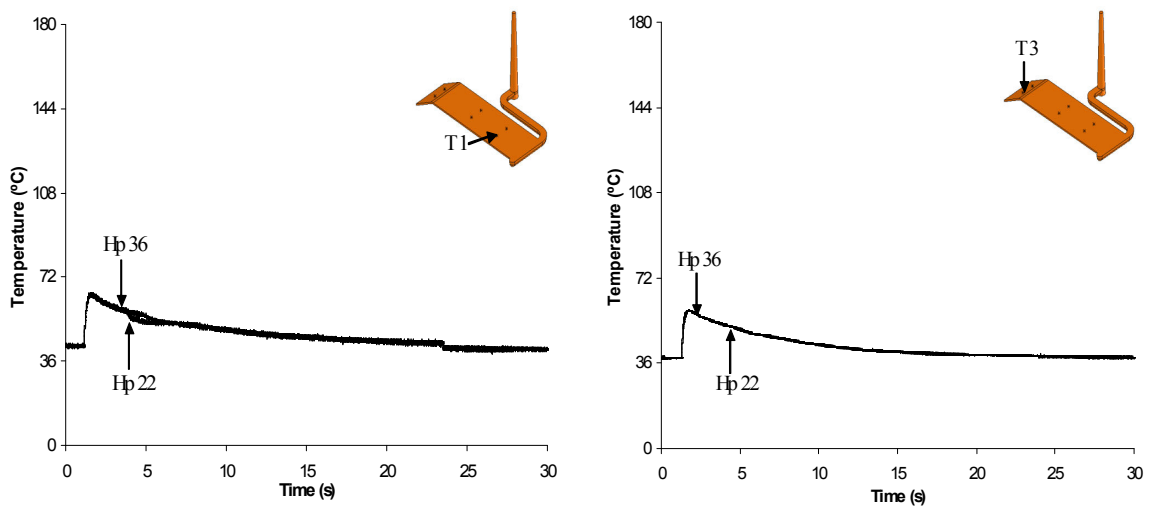


Figure A2.2.3– Influence of the holding pressure on the Temperature evolution at middle of fill. PP mouldings with Holding Pressure of 22 and 36MPa with Mould Temperature at 40°C



a) Position T1

b) Position T3

Figure A2.2.4– Influence of the holding pressure on the Temperature evolution curves in PP parts. Mouldings with Holding Pressure of 22 and 36MPa with Mould Temperature at 40°C

A2.3-Temperature evolution for reinforced PP20%

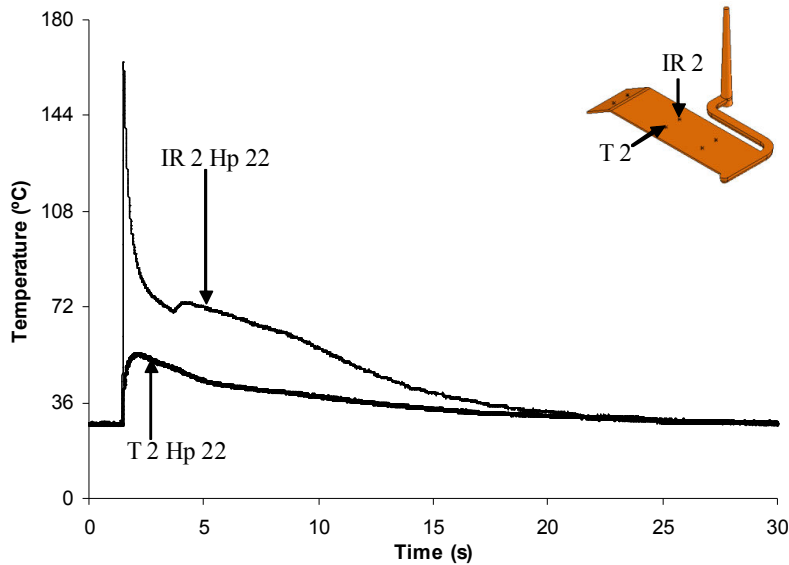
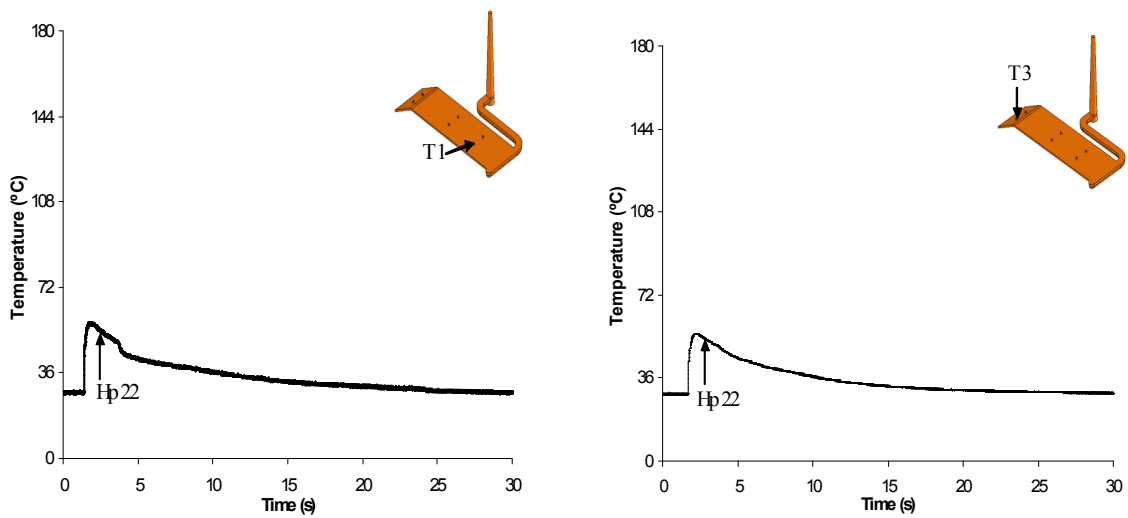


Figure A2.3.1– Influence of the holding pressure on the Temperature evolution at middle of fill. PP with 20% GF mouldings with Holding Pressure of 22MPa with Mould Temperature at 25°C



a) Position T1

b) Position T3

Figure A2.3.2– Influence of the holding pressure on the Temperature evolution curves in PP20%GF parts. Mouldings with Holding Pressure of 22MPa with Mould Temperature at 25°C

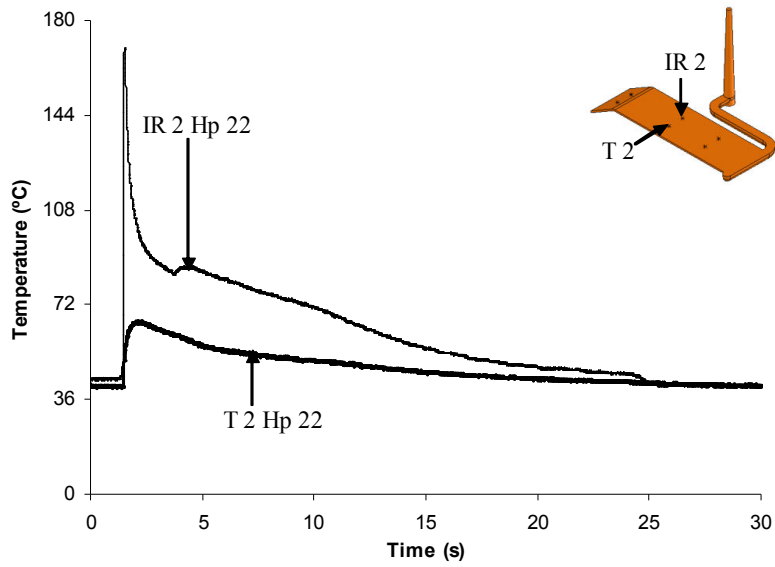


Figure A2.3.3– Influence of the holding pressure on the Temperature evolution at middle of fill. PP with 20% GF mouldings with Holding Pressure of 22MPa with Mould Temperature at 40°C

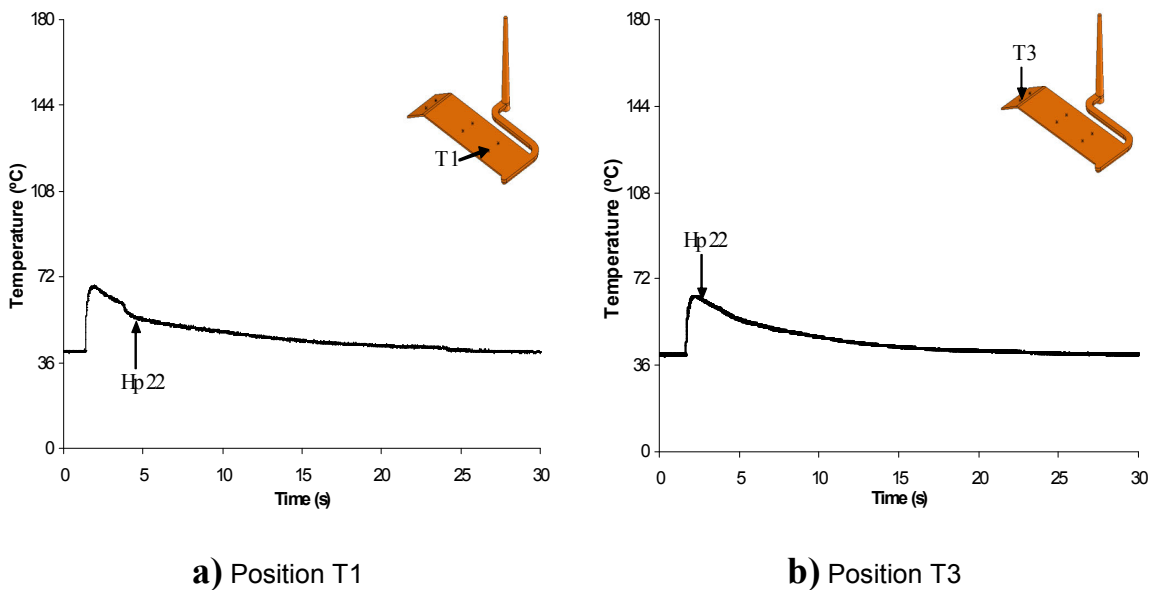


Figure A2.3.4– Influence of the holding pressure on the Temperature evolution curves in PP20%GF parts. Mouldings with Holding Pressure of 22MPa with Mould Temperature at 40°C

A2.4-Temperature evolution for reinforced PP30%

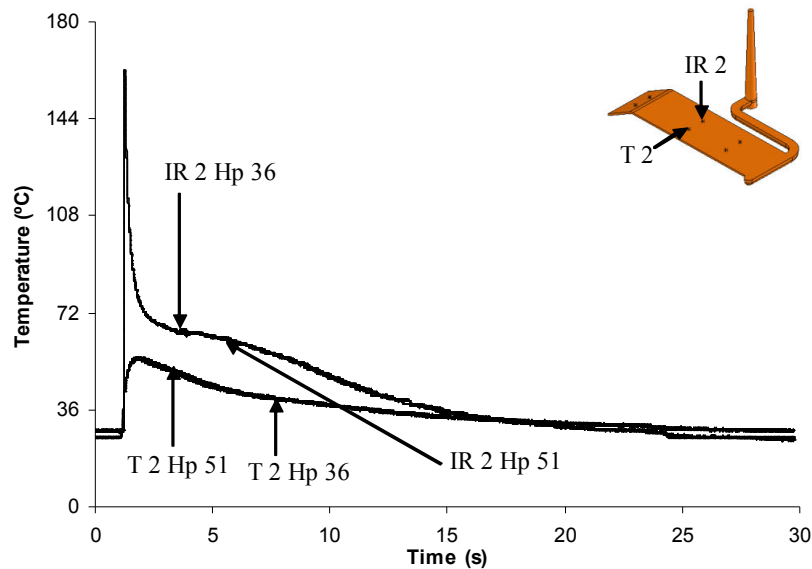
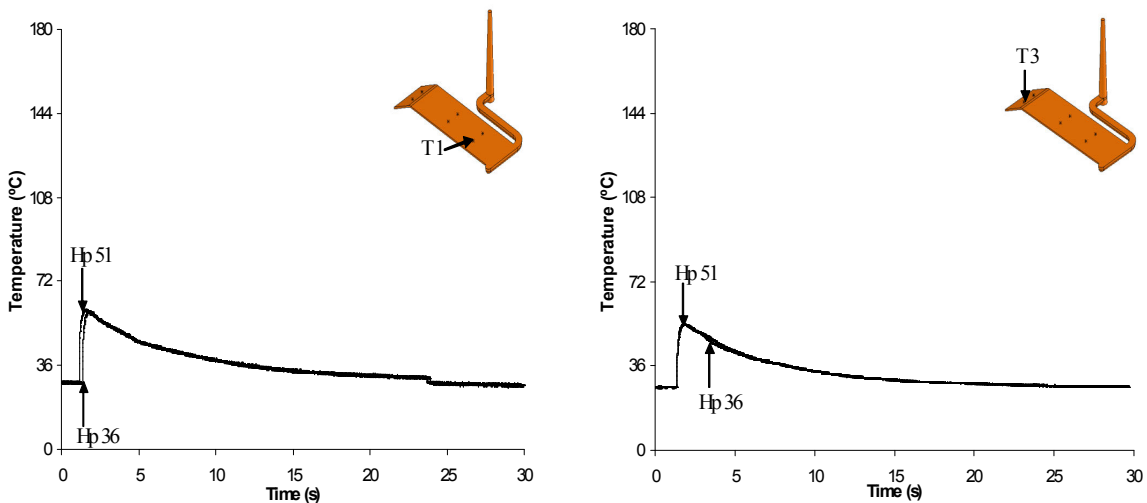


Figure A2.4.1– Influence of the holding pressure on the Temperature evolution at middle of fill. PP with 30% GF mouldings with Holding Pressure of 36 and 51MPa with Mould Temperature at 25°C



a) Position T1

b) Position T3

Figure A2.4.2– Influence of the holding pressure on the Temperature evolution curves in PP30%GF parts. Mouldings with Holding Pressure of 36 and 51MPa with Mould Temperature at 25°C

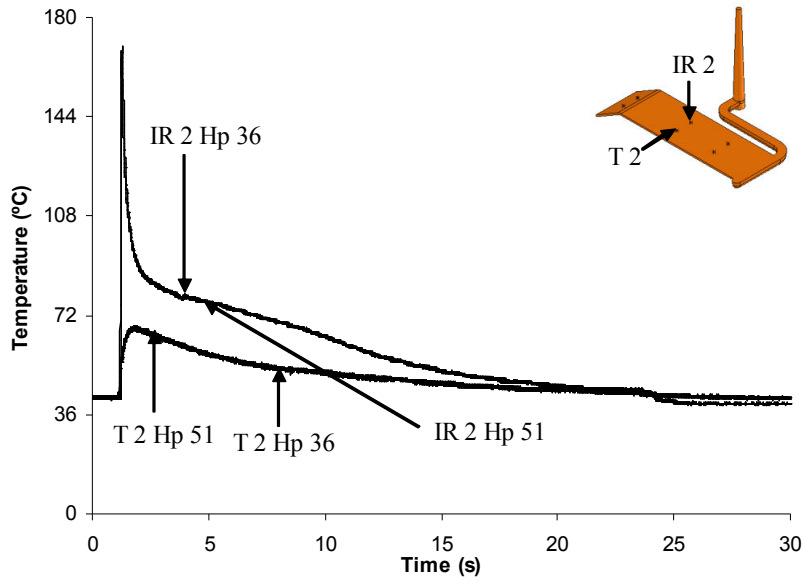
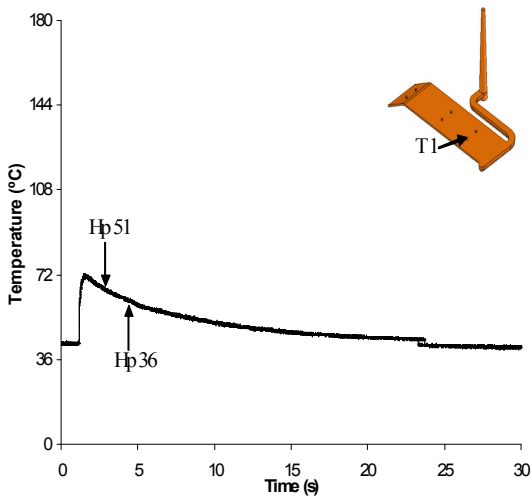
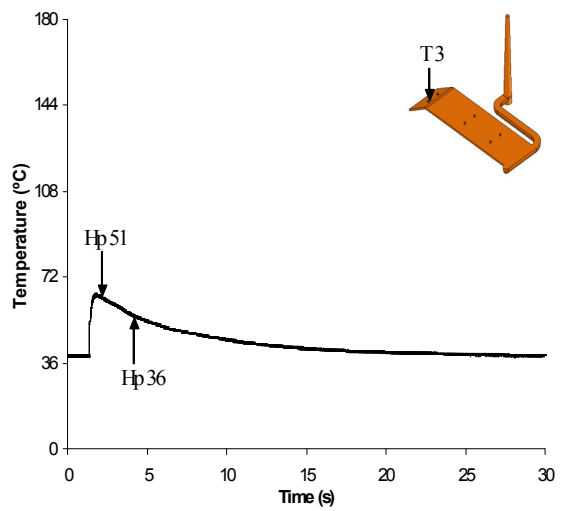


Figure A2.4.3– Influence of the holding pressure on the Temperature evolution at middle of fill. PP with 30% GF mouldings with Holding Pressure of 36 and 51MPa with Mould Temperature at 40°C



a) Position T1



b) Position T3

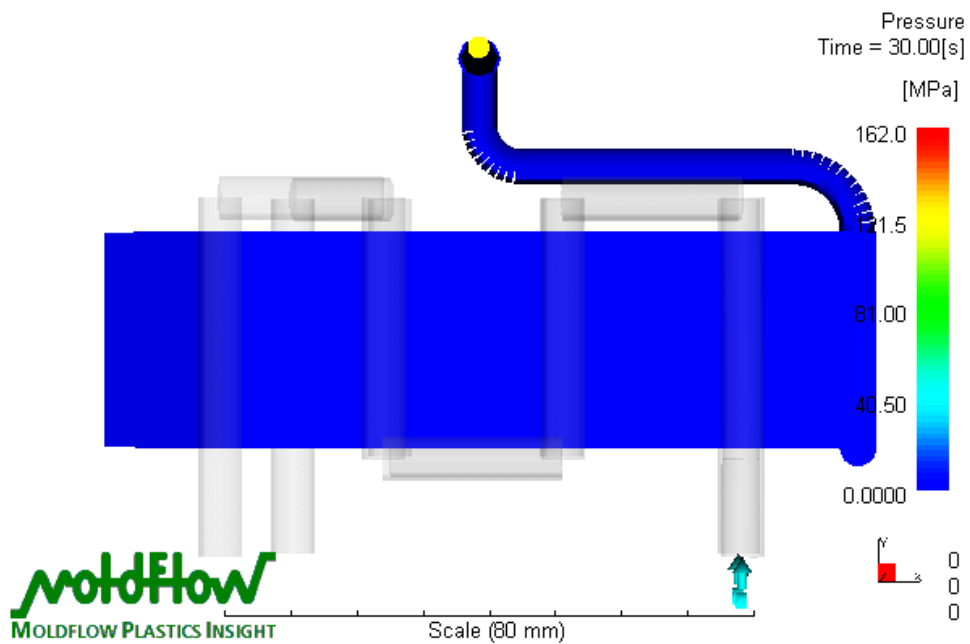
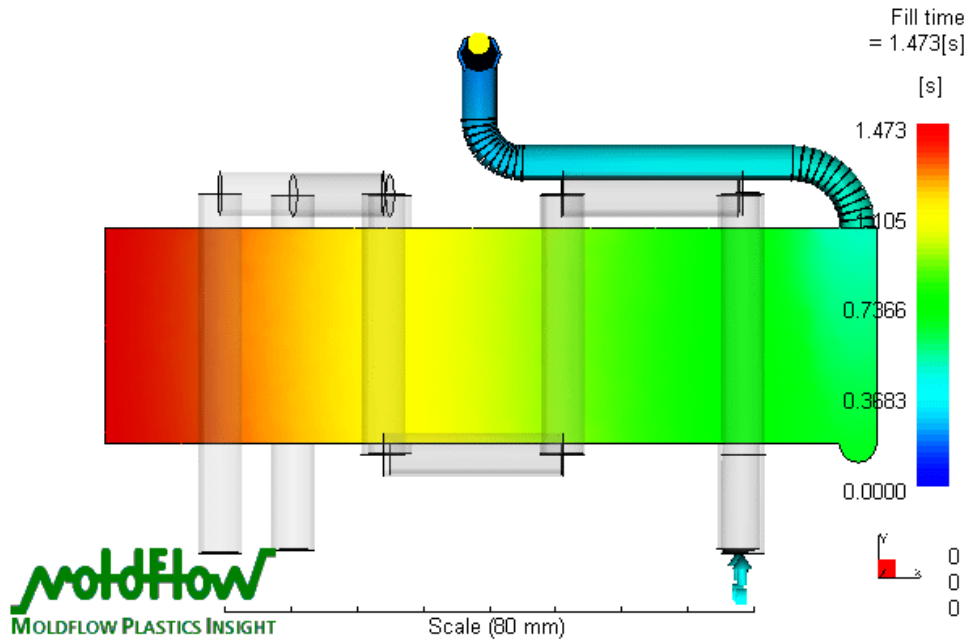
Figure A2.4.4– Influence of the holding pressure on the Temperature evolution curves in PP30%GF parts. Mouldings with Holding Pressure of 36 and 51MPa with Mould Temperature at 40°C

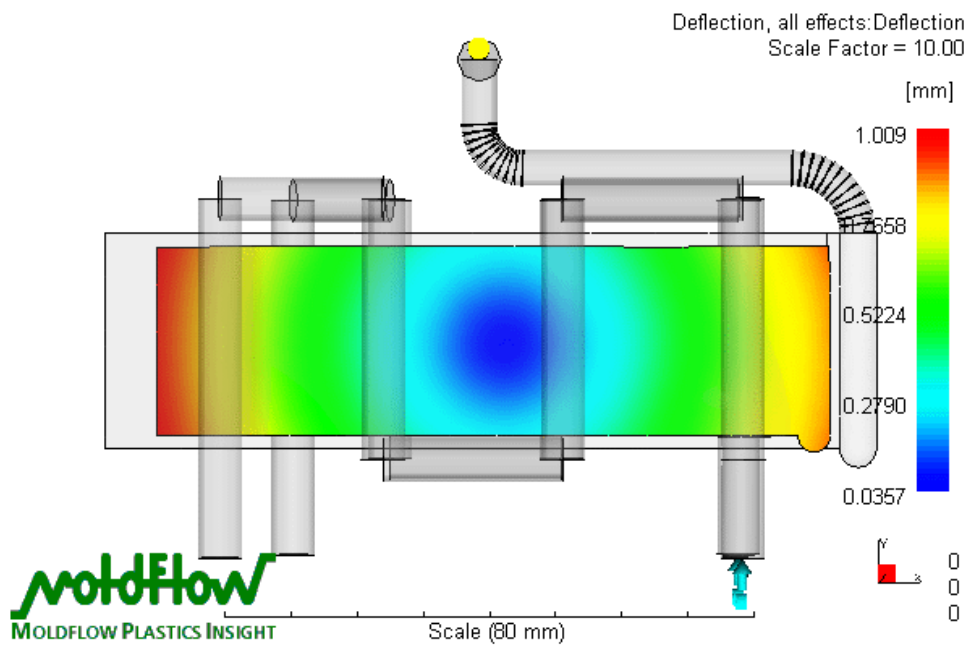
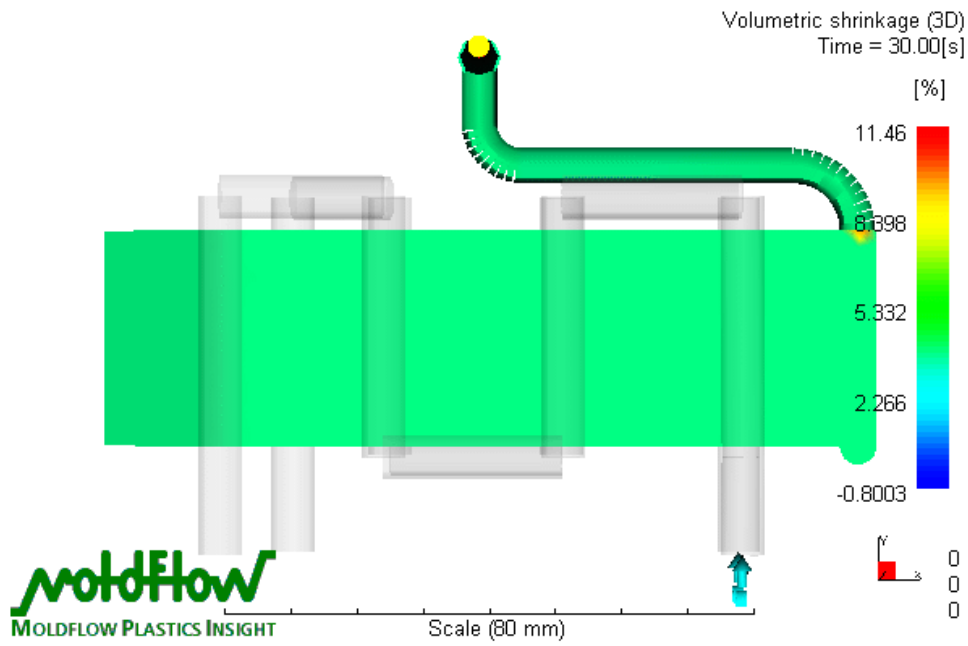
APPENDIX A3-3D Moldflow simulation results

(Cool, Flow, Warp)

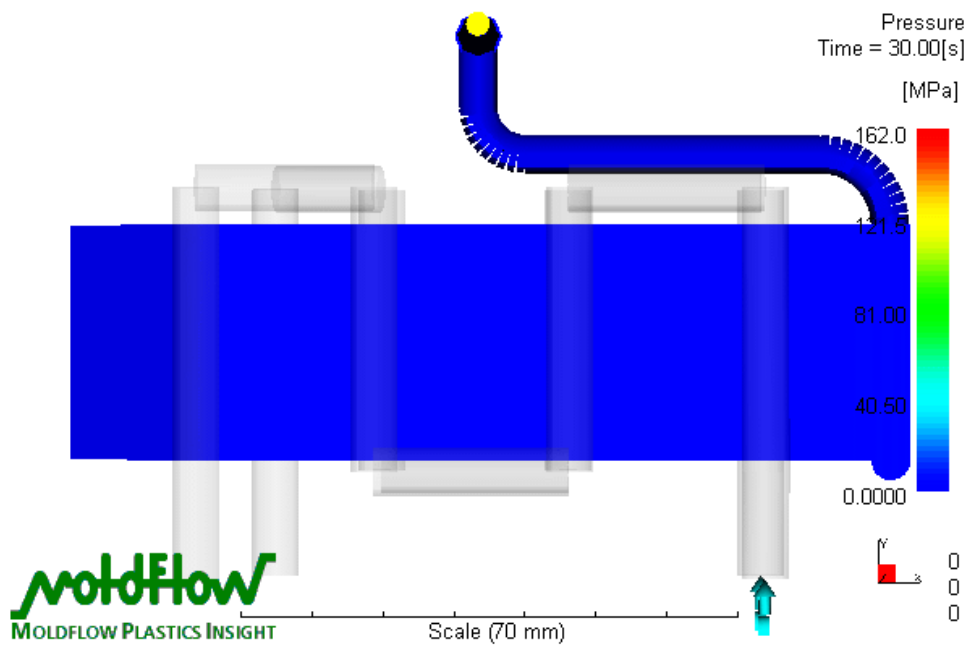
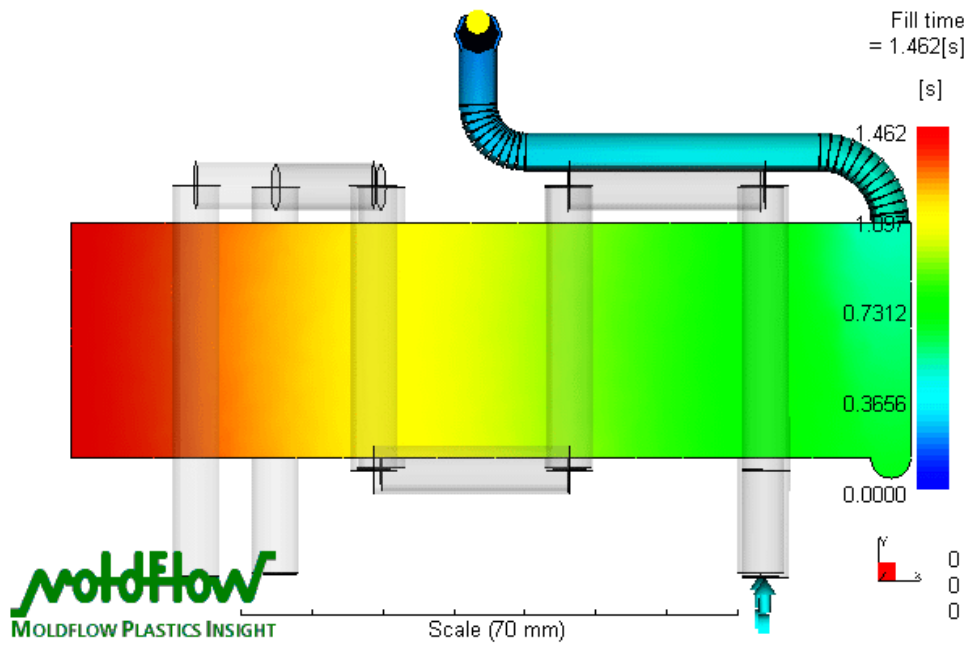
A3.1-Simulation results for PC

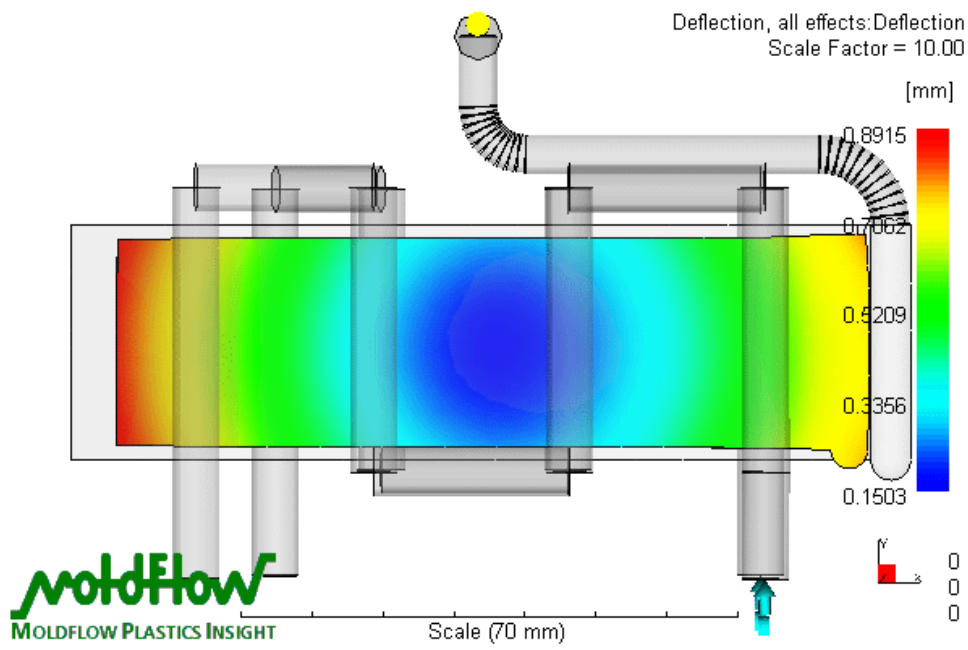
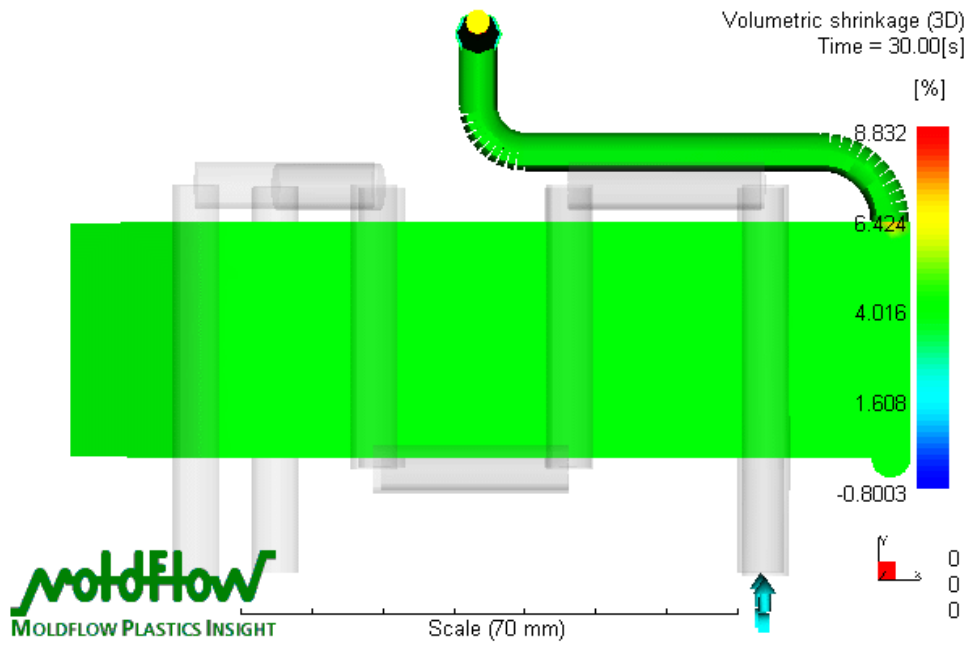
A.3.1.1-Condition of $H_p=7\text{MPa}$ and $T_m=80^\circ\text{C}$





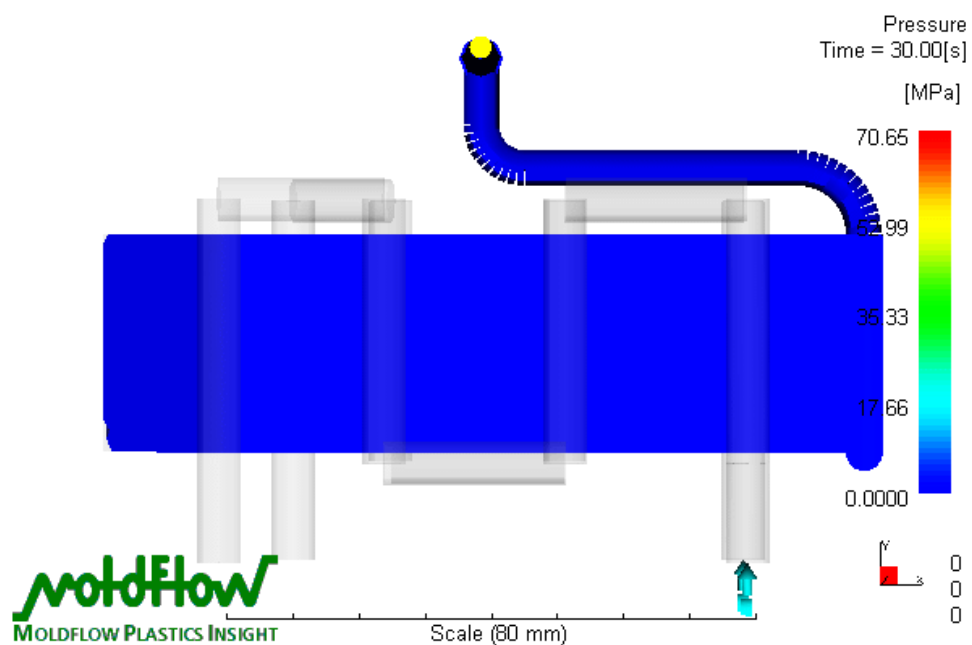
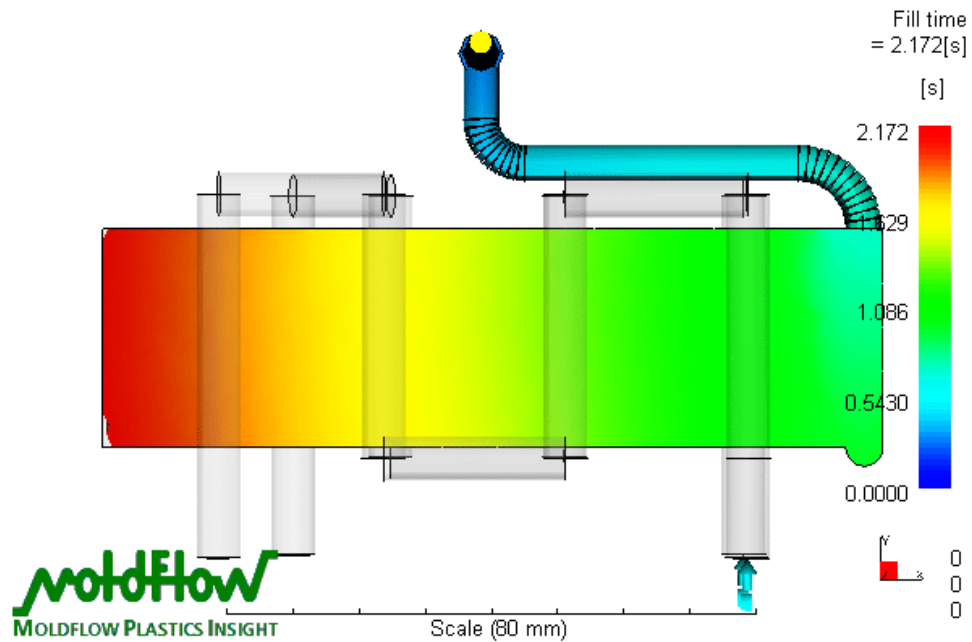
A.3.1.2-Condition of $H_p=51\text{MPa}$ and $T_m=80^\circ\text{C}$

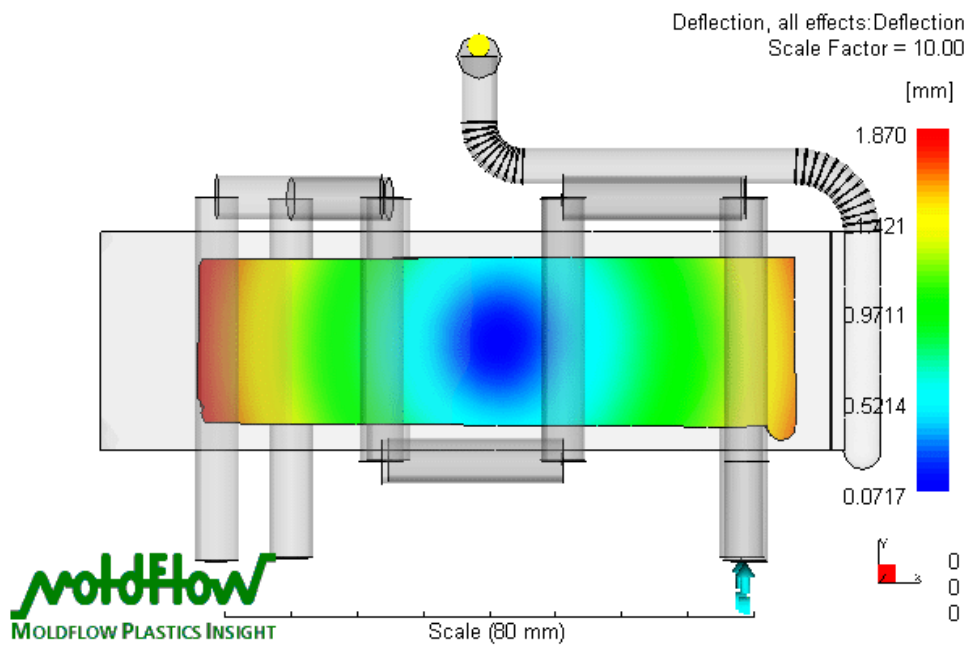
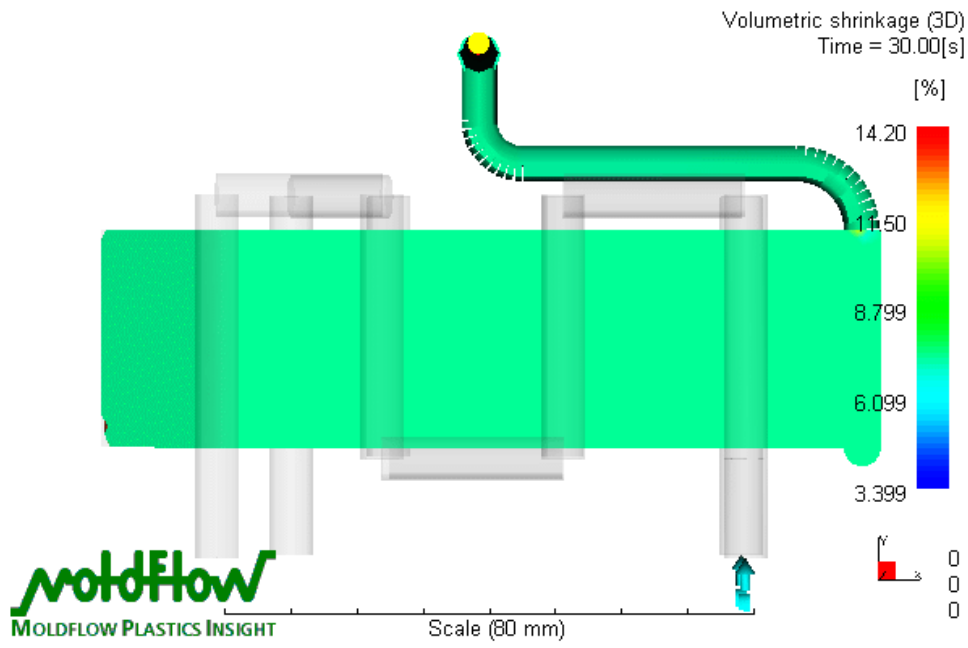




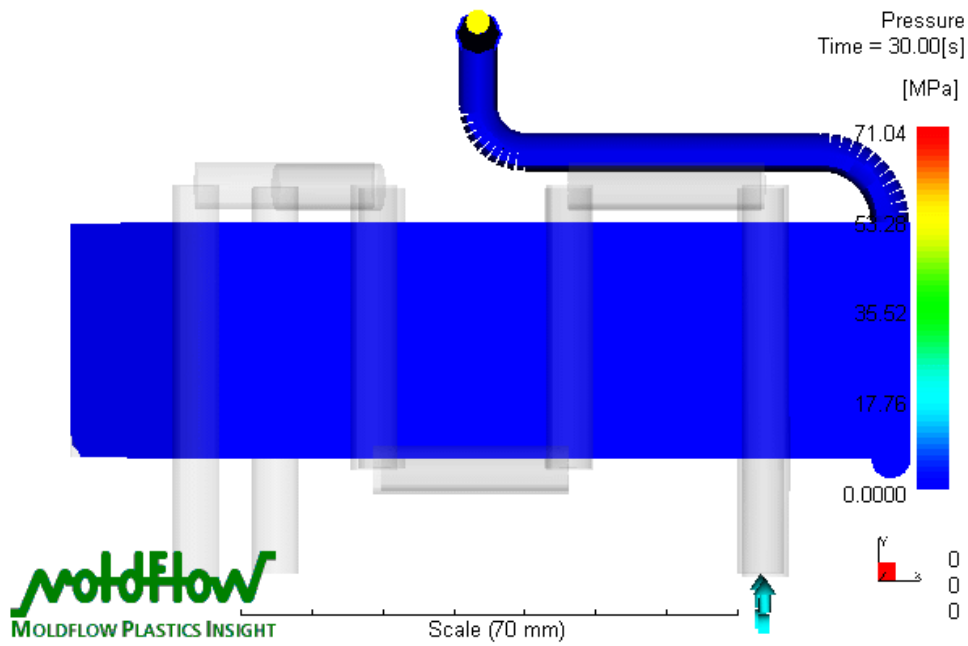
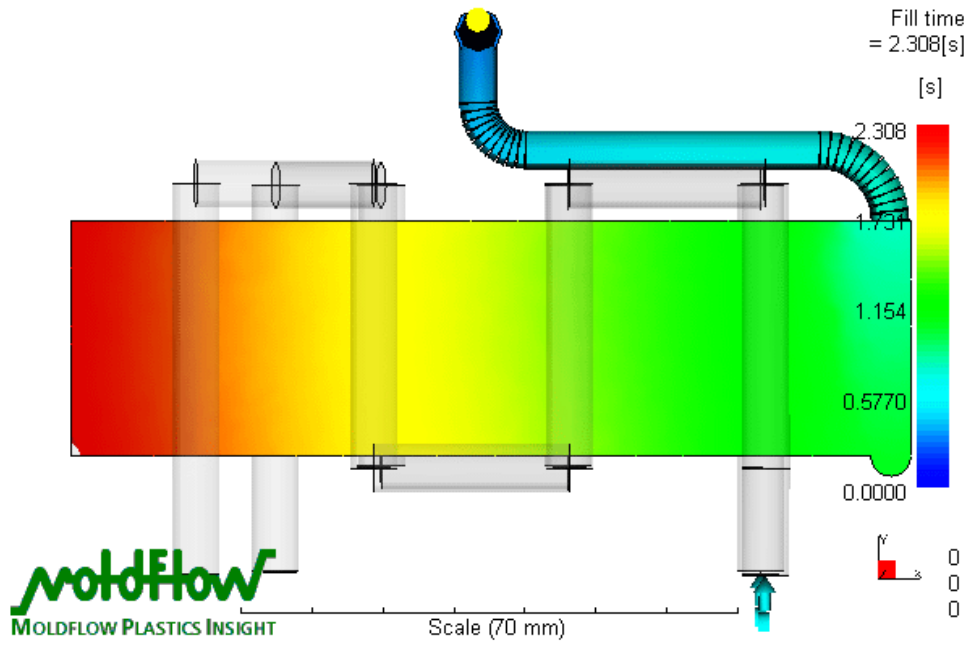
A3.2-Simulation results for PP

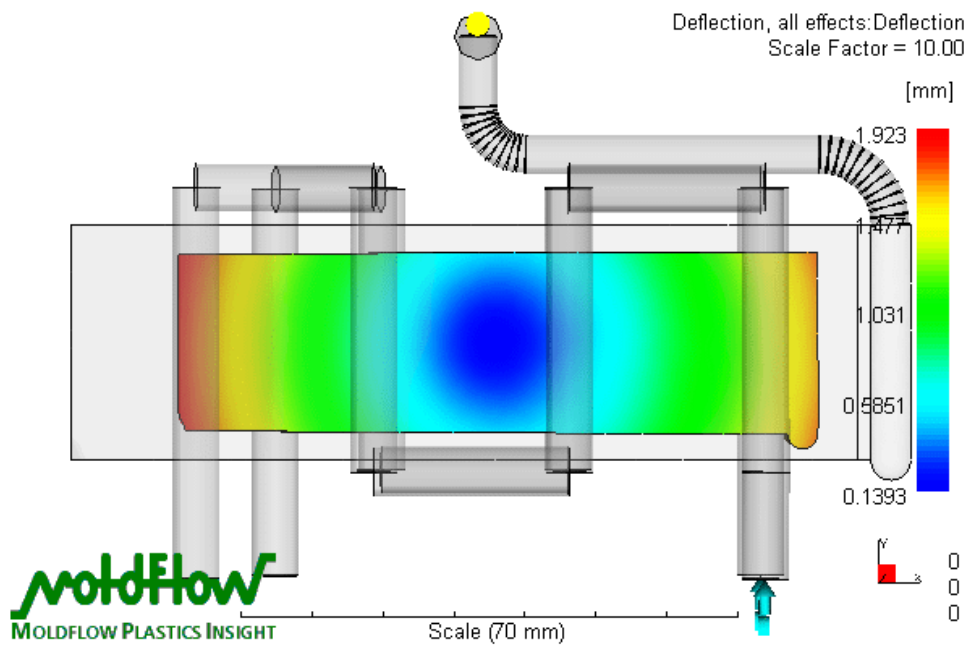
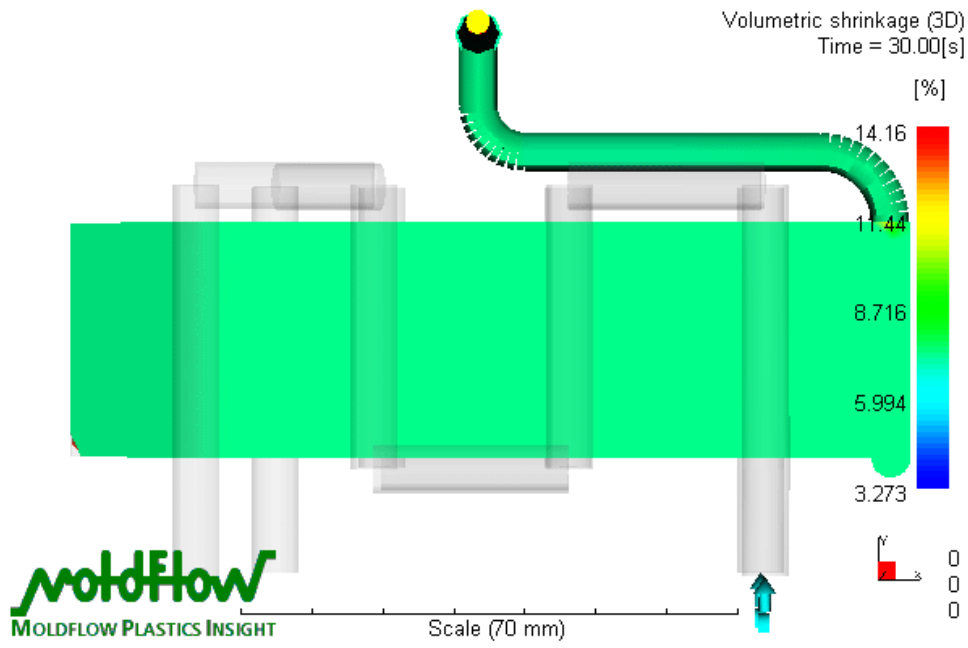
A.3.2.1-Condition of $H_p=7\text{MPa}$ and $T_m=25^\circ\text{C}$



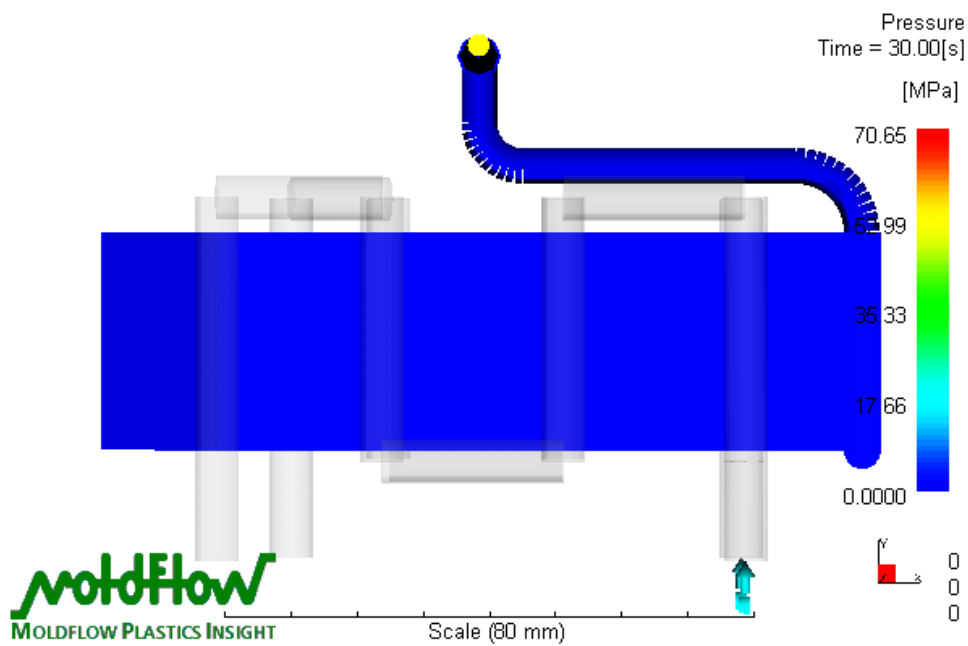
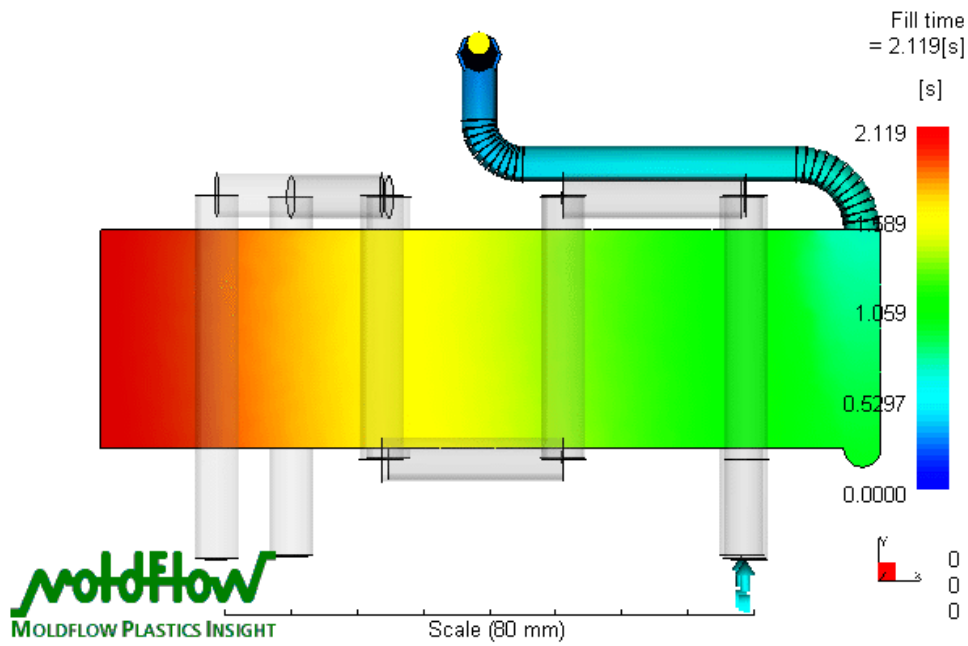


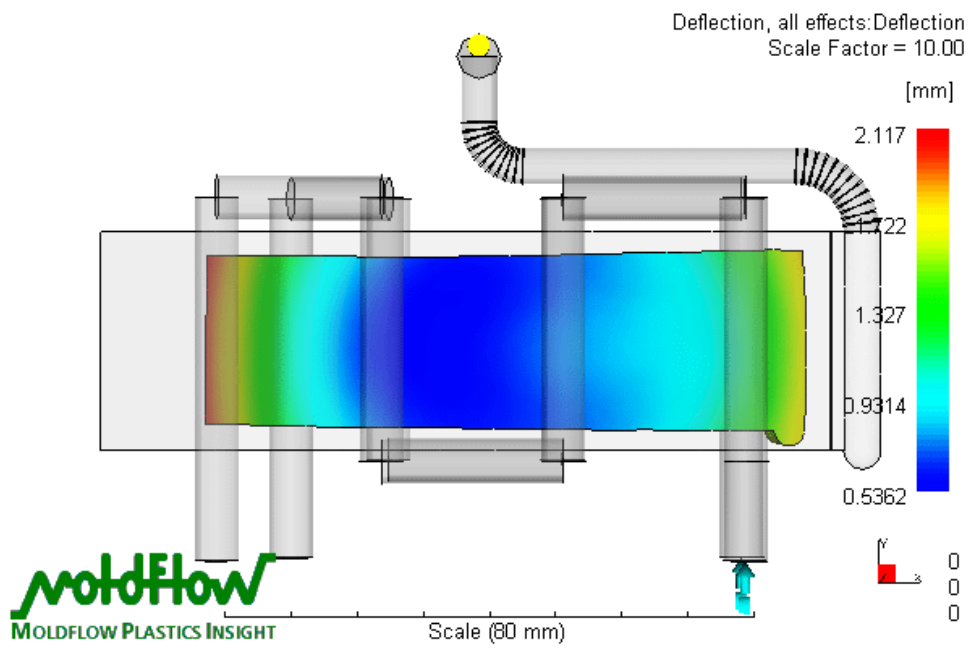
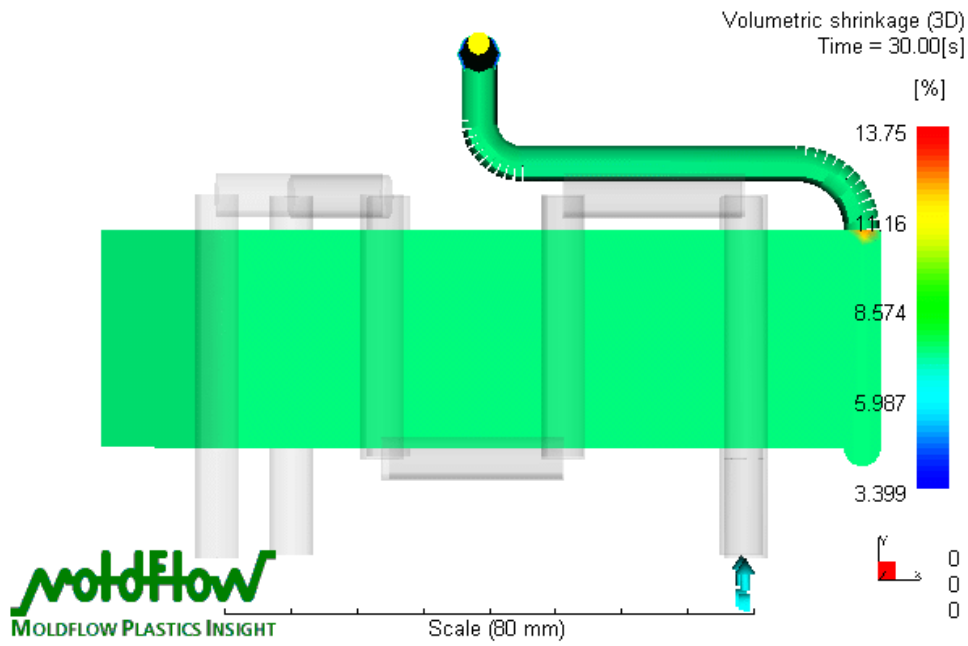
A.3.2.2-Condition of $H_p=7\text{MPa}$ and $T_m=40^\circ\text{C}$



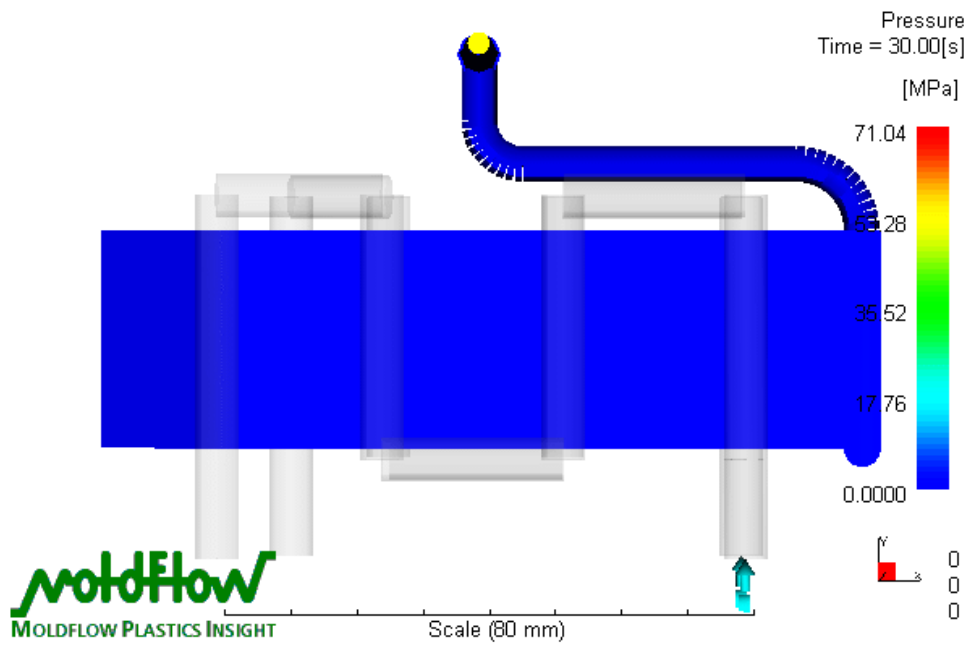
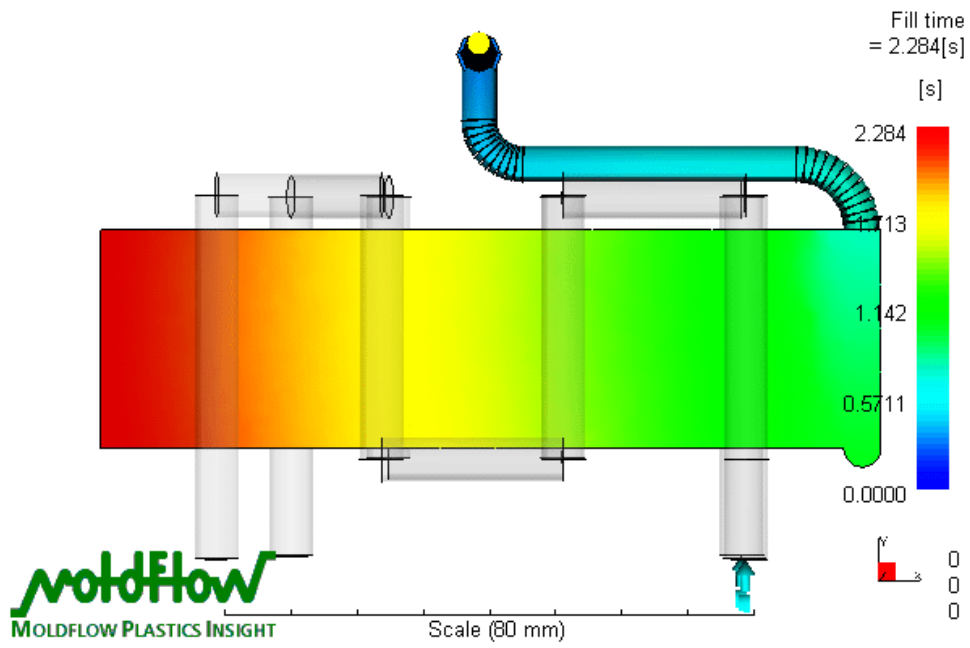


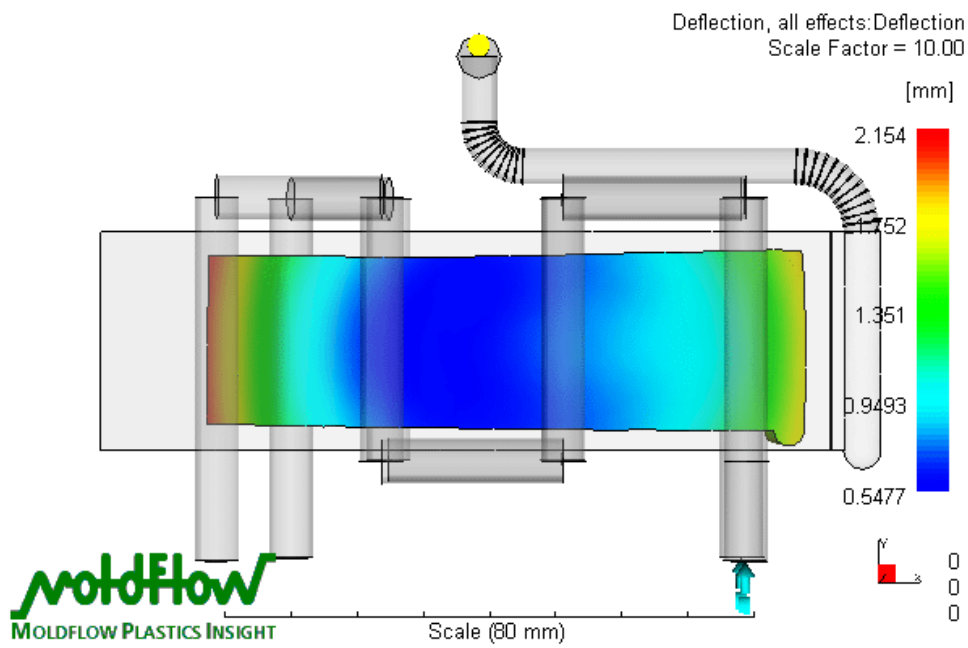
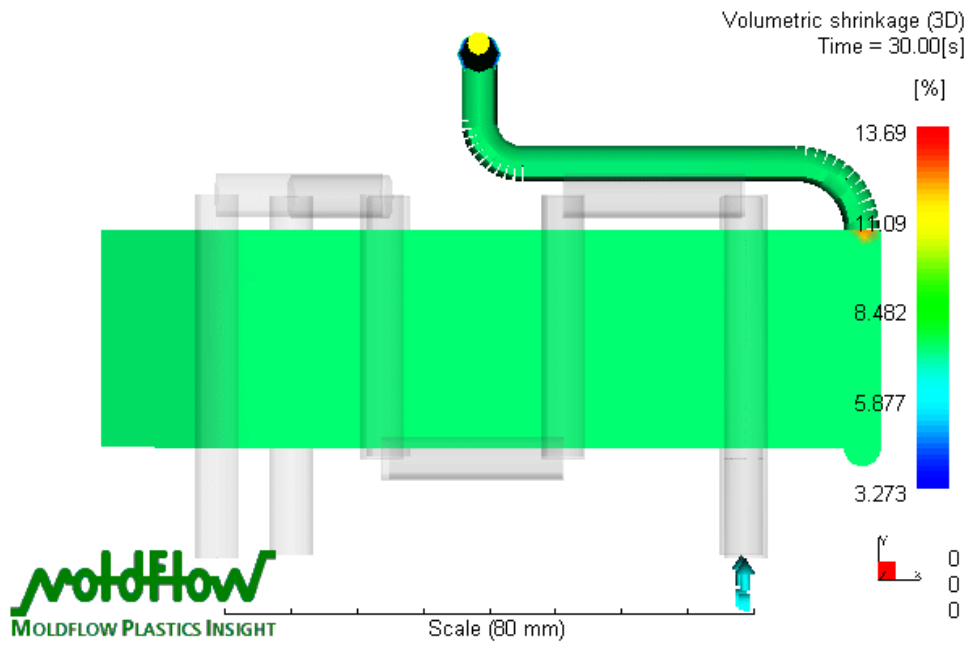
A.3.2.3-Condition of $H_p=51\text{MPa}$ and $T_m=25^\circ\text{C}$





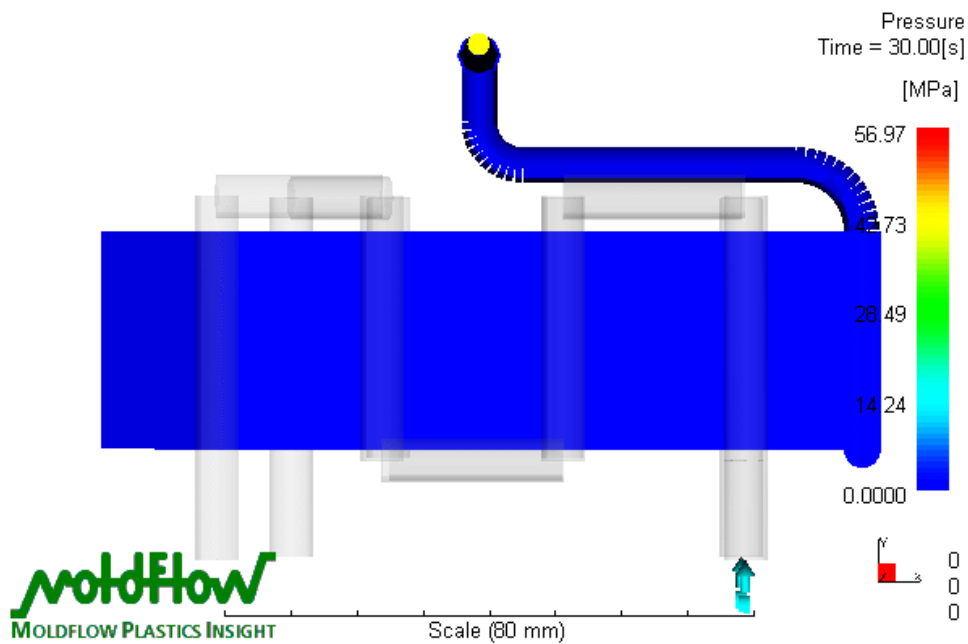
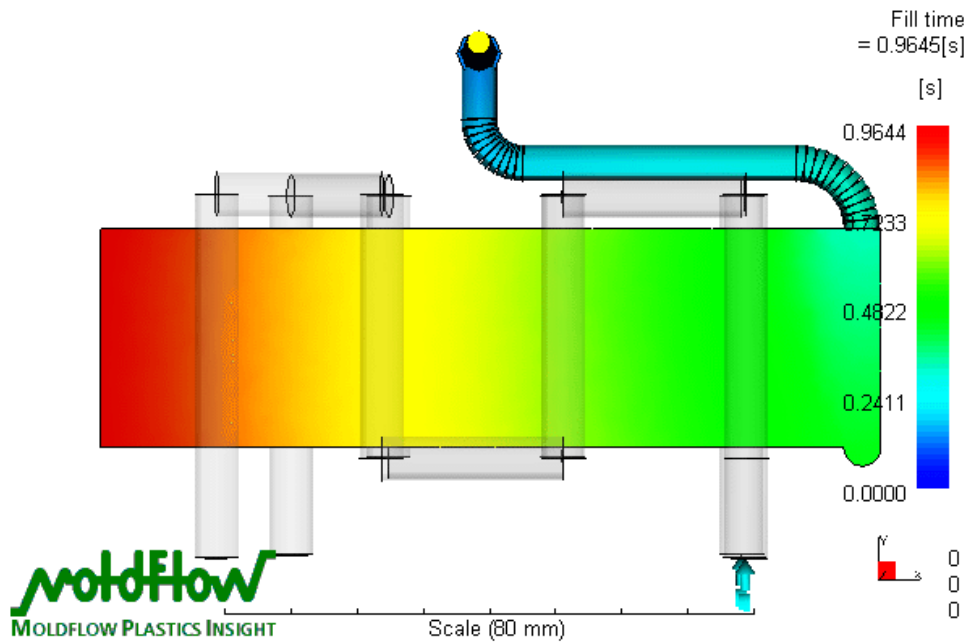
A.3.2.4-Condition of $H_p=51\text{MPa}$ and $T_m=40^\circ\text{C}$

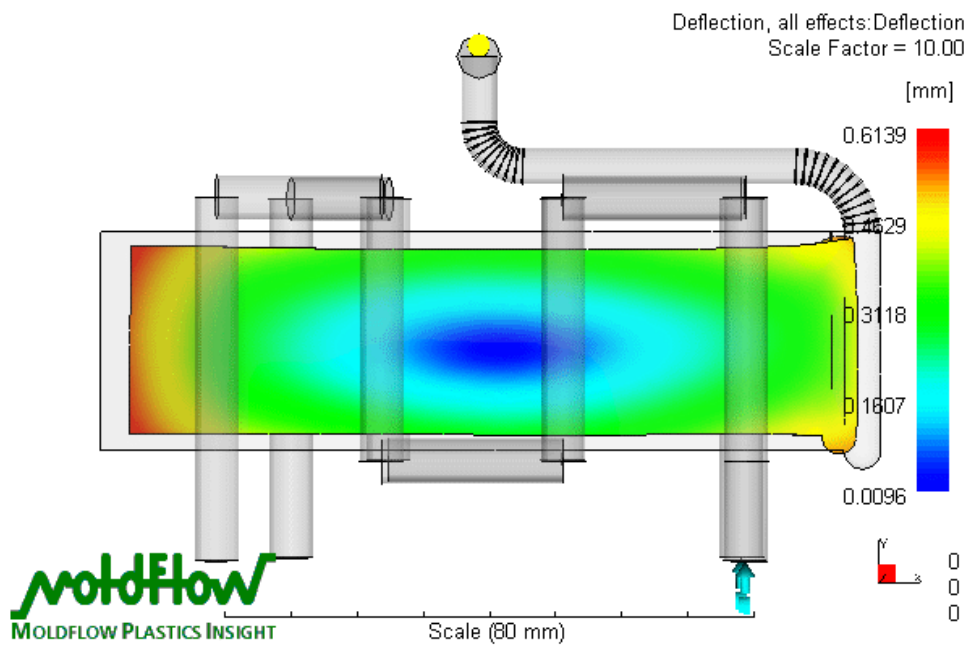
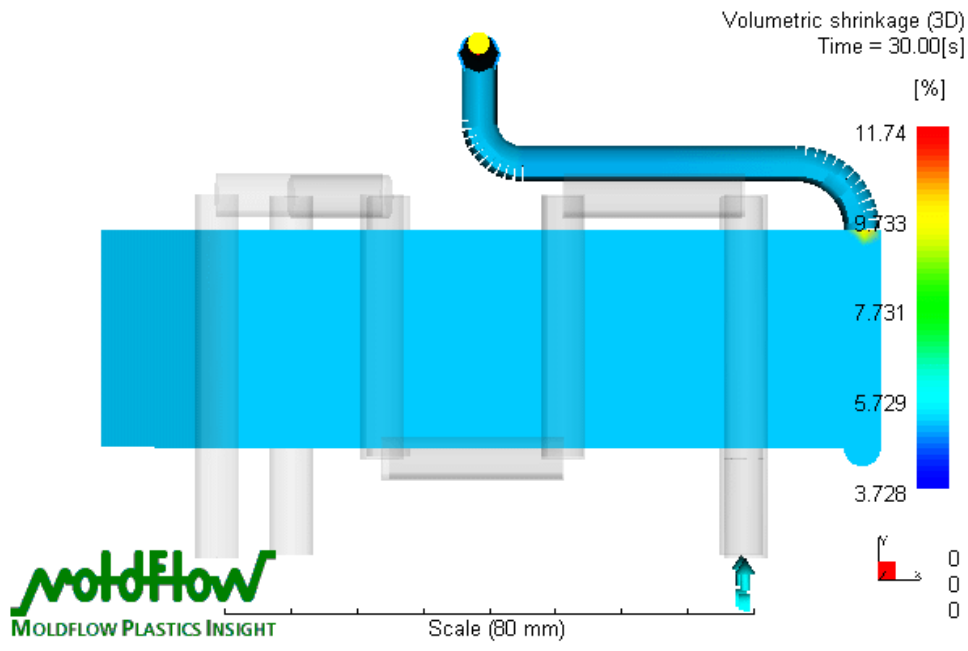




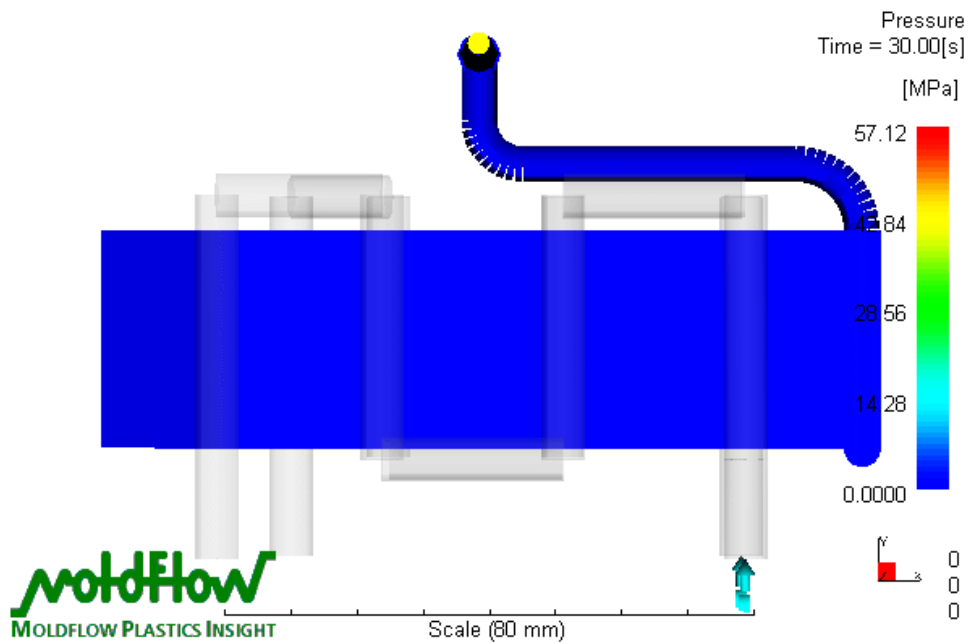
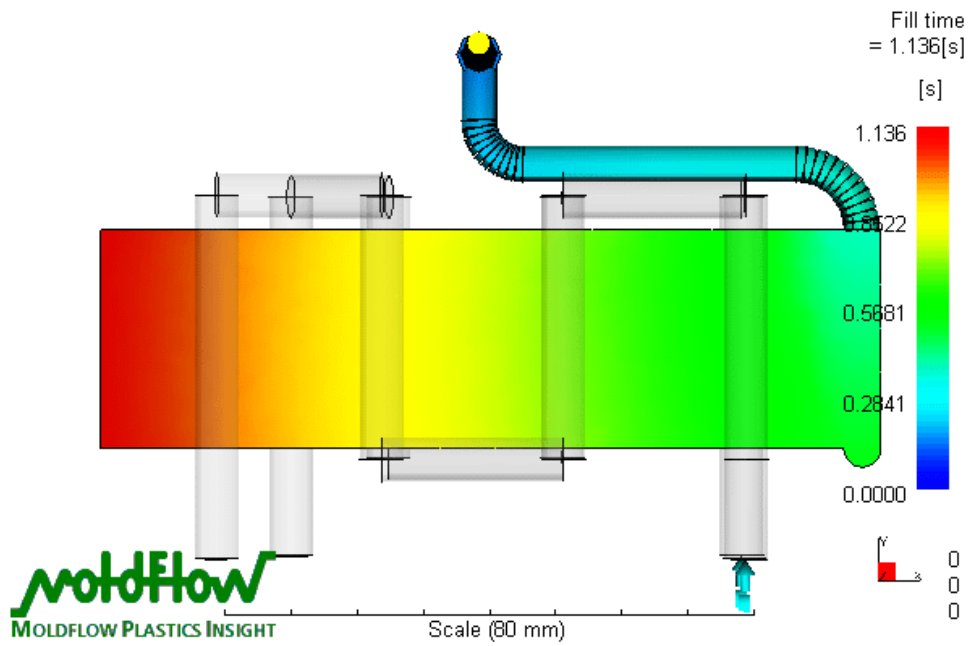
A3.3-Simulation results for reinforced PP with 20% of GF

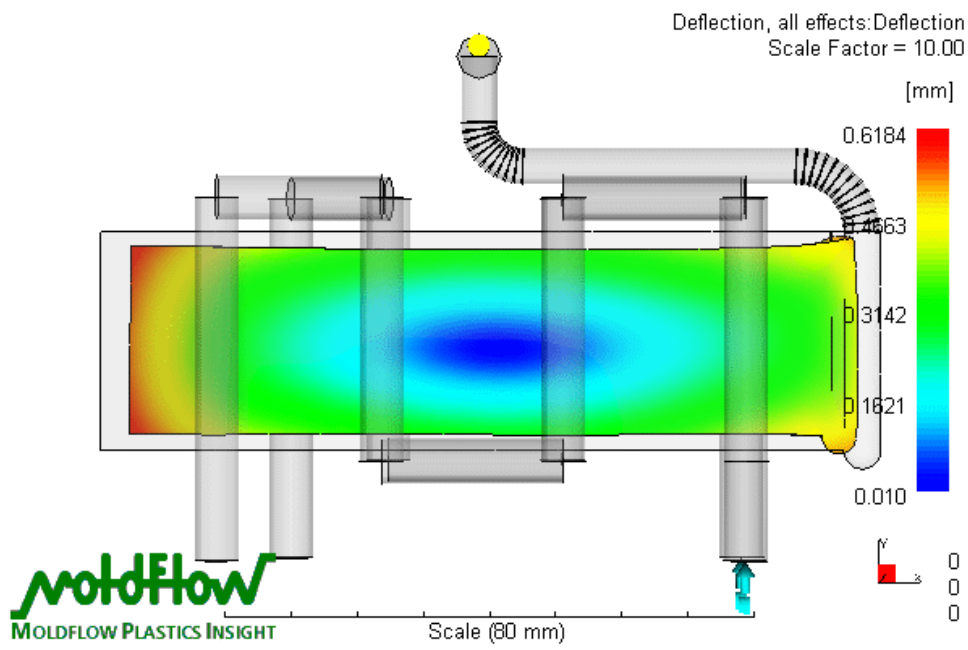
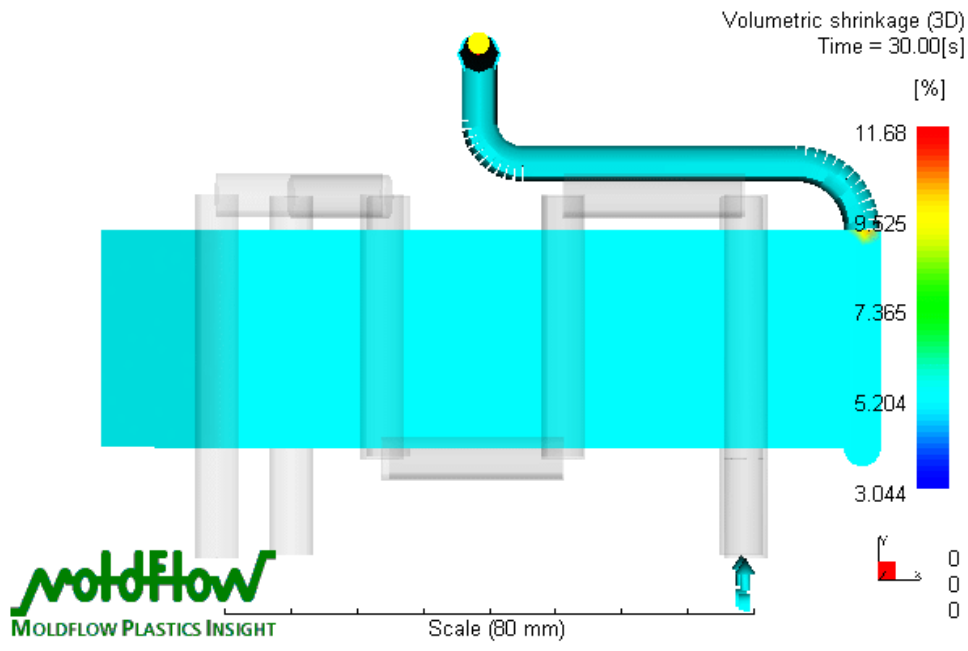
A.3.3.1-Condition of $H_p=7\text{MPa}$ and $T_m=25^\circ\text{C}$



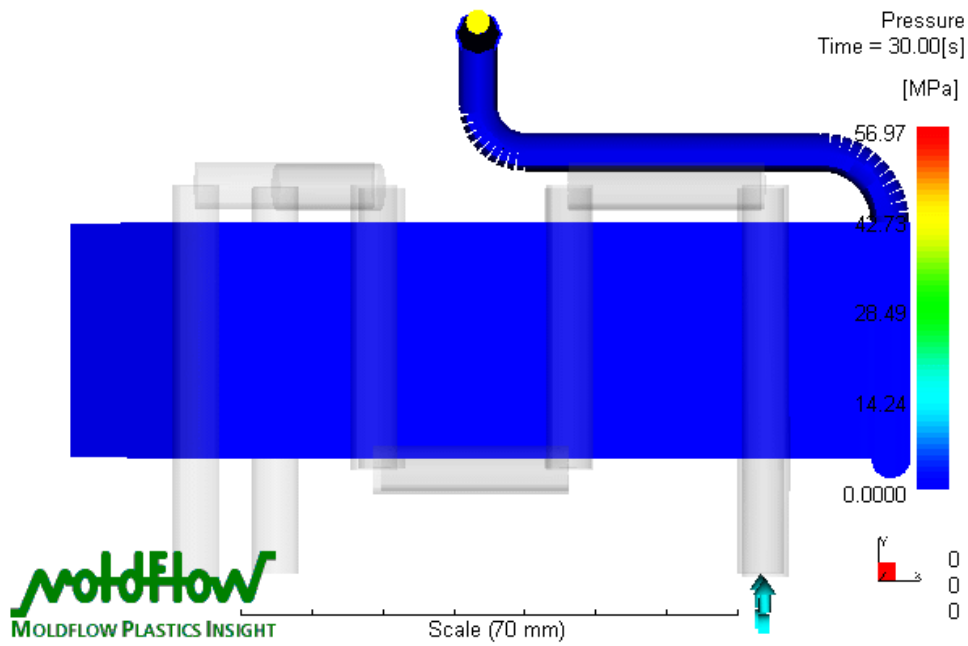
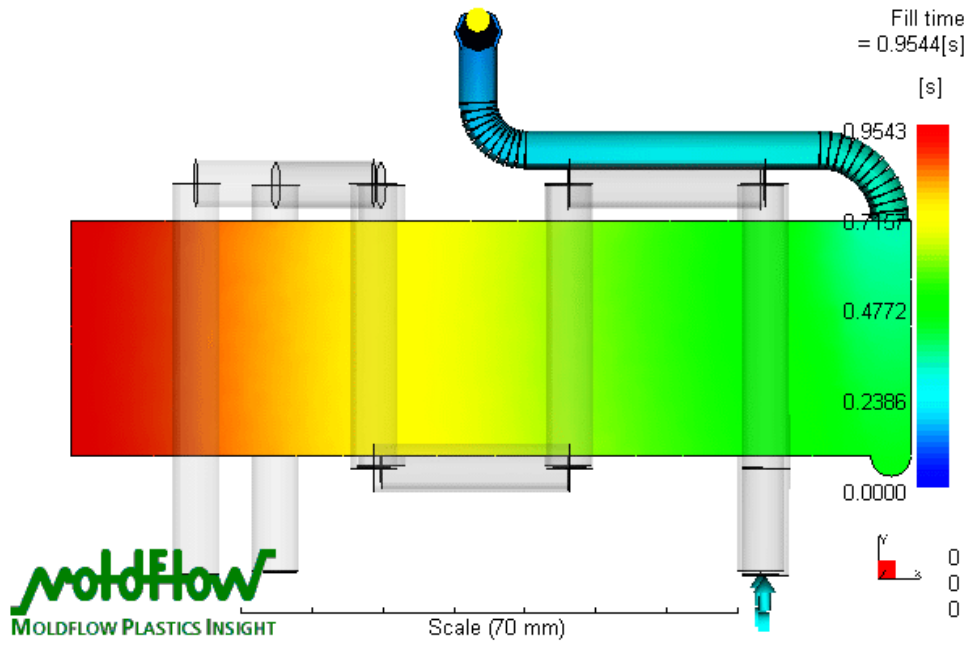


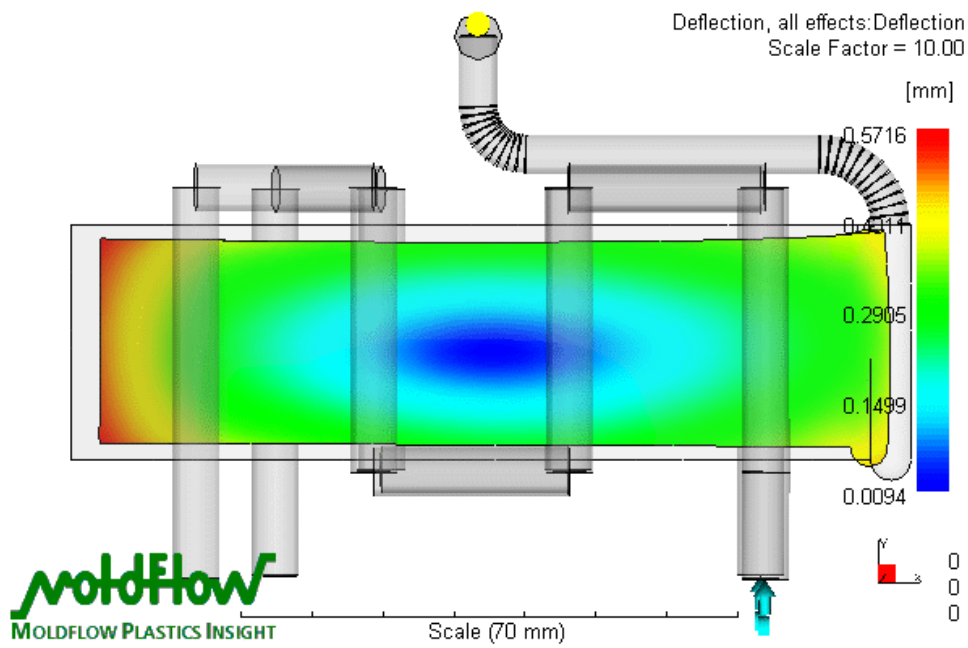
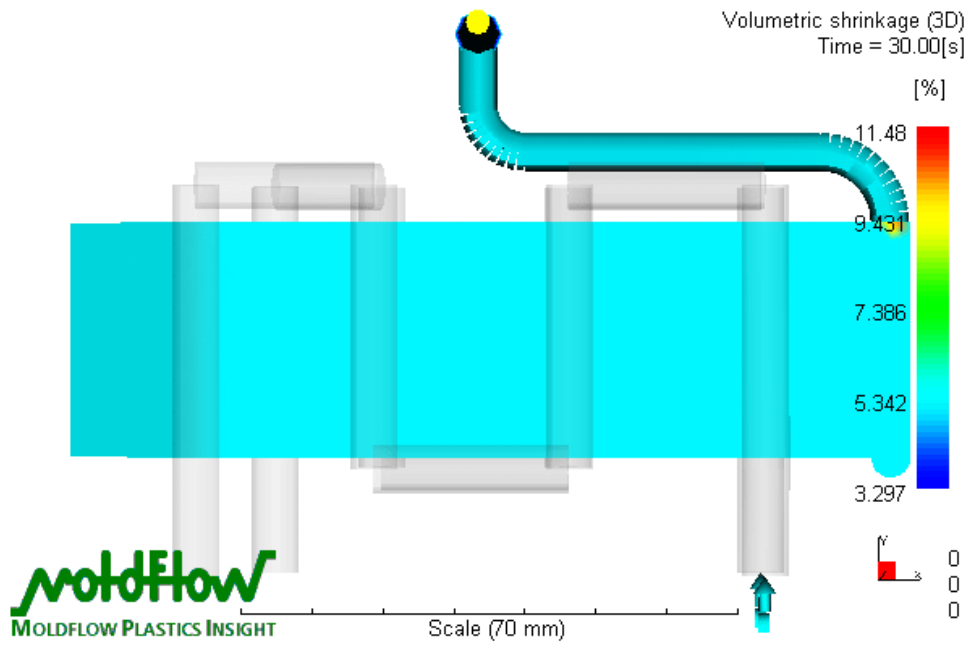
A.3.3.2-Condition of $H_p=7\text{MPa}$ and $T_m=40^\circ\text{C}$



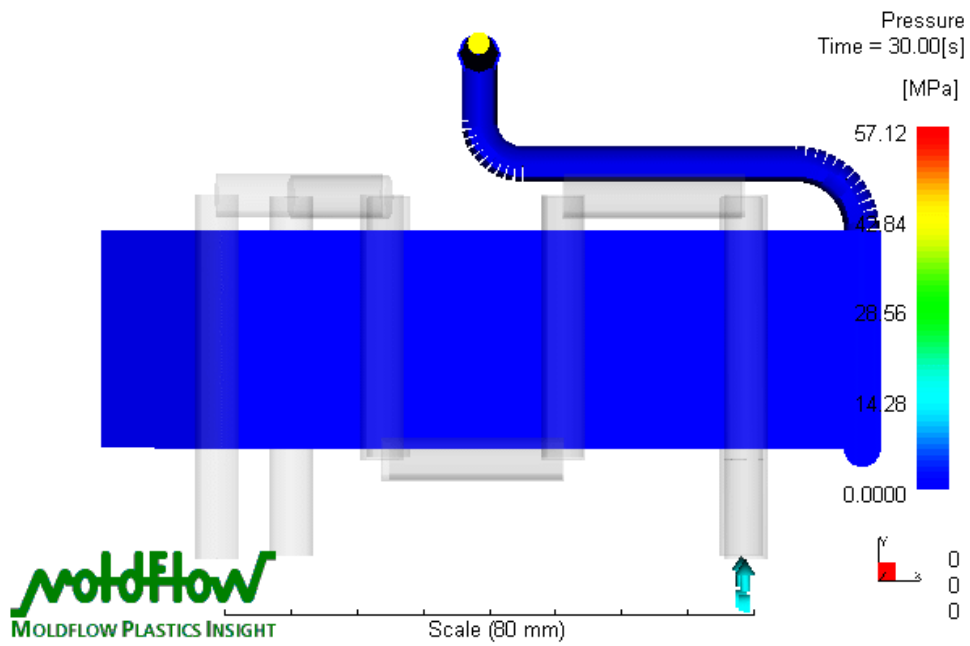
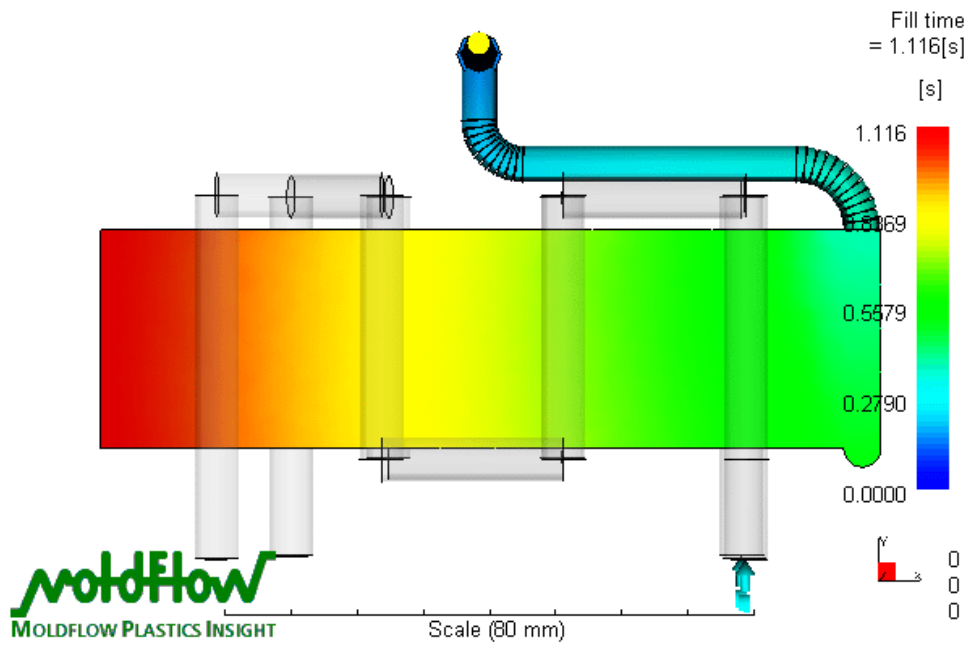


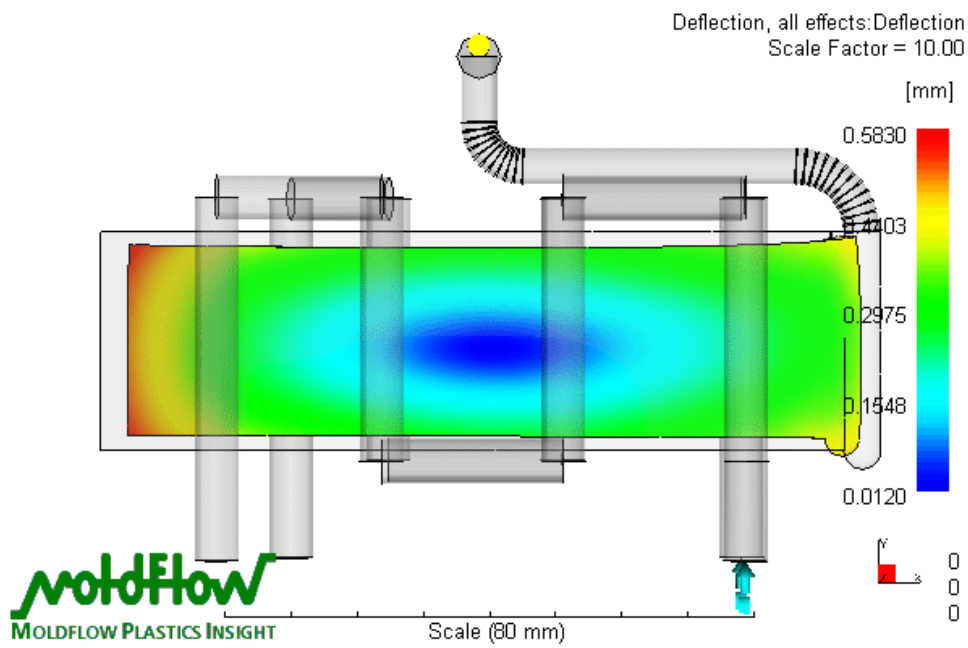
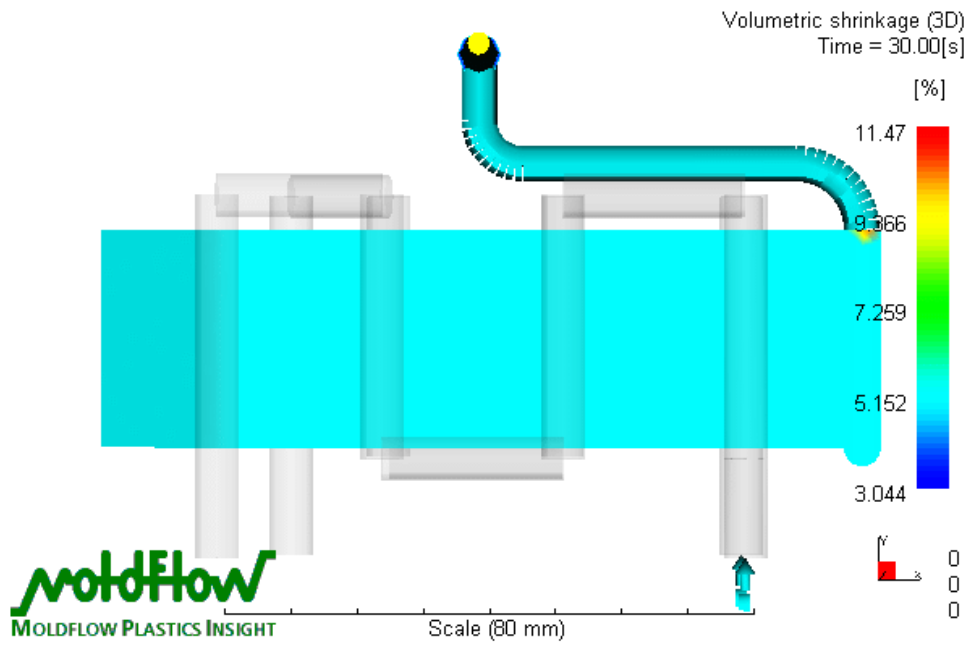
A.3.3.3-Condition of $H_p=36\text{MPa}$ and $T_m=25^\circ\text{C}$





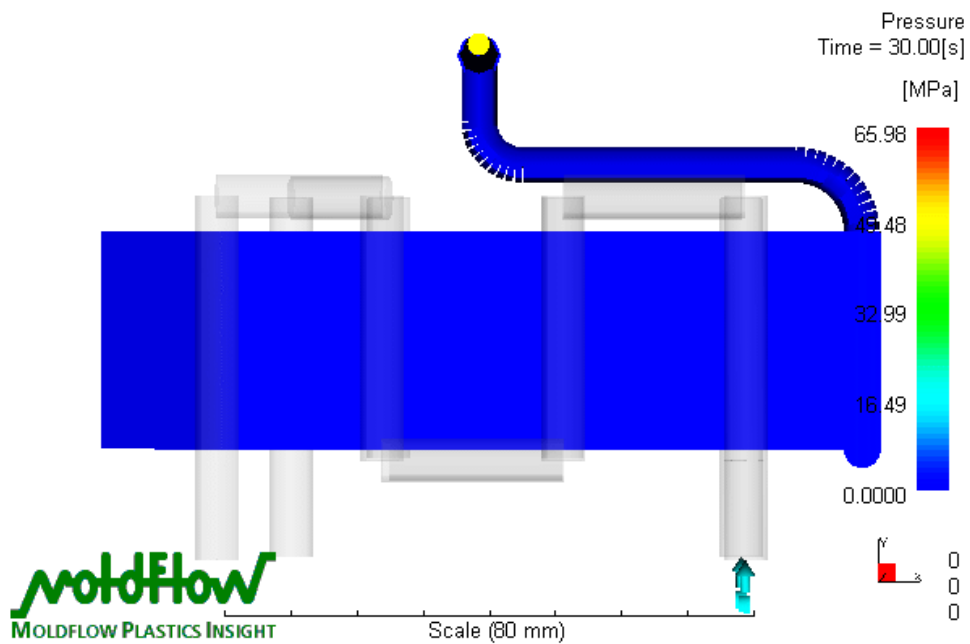
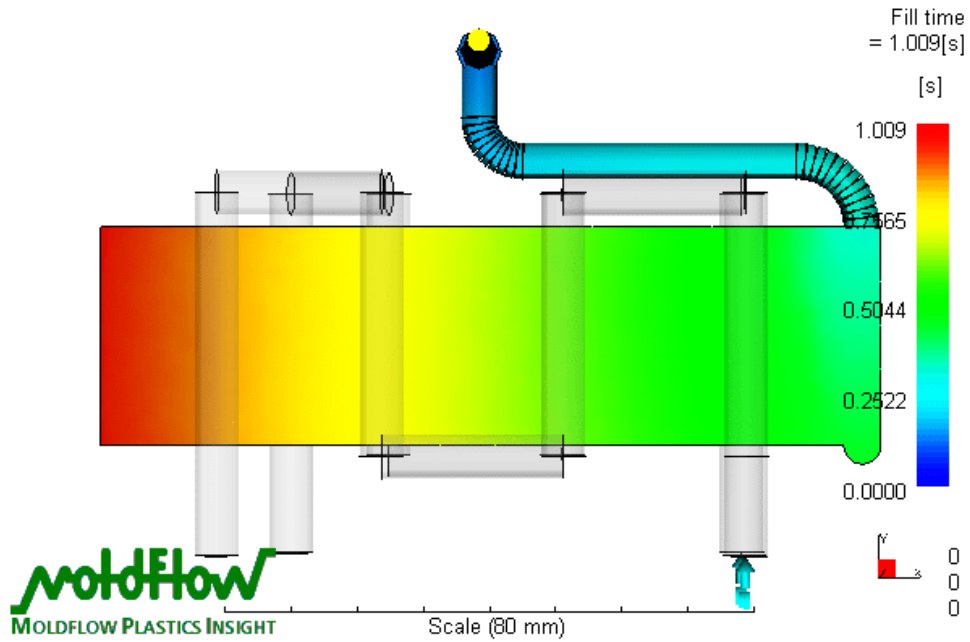
A.3.3.4-Condition of $H_p=36\text{MPa}$ and $T_m=40^\circ\text{C}$

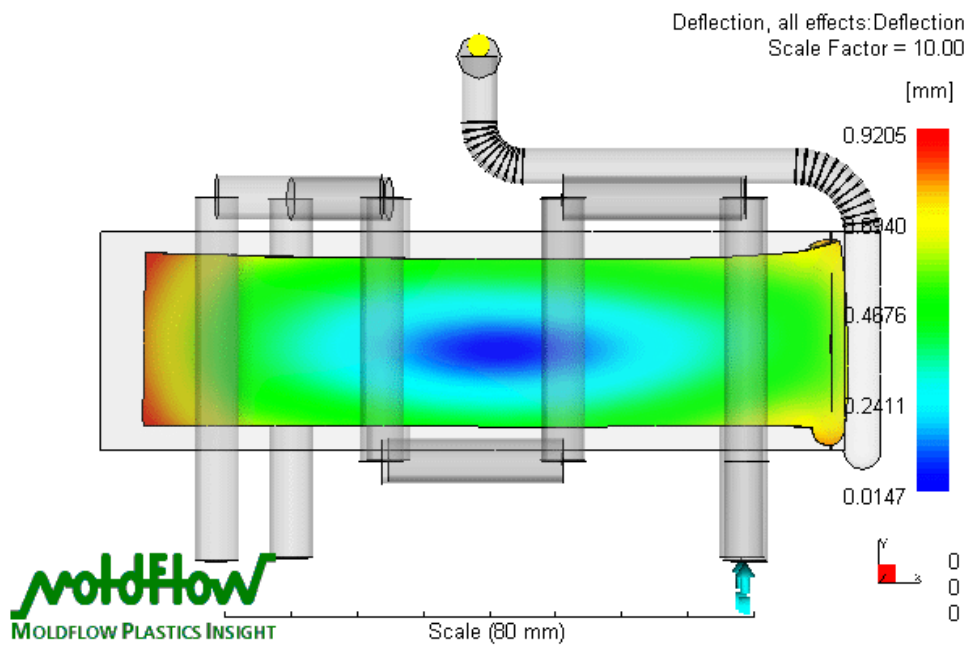
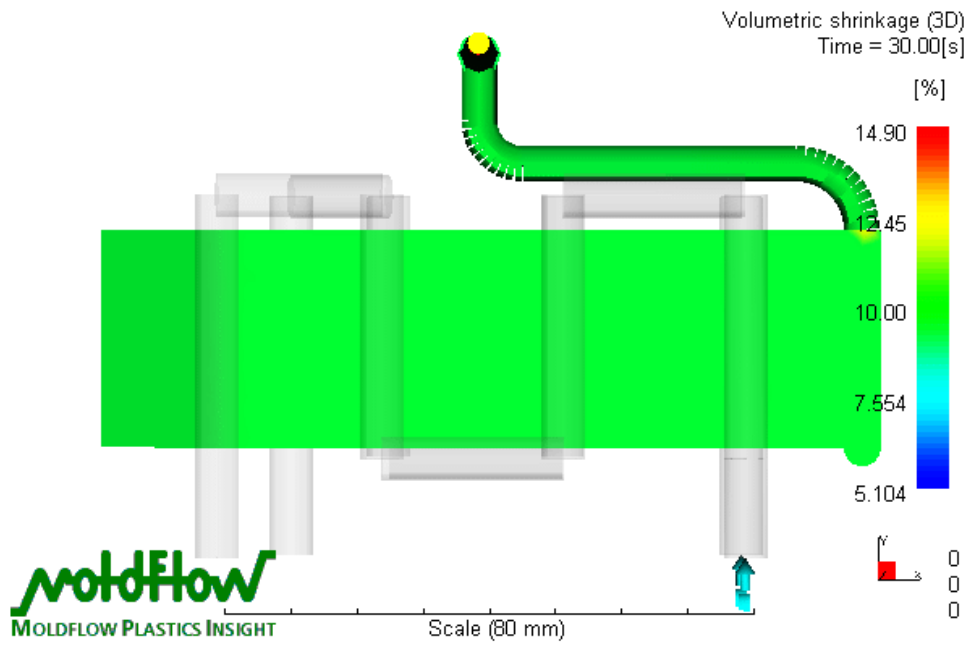




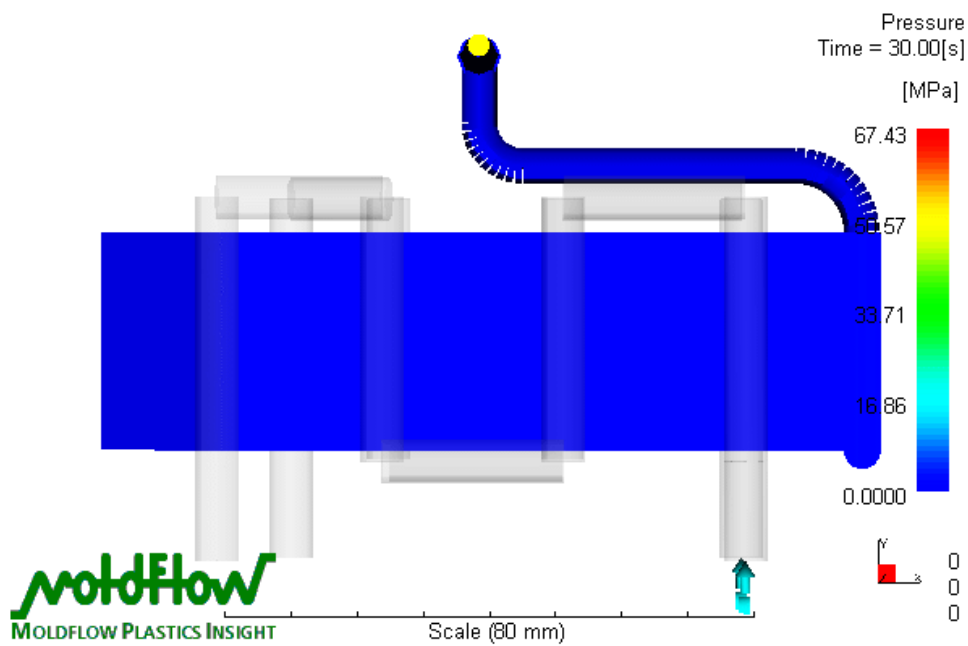
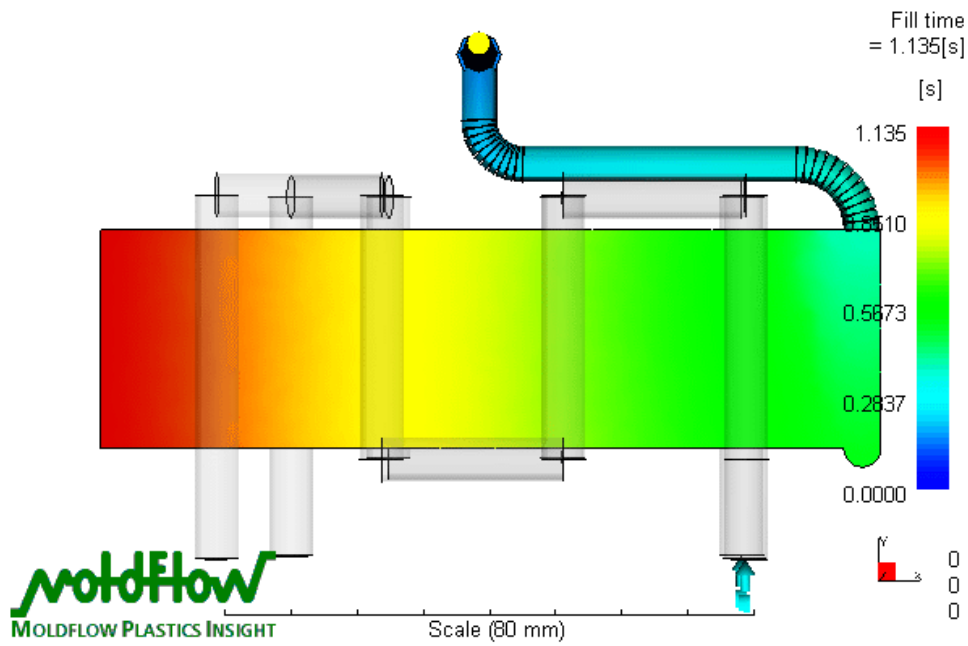
A3.4-Simulation results for reinforced PP with 30% of GF

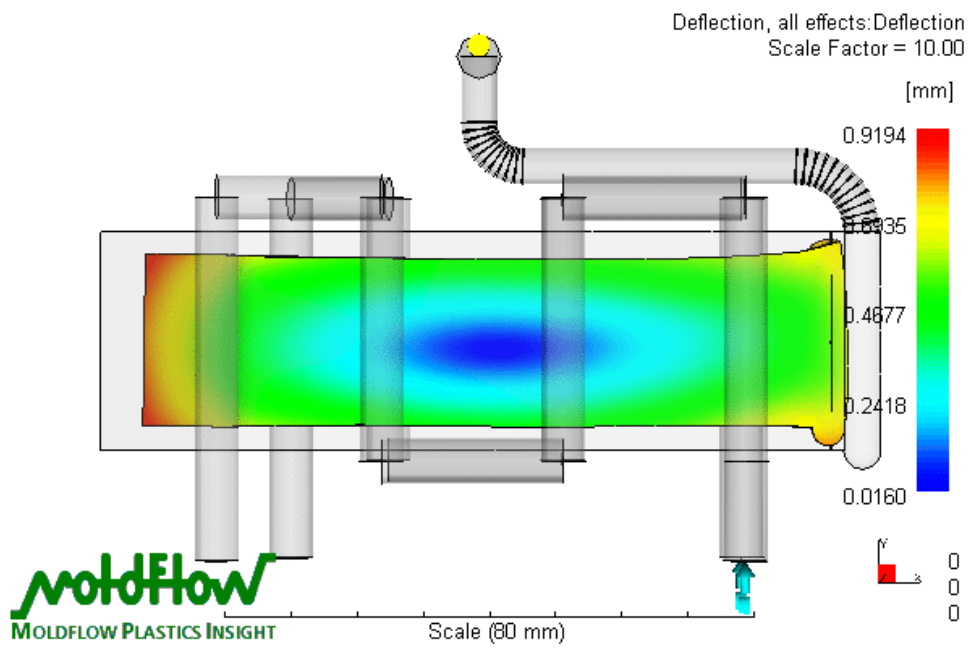
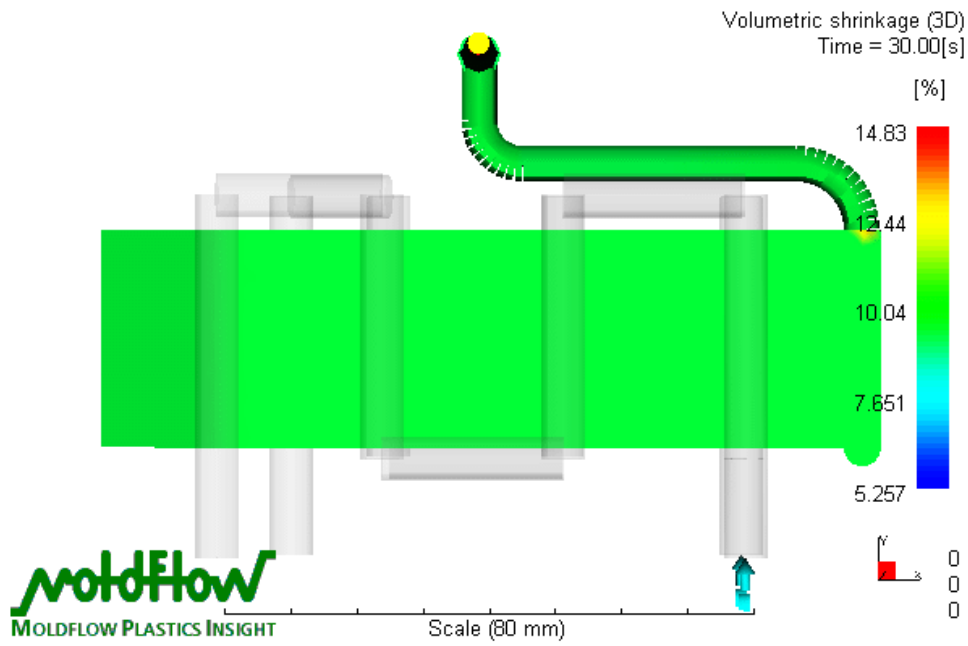
A.3.4.1-Condition of $H_p=7\text{MPa}$ and $T_m=25^\circ\text{C}$



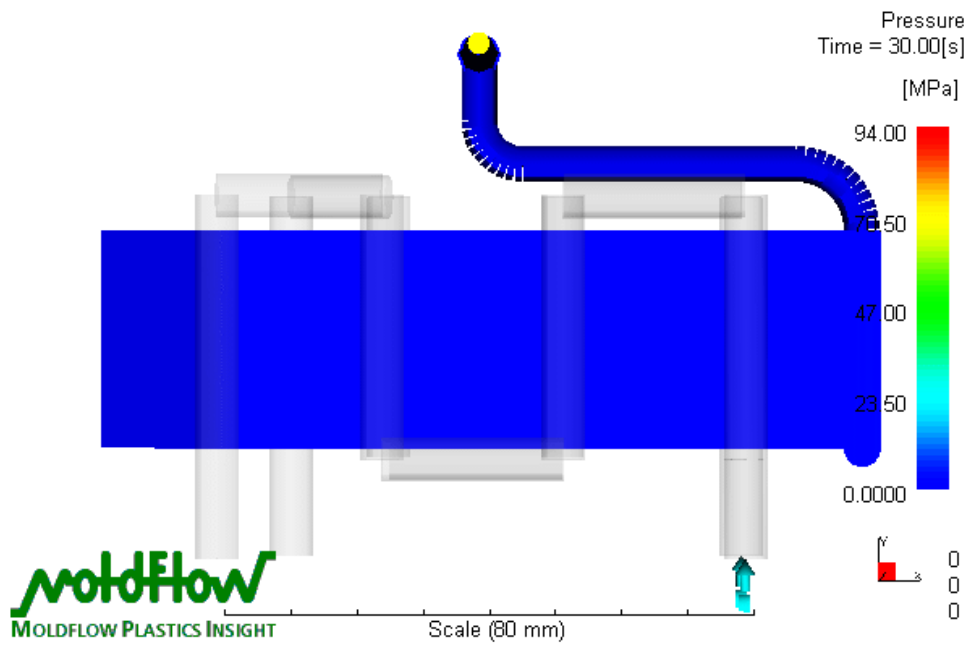
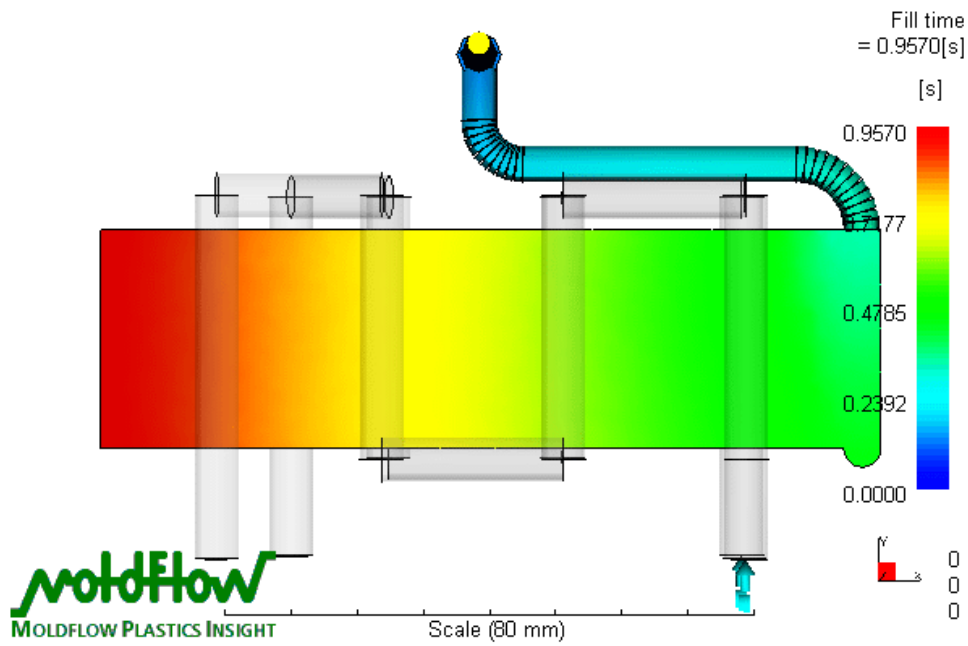


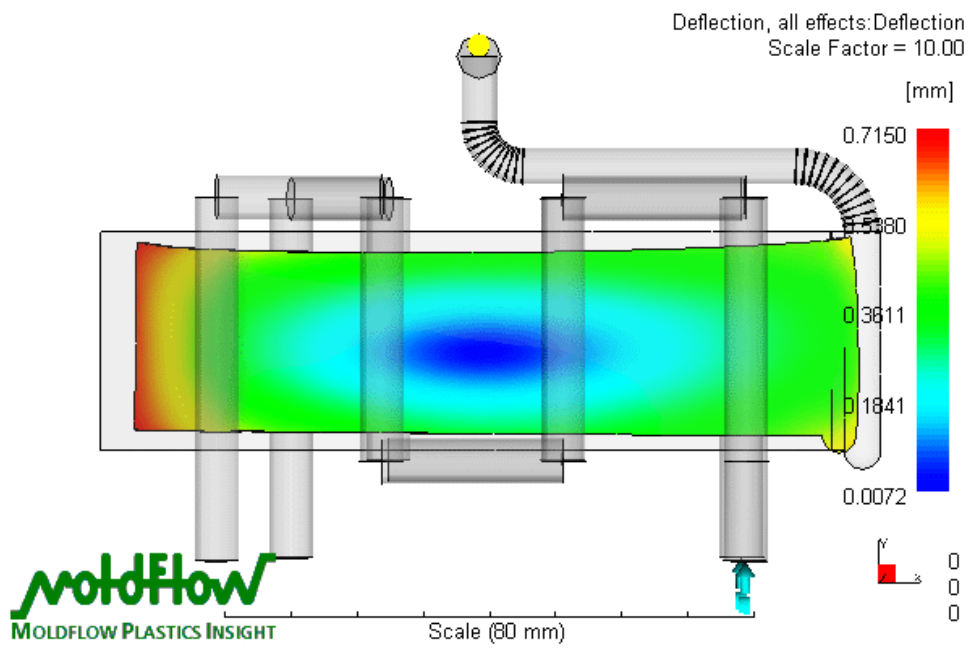
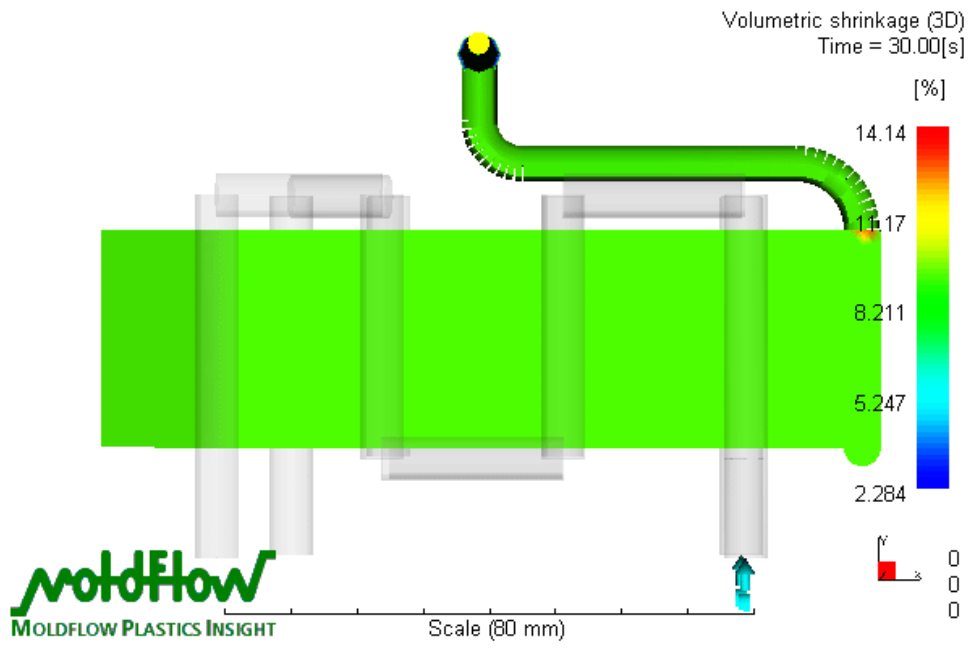
A.3.4.2-Condition of $H_p=7\text{MPa}$ and $T_m=40^\circ\text{C}$





A.3.4.3-Condition of $H_p=94\text{MPa}$ and $T_m=25^\circ\text{C}$





A.3.4.4-Condition of $H_p=94\text{MPa}$ and $T_m=40^\circ\text{C}$

